Pricing of risk in credit and equity index options—A role for option order flow?*

Pierre Collin-Dufresne† Anders B. Trolle‡

Abstract

We find consistent evidence across ratings and regions that delta-hedged credit index options have large negative Sharpe ratios and much more so than their equity index counterparts. Risk-factors extracted from equity index options have only moderate explanatory power for the time-series and cross-sectional variation in credit option returns, while a single credit-specific factor explains much of the remaining variation. We link this factor to credit option order flow in a manner that is consistent with the predictions of a demand-based option pricing model, in which order-flow risk is priced in equilibrium.

JEL Classification: G12, G13

Keywords: Credit risk, credit and equity index options, demand-based pricing

This version: June 20, 2025

Contains Internet Appendix

*We thank seminar participants at Copenhagen Business School, Tilburg University, and University of St. Gallen, for comments. Collin-Dufresne gratefully acknowledges research support from the Swiss Finance Institute. Trolle gratefully acknowledges support from the Center for Big Data in Finance (Grant no. DNRF167) and the Danish Finance Institute.

†EPFL and Swiss Finance Institute. E-mail: pierre.collin-dufresne@epfl.ch

‡Copenhagen Business School. E-mail: abtr.fi@cbs.dk

1 Introduction

Starting with the seminal work of Black and Scholes (1973) and Merton (1974), a large literature has focused on the relative pricing of debt and equity.[1] With the advent of an active market in credit index options, the focus has shifted to the pricing of higher order moments in credit and equity markets. Two recent papers (Collin-Dufresne, Junge, and Trolle (2024) and Doshi, Ericsson, Fournier, and Seo (2024)) study the relative pricing of credit and equity index options through the lens of structural credit risk models and reach different conclusions on the degree to which higher order risks are priced consistently across both markets. However, because both studies focus on a fairly narrow set of options (US investment-grade index options) using somewhat different structural models and quite different calibration strategies, it seems difficult to draw definitive conclusions from their studies.

Here, we seek to resolve the controversy. We considerably enlarge the option data set to cover the entire universe of liquid credit index options in terms of ratings (investment-grade, IG and high-yield, HY) and regions (US and Europe). Moreover, to circumvent the joint-hypothesis problem of previous studies, we address the relative valuation of credit and equity index options with a model-independent approach that relies on option trading strategies that are robust and implementable in real time. Finally, we tie differences in the relative valuation across markets to credit option order flow, in a manner that is consistent with the predictions of a demand-based option pricing model.

Our results strongly suggest that credit and equity index options are not priced consistently. Further, we find support for the hypothesis that the market structure and order-flow characteristics of credit index options contribute to driving a wedge between the pricing of these two classes of options.

First, we analyze portfolios of delta-hedged options sorted on moneyness (deep OTM

[1] See, for example, the large literature on the *credit spread puzzle*; see, e.g., Jones, Mason, and Rosenfeld (1984), Huang and Huang (2012), Cremers, Driessen, and Maenhout (2008), Chen, Collin-Dufresne, and Goldstein (2009), Culp, Nozawa, and Veronesi (2018), and Du, Elkamhi, and Ericsson (2019).

puts, OTM puts, ATM puts, and OTM calls) and maturity (1, 2, and 3 months). Sharpe ratios are much more negative for credit index options than equity index options (in the US, for example, averaging the annualized Sharpe ratios across portfolios gives -1.85 and -2.23 for the IG and HY credit index options compared to -0.60 for the equity index options) with the pricing differential being stable or even increasing over time. It follows that short-credit vs. long-equity strategies in options are highly profitable, and we show that it would be extremely unlikely to observe this degree of profitability in structural models where credit and equity index options are priced in a consistent fashion.[2]

Second, motivated by a return decomposition within a general stochastic-volatility model we identify four risk factors driving delta-hedged option returns, namely gamma (shocks to realized index return volatility), vega (shocks to implied volatility), vanna (shocks to downside risk), and volga (shocks to overall tail risk). We show how particular option trading strategies can be used as factor mimicking portfolios and study their risk-return characteristics across markets. Mean excess factor returns are uniformly negative, which is consistent with these factors paying off in adverse states. More importantly, there are significant differences in the pricing of the risk factors across markets with the gamma factor, and to a lesser extent the vega and vanna factors, having significantly more negative Sharpe ratios in credit than equity markets. This leads to short-credit vs. long-equity strategies in these factors being highly profitable (in the US, for example, the annualized Sharpe ratio on the credit vs. equity gamma factor is 1.19 and 1.51 for IG and HY, respectively).

Third, we construct a factor model from the equity-based risk factors. The model performs very well in pricing the equity index options; however, across a range of specifications, it does a poor job of pricing the credit index options explaining only about a quarter of the time-series variation in realized returns and having significantly negative alphas. Perform-

[2]We follow standard practice and compute option returns using mid-quotes. In the internet Appendix we show that, although transaction costs are higher for credit index options, significant differences in Sharpe ratios remain after taking transaction costs into account. We also note that our results are not affected by the look-ahead biases discussed in Duarte, Jones, Khorram, Mo, and Wang (2023).

ing a principal component analysis (PCA) on the unexplained credit option returns reveals large common variation, with the dominant factor explaining more than two-thirds of the variation across options and acting as a "level" factor that impacts all returns with the same sign. Adding this *credit option residual factor* to the model significantly reduces the alphas on credit index options.

Fourth, we investigate one important potential driver of this credit-specific factor: Industry professionals note that there exists a structural demand for credit index options for hedging purposes. Moreover, trades are typically very large and take place in a dealer-intermediated, over-the-counter environment—in contrast to exchange-traded equity index options. Consequently, we hypothesize that the credit option residual factor is linked to variation in option order flow; that is, demand-shocks that are difficult to hedge by the intermediaries.

We propose a simple demand-based option pricing model, where we characterize option prices—set by risk-averse dealers with limited risk-bearing capacity and facing stochastic option demand—as a solution to a system of coupled Black-Scholes type partial differential equations. The solution shows that, when markets are incomplete, order-flow risk is priced in equilibrium.

The model is consistent with the large negative Sharpe ratios on the credit index options and the credit option residual factor. In addition, we consider three testable model predictions regarding the relation between the credit option residual factor and option order flow: 1) a positive contemporaneous relation between the factor and order flow; 2) that the relation is stronger when dealers are more risk averse; and 3) that the expected excess return on the factor is more negative following high order flow.

To test these predictions, we first compute measures of daily order flow in credit index options using transaction data from swap data repositories. On average, trading volume is high, but is made up of relatively few, very large trades. Also, the order flow is highly volatile. Next, we run regressions involving the credit option residual factor and order flow. We find a significant positive relation between the factor and contemporaneous order flow consistent with 1). This relation is stronger when the capital ratio of intermediaries is low (proxying for higher dealer risk aversion in the model) consistent with 2). Finally, there is a negative relation between the factor and lagged order flow consistent with 3).

The paper is related to several strands of literature. A large literature has analyzed returns on equity index options; see, e.g. Coval and Shumway (2001), Bakshi and Kapadia (2003), Broadie, Chernov, and Johannes (2009), Santa-Clara and Saretto (2009), and Constantinides, Jackwerth, and Savov (2013). For credit index options, Collin-Dufresne et al. (2024) and Doshi et al. (2024) report some results on option returns. In this paper, we provide a much more comprehensive analysis of their risk and return characteristics, investigate the relative pricing of option risk factors across credit and equity markets, and explore the impact of option order flow.[3]

Several papers have proposed factor models for option returns; see, e.g., Jones (2006), Buchner and Kelly (2022), Horenstein, Vasquez, and Xiao (2023), and Fournier, Jacobs, and Orlowski (2024). Here, we consider a model based on tradable factors that are economically-motivated and easily implementable.

Starting with Bollen and Whaley (2004) and Gârleanu, Pedersen, and Poteshman (2009), a number of papers have explained the historically large negative Sharpe ratios on equity index options with a structural demand from end-users. The more recent reduction in the magnitude of Sharpe ratios has been attributed to a more balanced demand by end-users (Chen, Joslin, and Ni (2019)) and lower hedging costs for liquidity providers (Dew-Becker and Giglio (2023)). We show that demand pressure effects continue to be important for credit index options that trade in a dealer-driven, over-the-counter market (a very different

[3]Two recent papers construct synthetic credit variance swaps from credit index options, see Ammann and Moerke (2023) and Chen, Doshi, and Seo (2023). S&P Global recently launched official credit VIX indexes underscoring the high liquidity of credit index options, see Masabathula and Godec (2023).

market structure than for listed equity options), which explains part of the relative valuation of credit and equity index options.[4]

Our theoretical model linking option prices to order flow is related to the models in Gârleanu et al. (2009) and Chen et al. (2019). Our contribution is to provide a simple analytical framework using continuous-time trading, regime-switching order-flow and volatility risk, and a specific dealer utility-function, for which we obtain an explicit characterization of the equilibrium option price and many of its properties.

2 Credit indexes and options

2.1 Credit indexes

Credit indexes provide the basis for trading credit risk through index CDSs and options. We focus on the four most popular credit indexes, namely those for investment-grade and high-yield companies domiciled in North America (CDX.IG and CDX.HY) and Europe (iTraxx.main and iTraxx.Crossover).[5] The four indexes comprise 125, 100, 125, and 75 companies, respectively.

The index compositions are "refreshed" every six months in March and September, and each refreshed index is identified by its *series* number.[6] The most recent series is referred to as on-the-run. When an index member of a series defaults, a new *version* of the series without the defaulted name is launched. A credit derivative is always written on a particular index series, and for valuation purposes we need to keep track of the defaults that happen

[4] More generally, a number of papers have attributed valuation differences across credit and equity markets to intermediary frictions; see, e.g., Kapadia and Pu (2012), Friewald and Nagler (2019)), and He, Khorrami, and Song (2022).

[5] In addition to requirements on rating and geographical location, index constituents are also selected based on business sector and liquidity. Because the vast majority of firms in CDX.IG and CDX.HY are US firms, we refer to these as US indexes.

[6] For CDX.IG, iTraxx.main and iTraxx.Crossover, the refreshment takes place on March 20 and September 20. For CDX.HY, it takes place one week later on March 27 and September 27. In September 2014, there was a delay in the launch of the new series.

within that series. Assume that a series is launched at time 0 with N constituents. The number of constituents that remains at time t is

$$N_t = \sum_{i=1}^{N} \mathbf{1}_{\{\tau_i \geq t\}},$$

where τ_i is the default time of firm i.[7] The version number at time t is then $N - N_t + 1$.

2.2 Credit index returns

The most common credit derivatives are index CDSs. These are highly standardized contracts that allow for efficient trading of the credit risk in an index. At initiation, index CDSs typically have a maturity of five years and reference the current version of the on-the-run index series. These swaps are very liquid and have very low transaction costs, see Collin-Dufresne, Junge, and Trolle (2020b).

In an index CDS, the swap notional is divided evenly across the index constituents. We always assume an initial notional of one so that for a swap contract initiated at time t, each index constituent is associated with a notional of $\frac{1}{N_t}$. When entering the swap contract, the buyer of protection agrees to pay a fixed running coupon, *cpn*, of either 100 bps for IG indexes or 500 bps for HY indexes as well as an upfront amount U per unit of notional that varies with the market's perceived credit-risk of the underlying index constituents.[8] In return, whenever an index constituent defaults, the protection buyer receives the loss given default as in a single-name CDS with a notional of $\frac{1}{N_t}$. After that, the swap lives on with a reduced notional, referencing the series' new version.

The value of an index CDS is typically represented in terms of either spread or price. In

[7]Note that in case of a default, the new version of a series is not launched until the day after the settlement auction for the defaulted name in which the loss-given-default is determined. Therefore, strictly speaking, τ_i refers to the date of the settlement auction and not the actual default time.

[8]Note that the upfront amount will be negative if the risk-neutral expected loss rate of the underlying basket is less than the running coupon.

this paper, we work in price terms because it eases comparisons between credit and equity indexes. The time-t price of an index CDS is

$$S_t = 1 - U_t.$$

This can be interpreted as the price of a corporate bond index constructed by buying a risk-free floating-rate note with face value of one (and market value that constantly resets to one) and selling credit protection on an index CDS with notional value of one (and market value U_t).

When we colloquially refer to the return on a credit index, we are referring to the return on an index CDS characterized by index series and version as well as swap maturity. We always consider five-year swaps and that the index CDS references the current version of whichever series is on-the-run at the beginning of the holding period. Assuming that the coupon is paid continuously, the return over a short holding period of Δ is

$$R = \frac{S_{t+\Delta} + (r_t + cpn)\Delta}{S_t} - 1,$$

where r is the risk-free rate. If there is a default among the index constituents during the holding period, the series' original version is no longer quoted at the end of the holding period. Instead, its price can be computed as

$$S_{t+\Delta} = \frac{N_t - 1}{N_t}\tilde{S}_{t+\Delta} + \frac{1}{N_t}(1 - \ell),$$

where $1 - \ell$ is the recovery rate of the defaulted name and $\tilde{S}_{t+\Delta}$ is the price of the series' new version.[9]

[9]For the daily holding periods that we consider in this paper, there are never more than one default.

2.3 Credit index option returns

There is an active market for options on five-year on-the-run index CDSs.[10] Contractually, the options are settled in upfront terms and reference the version of the series that prevailed when the option was issued. For instance, the payoff of a call option bought at time t with unit notional is

$$\left(\frac{N_T}{N_t}\tilde{U}_T + \frac{1}{N_t}\sum_{i=1}^{N_t-N_T} \ell_i - K^U\right)^+,$$

where T is option expiration and K^U is the strike in upfront terms.[11] If exercising, the holder of the option will enter as a credit protection buyer in an index CDS with notional $\frac{N_T}{N_t}$ on the series' current version trading with an upfront of $\tilde{U}_T$. In addition, the option holder will receive credit protection payments on the $N_t - N_T$ defaults that happen in the index series over the life of the option—a feature known as *front end protection*.

The above payoff can be re-expressed in price terms; indeed, it is equivalent to the put option payoff

$$\left(K^S - S_T\right)^+,$$

where $K^S = 1 - K^U$ is the strike in price terms and

$$S_T = \frac{N_T}{N_t}\tilde{S}_T + \frac{1}{N_t}\sum_{i=1}^{N_t-N_T}(1-\ell_i).$$

is the time-T price of the series' original version (the one that prevailed at time t).[12]

Let $\mathcal{P}_t(T, K^S)$ denote the time-t price of a put options with expiration T and strike K^S. The return over a holding period of Δ is trivially $R = \frac{\mathcal{P}_{t+\Delta}(T,K^S)}{\mathcal{P}_t(T,K^S)} - 1$. However, in case

[10] Options are European style and expire on the third Wednesday of each month.

[11] Call options on the upfront are known as payer swaptions, while put options on the upfront are known as receiver swaptions.

[12] This is an approximation because in the underlying index CDS, defaults are settled as they occur, while in the option, defaults are settled at maturity. However, because option maturities are short and interest rates are low during most of the sample period, we can disregard this issue.

of a default during the holding period, options on the series' original version are no longer quoted at the end of the holding period. Instead, as we show in Section IA.1 in the Internet Appendix, $\mathcal{P}_{t+\Delta}(T, K^S)$ can be computed as

$$\mathcal{P}_{t+\Delta}(T, K^S) = \frac{N_t - 1}{N_t} \times \tilde{\mathcal{P}}_{t+\Delta}(T, \tilde{K}^S),$$

where $\tilde{\mathcal{P}}_{t+\Delta}$ is the price of an option on the series' new version with an adjusted strike of $\tilde{K}^S = \frac{N_t}{N_t - 1}\left(K^S - \frac{1}{N_t}(1-\ell)\right)$.

3 Option returns in a structural model

In this paper, we compare average returns on credit and equity index options. Before turning to the empirical analysis, this section assesses whether, and under what conditions, such a comparison is informative.

The central issue is as follows: Suppose that credit and equity index options are priced off of the same asset value process in a structural credit-equity framework, and consider a pair of options—one credit, one equity—with similar contract characteristics (type, maturity, and moneyness). To the extent that their exposures to the fundamental asset risk factors differ and risk premia vary across factors, the options will carry different risk premia. Therefore, observed differences in average option returns need not reflect mispricing, but may instead arise from differences in factor exposures.

We conduct a simulation exercise to investigate this issue. The true data-generating process is assumed to be the model proposed in Collin-Dufresne et al. (2024), with parameter estimates taken from Doshi et al. (2024).[13] The model features three priced sources of systematic asset risk: diffusive risk, jump risk, and variance risk (the model is reviewed in

[13]The two models have the same underlying asset dynamics; only the debt structure of the representative firm and the conditions triggering default differ somewhat. We base the simulation on the Collin-Dufresne et al. (2024) model because it features analytical option prices.

Section IA.5 of the Internet Appendix). We simulate excess returns for both equity and investment-grade credit index options, assuming a daily holding period as we do throughout the paper. We focus on one-month, at-the-money options, but results are robust to variations in maturity and moneyness. Returns are calculated for both outright options and delta-hedged options, where the delta is with respect to the underlying index (not the asset value, which is unobservable in reality) and computed using the Black-Scholes model as in our empirical analysis. Results are presented separately for equity and credit options, as well as for a long-equity/short-credit options strategy.

Panel A in Table 1 reports the factor exposures, defined as the regression coefficients obtained by regressing option excess returns on asset excess returns, returns squared and changes in the asset variance state variable. These are empirical measures of delta (directional asset exposure), gamma (exposure to realized asset variance), and vega (exposure to expected future asset variance).[14] For outright options, the most important observations are that i) credit options have strikingly different vegas for calls and puts, with calls having negative vega and puts having very large positive vega;[15] ii) for a given option type, credit and equity options have very different vegas; and iii) for the most part, delta dominates gamma and vega. Because the variance exposures are very different and, in any case, are dominated by the directional exposure, a comparison of credit and equity option returns is ill-suited towards studying the consistent pricing of volatility risk.

For the delta-hedged options, the situation is very different in that i) the risk exposures are the same across puts and calls (follows from put-call parity); ii) the risk exposures are similar for credit and equity options; and iii) the asset deltas are close to zero so that delta-neutrality

[14] The factor exposures are normalized to reflect a one standard derivation change in each of the risk factors. Note also that in our main analysis we also consider so-called vanna and volga risk, but these are not separate risk factors in the model.

[15] This has been noted in both Collin-Dufresne et al. (2024) and Doshi et al. (2024). The reason is that the underlying index itself incorporates options on firms' asset values (equity is long calls, while credit is short puts). This is especially important for the credit index where an increase in asset volatility both decreases the index level and increases index volatility, with the net effect being negative for the credit index call option and strongly positive for the credit index put options.

wrt. the underlying index also largely achieves delta-neutrality wrt. the fundamental asset value. Together, this means that comparing delta-hedged credit and equity option returns is indeed meaningful for detecting differential pricing of volatility risk.[16]

Panel B in Table 1 presents the finite-sample distribution of annualized mean excess returns, based on 1,000 simulations of 10 years of daily returns, which is the sample size in the paper. For outright options, the 95% confidence intervals are very wide—more than 500% for puts, a bit less for calls—which implies low statistical power to reject the model (i.e., the null of no mispricing) based on average option returns. This is largely due to their large directional exposures, and is consistent with Broadie et al. (2009) in the case of SPX options. Doshi et al. (2024) acknowledge the issue, but nevertheless focus on average outright option returns.

For the delta-hedged options, the 95% confidence intervals are much more narrow—about a third as wide as for outright options—making these positions much better at detecting mispricing of volatility risk in finite samples. The long-short strategy, in particular, has a narrow confidence interval; we compare with the sample mean of this strategy in Section 6.1.

4 Option risk factors and factor-mimicking portfolios

Based on the previous section, our focus is on delta-hedged option returns. These returns are analyzed through an intuitive factor model. In Section 4.1 we identify four relevant risk factors; next, in Sections 4.2 and 4.3 we show how particular option trading strategies can be used as factor-mimicking portfolios.

[16] As explained in Section 4.2, gamma and vega exposures can be separated by studying portfolios of options with different maturities.

4.1 Option risk factors

To motivate the factor model, assume that the price S_t of the underlying index follows a general stochastic-volatility process, with σ_t denoting the instantaneous return volatility (S_t can refer to either a credit or equity index). While σ_t is unobservable, it is well-known that the ATM Black-Scholes implied volatility converges to σ_t as option maturity goes to zero (e.g. Ledoit and Santa-Clara (1998), Durrleman (2010)). Therefore, we use a short-term ATM Black-Scholes implied volatility, denoted I_t, as an observable state variable in lieu of σ_t.[17]

Let P_t^i denote the price of option i on the index and consider a holding period of Δt (typically daily). The change in the option price is approximately

$$\Delta P^i \approx \frac{\partial P^i}{\partial t}\Delta t + P_S^i \Delta S + P_I^i \Delta I + \frac{1}{2}P_{SS}^i(\Delta S)^2 + \frac{1}{2}P_{II}^i(\Delta I)^2 + P_{IS}^i \Delta S \Delta I,$$

where P_S^i, P_I^i, P_{SS}^i, P_{II}^i and P_{IS}^i denote partial derivatives. The change in the value of the delta-hedged option, assuming that the index position is financed at the risk-free rate, is $\Delta V^i = \Delta P^i - P_S^i(\Delta S - (r-q)S\Delta t)$, where q is the payout rate of the index. Also, it is convenient to express the profit-loss in terms of the index return scaled by I, denoted $R^S = \frac{1}{I}\frac{\Delta S}{S}$, and the relative change in I, denoted $R^I = \frac{\Delta I}{I}$. This is because these quantities are much more uniform across indexes, as well as in the time series, giving better statistical properties to the various long-short portfolios that we will consider below. Then, we have

$$\Delta V^i \approx \big(\frac{\partial P^i}{\partial t} + P_S^i(r-q)S\big)\Delta t + P_I^i I R^I + \frac{1}{2}P_{SS}^i S^2 I^2 (R^S)^2 + \frac{1}{2}P_{II}^i I^2 (R^I)^2 + P_{IS}^i S I^2 R^S R^I. \quad (1)$$

Taking risk-neutral expectation of (1), imposing absence of arbitrage ($\bar{\mathbb{E}}[\Delta V^i] = rV^i\Delta t$,

[17] When applying the Black-Scholes model index options, the risk-neutral drift is not directly observable due to the risk of defaults in case of credit indexes and the presence of a dividend yield in case of equity indexes. We use a standard approach of inferring the risk-neutral drift from put-call parity using a cross-section of options.

where $\bar{\mathbb{E}}[\cdot]$ denotes conditional risk-neutral expectation), and subtracting the result from (1), we get an expression for the dollar return in excess of the risk-free rate:

$$\begin{aligned}\Delta V^i - rV^i\Delta t \approx & \frac{1}{2}\underbrace{P^i_{SS}S^2I^2}_{\gamma^i}\left((R^S)^2 - \bar{\mathbb{E}}[(R^S)^2]\right) + \underbrace{P^i_I I}_{\nu^i}\left(R^I - \bar{\mathbb{E}}[R^I]\right) \\ & + \underbrace{P^i_{IS}SI^2}_{\zeta^i}\left(R^S R^I - \bar{\mathbb{E}}[R^S R^I]\right) + \frac{1}{2}\underbrace{P^i_{II}I^2}_{\omega^i}\left((R^I)^2 - \bar{\mathbb{E}}[(R^I)^2]\right). \end{aligned} \tag{2}$$

Equation (2) shows that there are four risk factors driving excess returns, namely shocks to 1) realized index return volatility, 2) short-term ATM implied volatility, 3) covariance between returns and implied volatility, and 4) realized volatility of implied volatility. The corresponding factor exposures are measured by gamma (γ), vega (ν), vanna (ζ), and volga (ω).

The first two factors, realized and implied volatility, are well-known. The third factor, return-vol covariance, affects the asymmetry of the return distribution with higher covariance increasing the right tail and decreasing the left tail. This benefits OTM calls and hurts OTM puts making vanna positive for the former and negative for the latter. To ease interpretability, we use minus the covariance as a factor, replacing the term $\zeta^i\left(R^S R^I - \bar{\mathbb{E}}[R^S R^I]\right)$ in (2) with $-\zeta^i\left(-R^S R^I - \bar{\mathbb{E}}[-R^S R^I]\right)$. With this change of sign, the factor captures downside risk.

The fourth factor, vol-of-vol, affects both tails of the return distribution symmetrically, thus capturing overall tail risk. Higher vol-of-vol benefits all OTM options making volga positive for those.

Note that investors generally regard states with high volatility, more downside risk, and high overall tail risk as adverse. Therefore, we expect the associated factor risk premia to be negative, which we will check in the empirical analysis.

In the next two sections we form factor-mimicking portfolios; i.e., option portfolios that are highly correlated with each of the four factors. In doing so we need to compute the factor sensitivities of individual options. In order to obtain easily implementable option strategies we approximate these factor sensitivities with those from the Black-Scholes model.[18] The alternative of using a specific stochastic-volatility model, in addition to being more complex, would introduce model risk.

4.2 Gamma and vega factors

For the gamma and vega factors we use delta-hedged ATM options with different maturities. These options have positive gamma and vega, but approximately zero vanna and volga; see Section IA.2 in the Internet Appendix. Let P_j^x, R_j^x, γ_j^x, ν_j^x, ζ_j^x, ω_j^x, $x = \{p, c\}$ denote the price, excess return and greeks of an ATM put or call option with maturity T_j.

Consider first a straddle consisting of an ATM put and call option with maturity T_j. It has gamma $\gamma_j = \gamma_j^c + \gamma_j^p$, vega $\nu_j = \nu_j^c + \nu_j^p$, price $P_j = P_j^c + P_j^p$ and excess return

$$R_j = wR_j^c + (1-w)R_j^p, \quad w = \frac{P_j^c}{P_j}.$$

Next, following Cremers, Halling, and Weinbaum (2015) we can construct factor-mimicking portfolios that isolate gamma and vega risk using straddles with different maturities. The reason is that gamma is decreasing in option maturity and vega is increasing in option maturity. Consider two option maturities T_1 and T_2. The gamma factor (GMA) is constructed by buying one T_1-straddle and selling $N = \frac{\nu_1}{\nu_2}$ T_2-straddles. This strategy is vega-neutral, has large positive gamma exposure

$$\gamma_{GMA} = \gamma_1 - N\gamma_2 > 0,$$

[18]This is an approximation for two reasons: First, the Black-Scholes model is not an internally consistent model for computing vega, vanna, and volga exposures. Nevertheless, it is routinely used for this purpose due to its robustness; see, e.g., Castagna and Mercurio (2007) and Carr and Wu (2020). Second, the Black-Scholes model gives risk exposures with respect to the option's own implied volatility, not the common I in (2). However, in the construction of the factor mimicking portfolios we use relatively short-term options that are not too far away from ATM, so all implied volatilities are highly correlated with I.

and excess return

$$R_{GMA} = R_1 - \frac{NP_2}{P_1} R_2.$$

Note that throughout we assume that the proceeds from selling options are kept in a margin account and earn the risk-free rate.

The vega factor (VGA) is constructed by buying one T_2-straddle and selling $N = \frac{\gamma_2}{\gamma_1}$ T_1-straddles. This strategy is gamma-neutral, has large positive vega exposure

$$\nu_{VGA} = \nu_2 - N\nu_1 > 0,$$

and excess return

$$R_{VGA} = R_2 - \frac{NP_1}{P_2} R_1.$$

4.3 Vanna and volga factors

For the vanna and volga factors we use delta-hedged options with different moneyness but same maturity. We define moneyness of an option as

$$m = \frac{\log\left(\frac{K}{F_{t,T}}\right)}{\sigma^{ATM}\sqrt{T-t}}, \tag{3}$$

where σ^{ATM} is the (interpolated) ATM implied volatility with the same maturity, and $F_{t,T}$ is the forward index price.[19] Gamma and vega are roughly symmetric in moneyness, volga is also roughly symmetric (approximately zero around ATM and positive otherwise), while vanna is asymmetric (approximately zero around ATM, negative for low-strike options, and positive for high-strike options); again, see Section IA.2 in the Internet Appendix. Let P_j^x, R_j^x, γ_j^x, ν_j^x, ζ_j^x, ω_j^x, $x = \{p, c\}$, $j = \{-, 0, +\}$ denote the price, excess return and greeks of a

[19] Intuitively, m measures the number of standard deviations that an option is in or out of the money given log-normally distributed prices.

put or call option with moneyness m of -1, 0 (i.e. ATM), or $+1$.

The vanna factor (VNA) is a vega-neutral, risk-reversal strategy that buys one OTM put with moneyness $m = -1$ and sells $N = \frac{\nu_-^p}{\nu_+^c}$ OTM calls with moneyness $m = 1$. Because of the symmetry of gamma and volga, these exposures are small. However, because $\zeta_-^p < 0$ and $\zeta_+^c > 0$, the strategy has large negative vanna exposure

$$\zeta_{VNA} = \zeta_-^p - N\zeta_+^c < 0,$$

making it highly correlated with increases in downside risk. The excess return is

$$R_{VNA} = R_-^p - \frac{NP_+^c}{P_-^p} R_+^c.$$

The volga factor (VLG) is a vega-neutral, butterfly strategy that buys one OTM put with moneyness $m = -1$ and one OTM call with moneyness $m = 1$ (i.e., buys a strangle), and sells $N = \frac{\nu_-^p + \nu_+^c}{\nu_0^p + \nu_0^c}$ ATM straddles.[20] The gamma exposure is small. Further, because the straddle has approximately zero vanna and the OTM put and call have vanna of similar magnitudes but opposite sign, the strategy's vanna exposure is also small. However, because $\omega_-^p, \omega_+^c > 0$ while $\omega_0^p, \omega_0^c \approx 0$, the strategy has large positive volga exposure

$$\omega_{VLG} = \omega_-^p + \omega_+^c - N(\omega_0^p + \omega_0^c) \approx \omega_-^p + \omega_+^c > 0,$$

making it highly correlated with increases in overall tail risk. The excess return is

$$R_{VLG} = \frac{1}{P^{VLG}} \left(P_-^p R_-^p + P_+^c R_+^c - N \left(P_0^p R_0^p - P_0^c R_0^c \right) \right),$$

where $P^{VLG} = P_-^p + P_+^c$ is the cost of the strategy.

[20] In some markets, such as FX, risk-reversals and butterflys are routinely quoted directly (Carr and Wu (2007)) and used for pricing exotic derivatives via the so-called vanna-volga method (Castagna and Mercurio (2007)).

5 Data

Data on credit indexes, credit index options, defaults, and recovery rates is from Markit. For the equity index options we use SPX options in the US market and Eurostoxx 50 options in the European market. These are the benchmark equity index options in their respective markets, and data is from CBOE and OptionMetrics, respectively. In all cases, we use end-of-day quotes. We focus on mid quotes except in Section IA.4 in the Internet Appendix, where we use bid and offer quotes to analyze the impact of transaction costs. We apply a number of filters to the options data to ensure that we focus on the most liquid quotes, see Section IA.3 in the Internet Appendix.

For credit index options, Collin-Dufresne et al. (2024) show that most trading is in 1, 2, and 3-month options, and trading is skewed towards low strikes in terms of price (i.e., high strikes in terms of upfront/spread). Therefore, on each observation date we select the first three monthly expirations among the options that have more than two weeks to expiration. These options are denoted M1, M2, and M3. For each maturity, we consider four levels of moneyness, $m = -2, -1, 0, 1$, with m defined in (3). We only use actual quoted strikes, so for each target level of moneyness, we search for the strike that comes closest to the target with the constraint that the deviation from target cannot be greater than 0.5.

For the equity index options, on each observation date we search for the three option maturities that are closest to the three credit index option maturities.[21] For each maturity, we consider the same four levels of moneyness as the credit index options.

In the last part of the paper we use transaction data in credit index options. This data is provided by Clarus FT which sources it from swap data repositories.

Our sample period is determined by the intersection of the price and transaction data. It starts on January 1, 2013 (when transaction data becomes available) and ends on April 3,

[21] In our final dataset, there is a close correspondence between the maturities of equity and credit index options, with the equity index options expiring either two days after or five days before the corresponding credit index options.

2023 (when the Markit data ends). The frequency of the data is daily, and we always consider returns with a daily holding period. We use a separate grid of trading days for the US and European markets with the European trading days being the intersection of trading days in London (which determines availability of derivatives data on European credit indexes) and Eurex in Frankfurt (where Eurostoxx 50 options are traded), see Table IA.1 in the Internet Appendix.

6 Results

6.1 Option returns

For context, we first discuss the returns of the underlying indexes (summary statistics are given in Table IA.2 in the Internet Appendix). In our sample period there are no defaults in the on-the-run IG credit indexes, 21 defaults in the on-the-run CDX.HY index, and 5 defaults in the on-the-run iTraxx.Crossover index, see Tables IA.3 and IA.4 in the Internet Appendix. The Sharpe ratios are of similar magnitudes across credit and equity indexes. In the US, annualized Sharpe ratios are 0.68, 0.62, and 0.76 for the IG and HY credit indexes and the equity index, respectively. In Europe, the corresponding numbers are 0.78, 0.73, and 0.48.

Next, we turn to the risk-return tradeoff for index options. We consider portfolios of delta-hedged OTM and ATM options (puts for $m \leq 0$ and calls for $m > 0$). Specifically, for each index, we construct 7 equally-weighted portfolios by sorting options on moneyness ($m = -2, -1, 0, 1$) and maturity (1M, 2M, 3M). The annualized Sharpe ratios of the seven option portfolios for each index are shown in Figure 1. In general, Sharpe ratios are much more negative for credit index options than equity index options. Indeed, averaging the Sharpe ratios across portfolios we get -1.85 and -2.23 for the IG and HY indexes in the US compared to -0.60 for the equity index, while in Europe we get -1.81 and -1.88 for the IG and

HY indexes compared to -0.10 for the equity index. For credit options, the most negative Sharpe ratios are found for the portfolios of deep OTM put options ($m = -2$) and short-term options (M1).

Table 2 (IA.5 in the Internet Appendix) provides more details on the performance of the option portfolios sorted on moneyness (maturity). In particular, while mean excess returns on credit option portfolios are highly statistically significant, this is only the case for two equity option portfolios. Also, and not surprisingly, the return distributions are fat-tailed and positively skewed.

Table 3 (IA.6 in the Internet Appendix) shows that for all moneyness (maturity) portfolios and all indexes, a strategy that goes short credit index options and long equity index options delivers highly statistically significant mean excess returns and high Sharpe ratios (averaging the annualized Sharpe ratios across portfolios gives 0.83 and 1.12 for the IG and HY indexes in the US and 1.38 and 1.47 in Europe), while preserving positively skewed return distributions. For ATM options, these results largely mirror those in Collin-Dufresne et al. (2024) for trading CDX.IG options against SPX options; here we show that they hold true more generally across the option surface, across both IG and HY indexes, across regions, and in a longer time series.

It is instructive to compare the mean return for the US ATM equity vs. IG strategy in Table 3 with the finite-sample distribution for the same strategy reported in Table 1. The annualized sample mean is 0.85, while the 95% confidence interval is from -0.30 to 0.22 under the null of consistent pricing in the structural model. One caveat is that the parameter estimates underlying the small-sample distribution are for a sample period that only partly overlaps with the sample period of this paper. Nevertheless, the sample mean is so far outside of the 95% confidence interval that we interpret this as strong evidence against the null of consistent pricing.[22]

[22] Alternatively, we can compare the Sharpe ratio. The annualized sample Sharpe ratio is 1.15, while the 95% confidence interval is from -0.79 to 0.45 under the null (not reported in Table 1).

Dew-Becker and Giglio (2023) argue that the profitability of selling equity index volatility has decreased significantly in recent years. To see if this is also the case for credit index volatility, Figure 2 shows, for each index and each full year in the sample, the mean annualized Sharpe ratio across of the seven option portfolios. While there is a tendency for the Sharpe ratio of equity index options to become less negative (and even occasionaly positive) over the sample period, no such tendency is observed for the credit index options. Indeed, splitting the sample period in two, the mean of the five yearly Sharpe ratios across the four credit indexes is -2.38 in the first half of the sample and -2.46 in the second half. In contrast, across the two equity indexes, the corresponding numbers are -1.21 and -0.09.

A natural question is how transaction costs affect the profitability of selling volatility through index options. We analyze this issue in Section IA.4 of the Internet Appendix. Based on indicative bid-ask spreads, we find that transaction costs for credit index options are about four to five times larger than those for equity index options, on average. Nevertheless, even taking these higher transaction costs into account, selling credit index volatility remains significantly more profitable than selling equity index volatility.[23]

6.2 Factor returns

To understand the differential pricing of credit and equity index options, we next look at the performance of the factor-mimicking portfolios within each index. The vega and gamma factors are constructed from straddles with two different maturities. For each of these two greeks, we first construct three individual factors using the maturity pairs 1M vs. 2M, 1M vs. 3M, and 2M vs. 3M, and then form an equally-weighted portfolio of the three individual factors. The vanna, and volga factors are constructed from options with different strikes but the same maturity. For each of these two greeks, we first construct three individual factors

[23]We show this in a setting where options are sold at bid prices and delta-hedged until expiration. Such a strategy is closer to how volatility is traded in practice, and implies that transaction costs are only incurred once per option.

using either 1M, 2M, or 3M maturities, and then form an equally-weighted portfolio of the three individual factors.[24]

Table 4 shows the performance of the resulting factor-mimicking portfolios.[25] Mean excess factor returns are consistently negative. As explained in Section 4.1, this is in line with expectations because the factors are constructed so that they pay off in (i.e., provide insurance against) what are arguably adverse states of the world, namely higher realized volatility (GMA), higher implied volatility (VGA), more downside risk (VNA), and higher overall tail risk (VLG).

For the credit options, the Sharpe ratios are most negative for GMA and VNA followed by VGA and then VLG, with the mean excess return being statistically significant for the GMA, VGA, and VNA factors. Because short-term options have high GMA exposures and OTM puts have higher VNA exposures, this is consistent with the Sharpe ratio pattern in Figure 1 for the credit option portfolios. In contrast, for the equity options, the Sharpe ratios are most negative for VNA followed by VGA and VLG and then GMA, with virtually none of the mean excess returns being statistically significant. Averaging across all credit (equity) indexes, the annualized Sharpe ratios for the GMA, VGA, VNA, and VLG factors are -1.68 (-0.23), -0.89 (-0.40), -1.72 (-0.89), and -0.13 (-0.48), respectively.[26] As such, it appears that the differential pricing of index options across credit and equity is mostly due to the pricing of the GMA factor and to a lesser extent the VGA and VNA factors.

To investigate this further, we consider long-short strategies where we trade equity vs.

[24]For each of the greeks, the individual factors are very highly correlated. Forming equally-weighted portfolios removes the arbitrariness of the choice of maturity, reduces noise, and reduces the number of missing observations.

[25]The performance of the individual factor-mimicking portfolios are displayed in the Internet Appendix, Tables IA.7 to IA.10.

[26]In the case of the S&P 500, Cremers et al. (2015) and Dew-Becker, Giglio, and Kelly (2021) report Sharpe ratios on factor mimicking portfolios that are conceptually similar to the GMA and VNA factors (although Cremers et al. (2015) interpret them as mimicking "jump" and "volatility" risk and Dew-Becker et al. (2021) interpret them as mimicking "realized volatility" and "uncertainty" risk). In earlier sample periods, Cremers et al. (2015)) report annualized Sharpe ratios of -0.93 and -0.55, and Dew-Becker et al. (2021) report Sharpe ratios of -1.2 and -0.2. In contrast, Table 4 shows Sharpe ratios of -0.19 and -0.11. Therefore, it seems that it is primarily the pricing of the GMA factor that has changed over time.

credit factor-mimicking portfolios. These are constructed as follows: For each greek, we first construct long-short positions using the individual factor-mimicking portfolios; for instance, shorting the 1M-2M credit GMA portfolio and going long the 1M-2M equity GMA portfolio. The long and short legs are risk-weighted, so in the case of GMA, they are weighted by their gammas. Next, we form an equally-weighted portfolio of the three individual long-short positions. Table 5 shows the performance of the resulting long-short portfolios.[27] For all the indexes, the GMA factor has the highest annualized Sharpe ratios (ranging from 1.19 to 1.79 and averaging 1.47) with the mean excess returns always being highly statistically significant. The Sharpe ratios are somewhat lower for the VGA (ranging from 0.35 to 0.84 and averaging 0.52) and VNA (ranging from 0.22 to 1.03 and also averaging 0.52) factors for which only the HY indexes have (some) mean excess returns that are statistically significant. These long-short strategies display mostly small and positive skewness, but fairly large kurtosis.

6.3 Performance of equity-based factor model

We now turn to the question of how well an equity-based factor model performs in pricing the credit index options. This speaks to how well the markets for equity and credit index options are integrated, a subject of debate between Collin-Dufresne et al. (2024) and Doshi et al. (2024). The set of pricing factors always consists of the four option factors and the index return.

To put the results in perspective, we start with an in-sample analysis of how well index-specific factor models perform in pricing the associated index options. For each index, Table 6 reports the maximum Sharpe ratio constructed from the set of option portfolios, the factors, and the options and factors jointly—all of which are higher for credit than equity indexes in line with Sections 6.1 and 6.2.

[27] The performance of the individual long-short portfolios are displayed in the Internet Appendix, Tables IA.11 to IA.14.

For each index, the latter two Sharpe ratios are relatively close, which is indicative of good in-sample pricing performance. More formally, the table reports the p-value of the Gibbons, Ross, and Shanken (1989) test of equivalence between the squared Sharpe ratios (i.e., of the alphas from the factor model being jointly zero), which for half the indexes cannot be rejected at the one percent level. However, the GRS test relies on very restrictive assumptions, and it is standard practice to evaluate models based on statistics such as the cross-sectional average of the absolute alphas (very small relative to the mean excess returns reported in Section 6.1), absolute robust t-statistics (mostly below one), and R^2s (always very high).[28] Based on these statistics, the in-sample performances of the factor models are very good.

Next, we evaluate the performance of the equity-based factor model for pricing the credit index options. To align credit and equity option returns in terms of trading hours and non-trading days, we consider the US and European markets separately. Also, we always include both contemporaneous factors and factors lagged one day to control for any remaining non-synchronicity across returns.

We consider three factor model specifications: An unconditional model (*mdl1*); a conditional model (*mdl2*), where the factor loadings are linear functions of the option portfolio greeks (all option portfolios are delta-neutral so there is no conditioning on delta); and a further conditional model (*mdl3*), where the factor loadings in addition are linear functions of the average implied volatility within each option portfolio, I^i_{t-1}. We can write *mdl3* as

$$\begin{aligned} R^i_t =& \alpha^i + \left(\beta^{1,i} + \tilde{\beta}^{1,i} I^i_{t-1}\right) IDX_t + \left(\beta^{2,i} + \bar{\beta}^{2,i}\gamma^i_{t-1} + \tilde{\beta}^{2,i} I^i_{t-1}\right) GMA_t + \left(\beta^{3,i} + \bar{\beta}^{3,i}\nu^i_{t-1} + \tilde{\beta}^{3,i} I^i_{t-1}\right) VGA_t \\ &+ \left(\beta^{4,i} + \bar{\beta}^{4,i}\zeta^i_{t-1} + \tilde{\beta}^{4,i} I^i_{t-1}\right) VNA_t + \left(\beta^{5,i} + \bar{\beta}^{5,i}\omega^i_{t-1} + \tilde{\beta}^{5,i} I^i_{t-1}\right) VLG_t + \text{lags} + \epsilon^i_t, \end{aligned}$$

where R^i_t denotes the excess return on the i'th option portfolio, *mdl2* is a special case with

[28] See Fama and French (2015), Stambaugh and Yuan (2017), and Kozak, Nagel, and Santosh (2018) for recent examples.

$\tilde{\beta} = 0$, and *mdl1* is a further special case with $\bar{\beta} = \tilde{\beta} = 0$.

For each credit index, Table 7 reports the cross-sectional average of the absolute alphas, absolute robust t-statistics, and R^2s.[29] Regardless of specification, the model does a poor job of pricing the credit options. In case of the unconditional model and taking the US IG index as an example, the average $|\alpha|$ is 1.66 which is very high relative to both the average mean excess return of -2.71 and the in-sample average $|\alpha|$ of 0.14 reported in Table 6. Moreover, average $|t|$ is high at 3.57 and average R^2 is only 0.26. Adding conditioning variables leads to only slightly lower average $|\alpha|$ (1.61 and 1.56) and slightly higher average R^2 (0.27 and 0.28). The same picture holds true for the US HY index and the European indexes. The upshot is that the equity-based factor model captures only a small part of both the time-series variation in realized returns and the cross-sectional variation in average returns.

6.4 Credit option residual factor

The poor performance of the equity-based factor model could be due to noisy credit index option returns or credit-specific factors missing from the model. To distinguish between these explanations, we apply a principal component analysis (PCA) to the residual excess returns of the 14 credit option portfolios within each market. In doing so, we face the issue that even though overall relatively few credit option returns are missing, because some of the missing returns occur randomly, the proportion of the dates where at least one observation is missing is non-negligible.[30] This presents a problem for regular PCA; instead, we apply probabilistic PCA (Tipping and Bishop (1999)), which is designed to handle missing observations.

The PCA reveals large common variation in the residuals. For example, for the unconditional model, the first PC (PC1) explains more than two-thirds of the variation across

[29]The regression coefficients in case of the unconditional model are given in the Internet Appendix, Tables IA.15-IA.16

[30]Across the two US credit indexes, 2.3% of the option portfolio returns are missing but 9.5% of the dates have at least one observation missing. Across the European credit indexes, the corresponding numbers are 4.1% and 19.2%.

residuals (70% in the US market and 75% in the European market). Figure 3 shows the factor loadings for the unconditional model. All loadings have the same sign, which makes PC1 a credit market factor that affects all credit index options in the same direction. The loadings are highest for short-term options and OTM options, and the loading pattern is similar across the IG and HY indexes. The second PC (PC2) explains a much lower fraction of the residual variation (for the unconditional model, 15% in the US market and 13% in the European market) and affects IG and HY portfolios with opposite sign (see Internet Appendix Figure IA5 for the factor loadings), which largely makes it an HY vs. IG factor.

For each model specification, we then construct two residual factors as

$$F_t^j = \sum_{i=1}^{14} \left(\alpha^i + \epsilon_t^i\right) \lambda^{i,j}, \quad j = 1, 2,$$

where $\lambda^{i,j}$ is the loading of portfolio i on PCj. That is, the residual factors are weighted averages of the excess returns on the 14 credit option portfolios, orthogonalized with respect to the equity factors. For the unconditional model, the annualized Sharpe ratios of the two factors are -1.72 and 0.78 in the US market and -2.17 and 0.96 in the European market (because alphas are negative for all credit option portfolios and generally more so for HY than IG, the Sharpe ratio is negative for F_t^1, which is long all options, and positive for F_t^2, which is short HY options and long IG options).

Table 7 shows that adding F_t^1 to the factor model significantly improves its performance on credit index options, reducing the average $|\alpha|$ and $|t|$ and raising the average R^2. In case of the unconditional model and taking the US IG index as an example, the average $|\alpha|$ is reduced from 1.66 to 0.67 and the average R^2 is increased from 0.26 to 0.73. The effect is similar for the US HY index and the European indexes. Adding also F_t^2 to the factor model has a much smaller impact; therefore, in the remainder we will focus on F_t^1 and its determinants. We will refer to F_t^1 as the *credit option residual factor*.[31]

To illustrate the fit of the factor models, Figure 4 shows scatterplots of predicted mean excess returns on the credit option portfolios versus actual mean excess returns, where predicted returns are obtained from the risk exposures in two models, *mdl1* and *mdl1*+F_t^1. Clearly, adding the credit option residual factor leads to a very large improvement in model fit.

7 Credit option returns and end-user demand

For equity index options, Bollen and Whaley (2004) and Gârleanu et al. (2009) find that a structural demand from end-users contributes to options being expensive. More recent papers find that the net demand by end-users has become more balanced (Chen et al. (2019)) and that hedging costs for liquidity providers have decreased (Dew-Becker and Giglio (2023)), which is consistent with the downward trend in the profitability of selling equity index options documented in Dew-Becker and Giglio (2023) (and corroborated in Section 6.1).

In contrast, for credit index options, market participants note that there is a persistent structural demand from end-users. This demand largely stems from banks who use credit index options to hedge their credit valuation adjustment (CVA) exposures, which in turn reduces their regulatory capital (Becker (2014) and Rega-Jones (2020)). Moreover, credit index options trade in a purely institutional, dealer-intermediated, over-the-counter market where each trade involves the transfer of a large amount of credit risk.[32] Consequently, a plausible conjecture is that the credit option residual factor is linked to order flow in these options.

[31] Instead of performing PCA on IG and HY options jointly, one could do PCA on IG and HY options separately. In this case, the annualized Sharpe ratio of the first residual factor is -1.26 for IG and -1.81 for HY in the US (-1.91 and -2.23 in Europe) and the factors are highly correlated. In the interest of parsimony, we prefer to work with the first joint residual factor.

[32] Unlike the underlying index CDSs, which are required to trade on so-called swap execution facilities (SEFs), the credit index options trade almost exclusively on a bilateral basis and always via dealers. Indeed, in the transaction data only about 2% of the option trades were executed on SEFs.

7.1 Credit option order flow

We analyze transactions from swap data repositories. In total, during our sample period there are 130,473 option transactions referencing the four credit indexes. The data comprises all transactions involving at least one US-based counterpart; however, we lack transactions between non-US parties (presumably, this issue is more important for options referencing the European indexes and, indeed, these options constitute only about one-third of the transaction data).[33] Also, the size of each trade (in terms of the notional value of the underlying swap) is only reported up to a cap which most often is 100 million USD.[34] Nevertheless, the order flow that we can compute from the transaction data should be useful (if noisy) proxy for the true order flow.

Table 8 reports summary statistics for the daily order flow measured in terms of the total number of trades, number of capped trades, and reported trading volume in billions (USD in US market and EUR in European market).[35] We note three important characteristics about the order flow:

- *Low-frequent large trades.* As already noted in Collin-Dufresne et al. (2024) for CDX.IG options, credit index options trade much less frequently than equity index options, but transactions are typically very large with the swap notional often exceeding the reporting cap (especially for IG indexes). In our sample, the average daily number of trades in CDX.IG (CDX.HY) is 18.7 (14.9) of which 39.0% (24.8%) are capped. Very large trades with notionals in billions are not uncommon for CDX.IG, see below.

- *Large volume.* The average daily reported trading volume for CDX.IG (CDX.HY) is 1.55 (0.96) billion, but this is severely downward-biased because of the large number of

[33] In the transaction data, about 14% of the trades are listed as corrections to previous trades. In these cases, the time stamp refers to the time that the corrected trade report is submitted to the SDR and not the time of the original trade. Therefore, we discard these trades when computing daily order flow.

[34] The reporting cap varies with option characteristics, but the typical value is 100 million USD.

[35] Gârleanu et al. (2009) show how to aggregate demand across options with different moneyness and maturity. This depends on the source of unhedgable risks and introduces a degree of model-dependency.

capped trades. More recent data sheds light on the true size of the market. On October 7, 2024 the reporting caps were raised from 100 million to 400 million. We collect transaction data from October 7, 2024 to June 13, 2025 and find an average daily trading volume for CDX.IG (CDX.HY) of 6.86 (2.77) billion. Nevertheless, despite the fourfold increase in reporting threshold, 50.7% (6.5%) of trades are capped. As described in the Section IA.6 of the Internet Appendix, we can go one step further and use specific data points in CFTC (2024) to infer a power-law for the hidden (capped) part of the trade size distribution.[36] The resulting trade-size distributions are given in Figure 5. We estimate that 7.0% (2.8%) of CDX.IG trades have notional values above 1.2 (2.0) billion, and that the average daily trading volume for CDX.IG (CDX.HY) is 12.90 (3.50) billion.[37]

- *Volatile flow.* The daily order flow is highly volatile; some days see almost no trading and other days see very high trading activity. In Table 8, the 95th percentiles of the daily order flow measures are about three times the median values.

7.2 Option pricing with stochastic demand

7.2.1 Illustrative model

To illustrate the link between option returns and order flow, we develop a simple demand-based option pricing model. The model builds on the standard ideas of Gârleanu et al. (2009) (GPP) and others (e.g., Henderson and Hobson (2009), Hugonnier, Kramkov, and Schachermayer (2005)) in that we assume that a representative dealer takes the price of the underlying asset, S_t, and the risk-free rate, r, as given (i.e., set in a larger market) and instead

[36] Based on regulatory data from 2023, CFTC (2024) finds that CDX.IG option trades with notionals above 1.2 (2.0) billion account for 67% (75%) of the total traded notional in these options.

[37] By contrast, setting the reporting cap at 100 million, which is mostly the threshold on our main sample, we get an average daily trading volume of only 2.23 (1.62) billion showing that the trading volumes in Table 8 are vastly underestimated.

is the marginal trader for setting the price of a derivative so as to clear an exogenously given demand by end-users.[38] In contrast to GPP, we solve the model in continuous time and obtain a solution for the demand-based option price in terms of a Black-Scholes type PDE that is easily solved numerically.

We assume that S_t follows a stochastic-volatility process

$$\frac{dS_t}{S_t} = \mu dt + \sigma(x_{t^-}) dZ_t$$
$$dx_t = \sum_{i=1}^{\bar{x}} \mathbf{1}_{\{x_{t^-}=i\}} \sum_{j \neq i} (j-i) dN_{x,i,j}(t),$$

where, for all $i, j = 1, \ldots, \bar{x}$, the $N_{x,i,j}(t)$ are independent Poisson counting processes with intensity $\lambda_{x,i,j}$.[39] We assume that the dealer trades both the underlying and a derivative written on that underlying with payoff $P(T, S_T) = \Phi(S_T)$ at time T for some general function $\Phi(\cdot)$.[40]

Further, we assume an exogenous and stochastic (net) demand for the derivative by end-users such that in order to clear markets, the dealer must hold θ_t units. Like volatility, the dealer position also follows a continuous-time Markov chain:

$$\theta_t = \theta(y_t)$$
$$dy_t = \sum_{i=1}^{\bar{y}} \mathbf{1}_{\{y_{t^-}=i\}} \sum_{j \neq i} (j-i) dN_{y,i,j}(t),$$

where, for all $i, j = 1, \ldots, \bar{y}$, the $N_{y,i,j}(t)$ are (conditionally) independent Poisson counting

[38] We do not model the trading motive of end-users, but we assume that they receive some hedging benefits from options.

[39] For simplicity we assume that the asset does not pay dividends or coupons. Adding payouts is straightforward.

[40] For example for a put option $\Phi(S) = \max[K - S, 0]$, for a portfolio of put and call options $\Phi(S) = \sum_i n_i^p \max[K_i - S, 0] + \sum_j n_j^c \max[S - K_j, 0]$. More generally, we assume that $\Phi(\cdot)$ is sufficiently well-behaved for the system of PDEs in Proposition 1 below to have a solution.

processes with intensity $\lambda_{y,i,j}(x_t)$.[41]

Finally, we assume that the dealer maximizes the following objective function:[42]

$$\max_{n_t,q_t} \mathbb{E}[\int_0^T dW_t - \frac{\gamma}{2}(dW_t)^2]$$
$$dW_t = rW_t dt + n_{t^-}(dS_t - rS_t dt) + q_{t^-}(dP_t - rP_t dt).$$

We define an equilibrium in the derivatives market as follows: Taking (r, S_t) as given, the derivative price $P(t, S, x, y)$ is set such that the optimal position of the dealer clears the market; that is, such that $q_t^* = \theta_t$. The resulting price is given in the following proposition:

Proposition 1. *In equilibrium, the demand-based derivative price $P(t, S, x, y)$ solves a set of coupled PDEs:*

$$\begin{aligned} 0 =& \frac{\partial}{\partial t}P(t,S,x,y) + rS\frac{\partial}{\partial S}P(t,S,x,y) + \frac{1}{2}\sigma(x)^2 S^2 \frac{\partial^2}{\partial S^2}P(t,S,x,y) - rP(t,S,x,y) \\ &+ \sum_{i,j} \mathbf{1}_{\{x=i\}} \lambda_{x,i,j} \Delta_{x,i,j} P(t,S,x,y)(1 - \gamma\,\theta(y)\Delta_{x,i,j}P(t,S,x,y)) \\ &+ \sum_{i,j} \mathbf{1}_{\{y=i\}} \lambda_{y,i,j}(x) \Delta_{y,i,j} P(t,S,x,y)(1 - \gamma\,\theta(y)\Delta_{y,i,j}P(t,S,x,y)) \end{aligned} \tag{4}$$

subject to the boundary condition $P(T, S, x, y) = \Phi(S)$ for all $x = 1, \ldots, \bar{x}$ and $y = 1, \ldots, \bar{y}$.

- *If $\sigma(x) = \bar{\sigma}\ \forall x$, then $P(t, S, x, y) = \int_{-\infty}^{+\infty} e^{-r(T-t)}\Phi(Se^{(r-\frac{\bar{\sigma}^2}{2})(T-t)+\bar{\sigma}\sqrt{T-t}\,z})\frac{e^{-\frac{z^2}{2}}}{\sqrt{2\pi}}dz$ satisfies the Black-Scholes pricing PDE and the derivative price is independent of demand.*

- *Instead, if there are (at least) two distinct volatility states ($\sigma(1) \neq \sigma(2)$) that occur*

[41] Empirically, option demand and volatility are often correlated. Therefore, we allow the transition probability in the exogenous demand to depend on the volatility state of the underlying. For parsimony, in the numerical illustration we abstract from this effect.

[42] This myopic mean-variance utility function reduces to $\max E[-e^{-\gamma W_T}]$ if the wealth process has deterministic expected return and variance. When W_t follows a more general process, then under some conditions discussed in Collin-Dufresne, Daniel, and Saglam (2020a), it can be interpreted as a 'source-dependent' recursive utility agent, who is CARA with respect to wealth-level shocks but risk-neutral with respect to shocks in the investment opportunity set (i.e., changes in the mean and volatility of wealth).

with positive probability, then the derivative price is independent of demand if and only if the representative dealer is risk-neutral. That is:

$$\{P(t,S,x,y) = P(t,S,x)\ \ \forall x,y\} \iff \{\gamma\theta(y) = 0\ \ \forall y\}.$$

Proof. See Appendix A.1 □

Note that within each volatility and demand state indexed by (x, y), the equilibrium derivative price must satisfy a Black-Scholes type PDE given by equation (4). These PDEs are interdependent as long as volatility and demand are stochastic.

Because of stochastic volatility, markets are incomplete and the risk premium on the derivative is affected by demand. As the paper focuses on delta-hedged options, the following lemma shows the risk premium on the delta-hedged derivative:

Lemma 1. *The conditional expected excess dollar return on the delta-hedged derivative is given by:*

$$\mu_V(t,S,x,y) = \gamma\,\theta(y)\left(\sum_{i,j}\mathbf{1}_{\{x=i\}}\lambda_{x,i,j}\left(\Delta_{x,i,j}P(t,S,x,y)\right)^2 + \sum_{i,j}\mathbf{1}_{\{y=i\}}\lambda_{y,i,j}(x)\left(\Delta_{y,i,j}P(t,S,x,y)\right)^2\right).$$

The expected excess return is zero if dealers are risk-neutral. Further, if dealers are risk-averse ($\gamma > 0$), then it has the same sign as the dealer's position:

$$\mu_V \gtreqless 0 \quad\iff\quad \gamma\,\theta(y) \gtreqless 0\ \ \forall y.$$

Proof. See Appendix A.2 □

7.2.2 Testable predictions

To illustrate how end-user demand affects option prices and risk premia, we consider a 3-month ATM put option. We allow for two volatility states $\sigma = \{0.1, 0.3\}$ and two demand states $\{1, 3\}$ resulting in $\theta = \{-1, -3\}$ (we assume that end-user demand is positive in both states so that dealer positions are negative), and assume constant transition intensities, $\lambda_x = 3$ and $\lambda_y = 1$.[43] We solve the system of four coupled PDEs using an explicit finite difference scheme described in Appendix A.3.

Figure 6 shows option prices (expressed in terms of implied Black-Scholes volatilities) in Panel A and expected excess delta-hedged option returns in Panel B as a function of end-user demand. Values are shown for two levels of dealer risk aversion, $\gamma = 5$ and 10, and conditional on being in the low-volatility state (the figure is qualitatively similar in the high-volatility state).[44]

Clearly, because the unconditional end-user demand is positive, the unconditional expected excess option return is negative. This is consistent with the large negative Sharpe ratios on the credit index options (Section 6.1) and the credit option residual factor (Section 6.4).

Furthermore, we can infer how variation in end-user demand affects realized and expected excess returns: an increase in demand causes an increase in the option price and, therefore, a positive contemporaneous excess return. At the same time, it causes a decrease in (that is, more negative) expected future excess return. Moreover, the option price is more sensitive to variation in demand when dealer risk aversion is higher.

When mapping these results into testable predictions regarding the credit option residual factor, it is important to recognize that we do not observe the stock of credit index options held by end-users (i.e., the total demand); rather, we observe the anonymized order flow as described in Section 7.1. To circumvent this issue, we make the identifying assumption (supported by industry publications, see above) that end-users are predominantly net buyers of credit index options in order to hedge existing credit-risk related exposures. Further, because virtually all options have short maturities, a certain "base flow" is necessary to

[43]Further, $S_0 = K = 10$ and $r = 0.05$.

[44]Naturally, option prices and expected excess returns also respond to changes in volatility. However, because we aim to explain the credit option residual factor—which is orthogonal to fundamental market volatility as captured by equity index options—we focus on the demand dimension.

maintain a given hedge exposure.[45] Under these assumptions, high daily order flow (above the base flow) is associated with an increase in end-user demand, while low daily order flow (below the base flow) is associated with a decrease.

Then, we get the following testable predictions regarding the relation between the credit option residual factor and order flow in credit index options:

1. A positive contemporaneous relation between the factor and order flow
2. The contemporaneous relation is stronger when dealers are more risk averse
3. The expected excess return on the factor is more negative following high order flow

7.3 Linking the credit option residual factor to credit option order flow

In the credit option residual factor, the IG and HY options have roughly equal weight (compare the IG and HY factor loadings in Figure 3). Therefore, to appropriately aggregate order flow, we first standardize the order flow in IG and HY options and then sum across the two (not standardizing the order flow would overweigh IG options). We focus on order flow measured in terms of the number of capped trades and trading volume.

Next, we regress the credit option residual factor on contemporaneous and lagged daily order flow. We also interact the contemporaneous order flow with the (de-meaned) intermediary capital ratio (HKM) from He, Kelly, and Manela (2017), which can be interpreted as being inversely related to dealer risk aversion in the model. Specifically, we estimate versions of the regression

$$F_t^1 = \beta^0 + (\beta^1 + \beta^2 \mathrm{HKM}_{t-1})\mathrm{flow}_t + \beta^3 \mathrm{flow}_{t-1} + u_t$$

[45] Strictly speaking, options expire only on the third Wednesday of each month, but the greeks continually change as option maturities shorten.

with lagged order flow averaged over the past two trading days. The testable predictions laid out in Section 7.2.2 map into $\beta^1 > 0$, $\beta^2 < 0$, and $\beta^3 < 0$.[46]

Table 9 reports the regression results, which are very consistent across the US and European markets. Consistent with Prediction 1, on its own, or with lagged order flow included, the coefficient on contemporaneous order flow is always positive and highly statistically significant. Consistent with Prediction 2, the coefficient on the HKM capital ratio always has the expected negative sign, although it is only statistically significant in one regression. Finally, consistent with Prediction 3, the coefficient on lagged order flow always has the expected negative sign, although it too is only statistically significant in one regression. Taken together, the results support the hypothesis that the market structure and order-flow characteristics of credit index options drive a wedge between the pricing of credit and equity index options.

8 Conclusion

We study the relative valuation of credit and equity index options. We find consistent evidence across ratings and regions that delta-hedged credit index options have very large negative Sharpe ratios—much more so than their equity index counterparts. Risk-factors extracted from equity index options have only moderate explanatory power for the time-series and cross-sectional variation in credit option returns, while a single credit-specific factor explains much of the remaining variation. We link this factor to credit-specific order flow in a manner that is consistent with the predictions of a demand-based option pricing model, in which order-flow risk is priced in equilibrium.

[46] Given that we link daily order flow to daily close-to-close returns, it is important to verify that the order flow predominantly takes place before the end-of-day prices are recorded by Markit. Figure IA6 in the Internet Appendix shows that this is indeed the case. That is, trading in options on the European (US) credit indexes predominantly takes place during European (US) trading hours.

A.1 Proof of Proposition 1

It is natural to conjecture that in the proposed equilibrium, the derivative price will be a function of the volatility and demand state variables. Specifically, we conjecture that $P(t, S_t) \equiv P(t, S_t, x_t, y_t)$. It follows that the dynamics of P can be found by Itô's formula:

$$
\begin{aligned}
dP(t) =& \mu_P(t,S,x,y)dt + \sigma_P(t,S,x,y)dZ_t + \sum_{i,j} \Delta_{x,i,j} P(t,S,x,y) \mathbf{1}_{\{x_{t-}=i\}} dN_{x,i,j} \\
&+ \sum_{i,j} \Delta_{y,i,j} P(t,S,x,y) \mathbf{1}_{\{y_{t-}=i\}} dN_{y,i,j} \qquad (5) \\
\mu_P(t,S,x,y) =& \frac{\partial}{\partial t} P(t,S,x,y) + \mu S \frac{\partial}{\partial S} P(t,S,x,y) + \frac{1}{2}\sigma(x)^2 S^2 \frac{\partial^2}{\partial S^2} P(t,S,x,y) \qquad (6) \\
\sigma_P(t,S,x,y) =& \sigma(x) S \frac{\partial}{\partial S} P(t,S,x,y) \qquad (7) \\
\Delta_{x,i,j} P(t,S,x,y) =& P(t,S,j,y) - P(t,S,i,y) \qquad (8) \\
\Delta_{y,i,j} P(t,S,x,y) =& P(t,S,x,j) - P(t,S,x,i). \qquad (9)
\end{aligned}
$$

Since the objective function of the representative dealer is myopic, we can rewrite the instantaneous objective function as

$$\max_{n_t,q_t} \mathbb{E}_t[dW_t] - \frac{\gamma}{2}\mathbb{E}_t[(dW_t)^2]$$

$$\frac{1}{dt}\mathbb{E}_t[dW_t] = rW_t + n(\mu - r)S + q\{\mu_P - rP + \sum_{i,j} \mathbf{1}_{\{x=i\}}\lambda_{x,i,j}\Delta_{x,i,j}P + \sum_{i,j} \mathbf{1}_{\{y=i\}}\lambda_{y,i,j}\Delta_{y,i,j}P\}$$

$$\frac{1}{dt}\mathbb{E}_t[(dW_t)^2] = (n\sigma S + q\sigma_P)^2 + q^2\sum_{i,j} \mathbf{1}_{\{x=i\}}\lambda_{x,i,j}(\Delta_{x,i,j}P)^2 + q^2\sum_{i,j} \mathbf{1}_{\{y=i\}}\lambda_{y,i,j}(\Delta_{y,i,j}P)^2.$$

Her first-order conditions read

$$(\mu - r)S = \gamma(nS\sigma(x) + q\sigma_P(t,S,x,y))S\sigma(x) \tag{10}$$

$$\begin{aligned}(\mu_P(t,S,x,y) - rP(t,S,x,y)) =& \gamma(nS\sigma(x) + q\sigma_P(t,S,x,y))\sigma_P(t,S,x,y) \\ &- \sum_{i,j} \mathbf{1}_{\{x=i\}}\lambda_{x,i,j}\Delta_{x,i,j}P(t,S,x,y)(1 - \gamma\, q\Delta_{x,i,j}P(t,S,x,y)) \\ &- \sum_{i,j} \mathbf{1}_{\{y=i\}}\lambda_{y,i,j}(x)\Delta_{y,i,j}P(t,S,x,y)(1 - \gamma\, q\Delta_{y,i,j}P(t,S,x,y)).\end{aligned} \tag{11}$$

In equilibrium, we have $q_t = \theta_t$, and thus we can solve for the equilibrium price by substituting the optimal position in the underlying asset from equation (10):

$$n^*S = \frac{\mu - r}{\gamma\sigma(x)^2} - \theta(y)\frac{\sigma_P(t,S,x,y)}{\sigma(x)}$$

into equation (11) along with the definitions from (6)-(9) to get the PDE (4).

A.1.1 Proof of bullet 1

Substituting the constant-volatility assumption into the PDE (4), we get

$$\frac{\partial}{\partial t}P(t,S) + rS\frac{\partial}{\partial S}P(t,S) + \frac{1}{2}\sigma^2S^2\frac{\partial^2}{\partial S^2}P(t,S) - rP(t,S) = 0$$

subject to the boundary condition $P(T,S) = \Phi(S)$. This is the Black-Scholes PDE. The solution in terms of the expectation follows from the Feynman-Kac theorem:

$$P(t, S_t) = \bar{\mathbb{E}}_t[e^{-r(T-t)}\Phi(S_T)].$$

A.1.2 Proof of bullet 2

The proof is by contradiction. Suppose that under the assumptions of the proposition, the equilibrium price were actually a function independent of the demand state; i.e., $P(t,S,x)$. Substituting into the PDE (4) we see that it should satisfy (for all values of x, y):

$$\begin{aligned} 0 =& \frac{\partial}{\partial t}P(t,S,x) + rS\frac{\partial}{\partial S}P(t,S,x) + \frac{1}{2}\sigma(x)^2S^2\frac{\partial^2}{\partial S^2}P(t,S,x) - rP(t,S,x) \\ &+ \sum_{i,j}\mathbf{1}_{\{x=i\}}\lambda_{x,i,j}\Delta_{x,i,j}P(t,S,x)(1-\gamma\,\theta(y)\Delta_{x,i,j}P(t,S,x)). \end{aligned}$$

Clearly, if $\sigma(1) \neq \sigma(2)$, then we must have that $\Delta_{x,i,j}P(t,S,x) \neq 0$ for $t < T$. Indeed, suppose instead that $P(t,S,1) = P(t,S,2) = P(t,S)$, then this implies (since the right-hand side equals zero in that case) that the same function must satisfy the Black-Scholes PDE for two distinct volatility values, a contradiction. But, if necessarily there must be a jump in the price when the volatility regime shifts, then we can rewrite the PDE simply as:

$$\frac{\frac{\partial}{\partial t}P(t,S,x) + rS\frac{\partial}{\partial S}P(t,S,x) + \frac{1}{2}\sigma(x)^2S^2\frac{\partial^2}{\partial S^2}P(t,S,x) - rP(t,S,x) + \sum_{i,j}\mathbf{1}_{\{x=i\}}\lambda_{x,i,j}\Delta_{x,i,j}P(t,S,x)}{\sum_{i,j}\mathbf{1}_{\{x=i\}}\lambda_{x,i,j}(\Delta_{x,i,j}P(t,S,x))^2} = \gamma\,\theta(y).$$

The left-hand side is independent of y, but the right hand-side is not iff $\gamma\,\theta(y) \neq 0$. The result follows.

A.2 Proof of Lemma 1

Taking expectations of (5) yields

$$\frac{1}{dt}\mathbb{E}[dP(t,S,x,y)] = \mu_P(t,S,x,y)+\sum_{i,j}\mathbf{1}_{\{x=i\}}\lambda_{x,i,j}\Delta_{x,i,j}P(t,S,x,y)+\sum_{i,j}\mathbf{1}_{\{y=i\}}\lambda_{y,i,j}\Delta_{y,i,j}P(t,S,x,y)$$

Using the expression for $\mu_P(t,S,x,y)$ in (6) and the pricing PDE (4) gives

$$\begin{aligned}\frac{1}{dt}\mathbb{E}[dP(t,S,x,y)] =& rP(t^-,S,x,y) + (\mu - r)S\frac{\partial}{\partial S}P(t,S,x,y)\\ &+\sum_{i,j}\mathbf{1}_{\{x=i\}}\lambda_{x,i,j}\gamma\,\theta(y)\left(\Delta_{x,i,j}P(t,S,x,y)\right)^2\\ &+\sum_{i,j}\mathbf{1}_{\{y=i\}}\lambda_{y,i,j}(x)\gamma\,\theta(y)\left(\Delta_{y,i,j}P(t,S,x,y)\right)^2.\end{aligned}$$

The expected excess return (in dollar terms) on the delta-hedged derivative (i.e., long one unit of the derivative and short $\frac{\partial P}{\partial S}$ units of the underlying asset) is given by

$$\mu_V = \frac{1}{dt}\mathbb{E}[dP(t,S,x,y)] - rP(t^-,S,x,y) - (\mu - r)S\frac{\partial}{\partial S}P(t,S,x,y),$$

and the result follows.

A.3 Numerical solution of the coupled system of PDEs

In order to solve the system of equation (4), we use an explicit finite difference scheme. We note that, effectively, we need to solve for four functions ($P(t,S,1,1)$, $P(t,S,1,2)$, $P(t,S,2,1)$, $P(t,S,2,2)$) that each satisfy a one-dimensional PDE and are connected through the jump terms. We can effectively solve each function on the same stock price grid, and by continuity of each of the functions (in t,S) we can approximate the jump term with the previous steps values. This makes the explicit scheme very easy to implement.

- We first make the change of variable $s = \ln S$ and define $p(t, s, x, y) = P(t, S, x, y) \equiv P(t, e^s, x, y)$.

- Substituting into the PDE (with $p_t = P_t$, $p_s = SP_S$, $p_{ss} = S^2 P_{SS} - SP_S$), we obtain the PDE to be solved:

$$
\begin{aligned}
0 = & p_t(t,s,x,y) + (r - \frac{1}{2}\sigma(x)^2)p_s(t,s,x,y) + \frac{1}{2}\sigma(x)^2 p_{ss}(t,S,x,y) - rp(t,s,x,y) \\
& + \sum_{i,j} \mathbf{1}_{\{x=i\}} \lambda_{x,i,j} \Delta_{x,i,j} p(t,s,x,y)(1 - \gamma\,\theta(y)\Delta_{x,i,j} p(t,s,x,y)) \\
& + \sum_{i,j} \mathbf{1}_{\{y=i\}} \lambda_{y,i,j}(x) \Delta_{y,i,j} p(t,s,x,y)(1 - \gamma\,\theta(y)\Delta_{y,i,j} p(t,s,x,y)).
\end{aligned}
$$

- Set $t = n \times \Delta t$ and $s = m \times \Delta s$ for some small Δt and Δs steps.

- Define $p_{xy}(n, m) = p(n \times \Delta t, m \times \Delta s, x, y)$

- Then the system of PDE can be approximated as:

$$
\begin{gathered}
0 = \tfrac{p_{xy}(n,m) - p_{xy}(n-1,m)}{\Delta t} + (r - \tfrac{1}{2}\sigma(x)^2)\tfrac{p_{xy}(n,m+1) - p_{xy}(n,m-1)}{2*\Delta s} + \\
\tfrac{1}{2}\sigma(x)^2 \tfrac{p_{xy}(n,m+1) - 2p_{xy}(n,m) + p_{xy}(n,m-1)}{\Delta s^2} - rp_{xy}(n-1,m) + \lambda_x(p_{x^+y}(n,m) - p_{xy}(n,m))(1 - \\
\gamma\theta(y)(p_{x^+y}(n,m) - p_{xy}(n,m)) + (\alpha + \beta x)(p_{xy^+}(n,m) - p_{xy}(n,m))(1 - \\
\gamma\theta(y)(p_{xy^+}(n,m) - p_{xy}(n,m))),
\end{gathered}
$$

where we denote by x^+ (y^+) the value of the volatility (demand) state after the jump from the current state x (y).

Given the "explicit scheme" approximation, we can recursively solve the value by solving the recursion:

$$
\begin{gathered}
(1 + r\Delta t)p_{xy}(n-1,m) = \\
\tfrac{1}{2}(\sigma(x)^2 \tfrac{\Delta t}{\Delta s^2} + (r - \tfrac{1}{2}\sigma(x)^2)\tfrac{\Delta t}{\Delta s})p_{xy}(n,m+1) + (1 - \sigma(x)^2 \tfrac{\Delta t}{\Delta s^2})p_{xy}(n,m) + \tfrac{1}{2}(\sigma(x)^2 \tfrac{\Delta t}{\Delta s^2} -
\end{gathered}
$$

$(r - \frac{1}{2}\sigma(x)^2)\frac{\Delta t}{\Delta s})p_{xy}(n, m-1) + \Delta t \lambda_x (p_{x^+y}(n, m) - p_{xy}(n, m))(1 - \gamma\theta(y)(p_{x^+y}(n, m) - p_{xy}(n, m)) + \Delta t(\alpha + \beta x)(p_{xy^+}(n, m) - p_{xy}(n, m))(1 - \gamma\theta(y)(p_{xy^+}(n, m) - p_{xy}(n, m)))$.

Starting from the terminal condition $p_{xy}(\frac{T}{\Delta t}, m) = \max[K - e^{m\,\Delta s}, 0]$ $\forall x, y$, we can work back through the 'trees'.

References

Ammann, Manuel, and Mathis Moerke, 2023, Credit variance risk premiums, *European Financial Management* 29, 1304–1335.

Bakshi, Gurdip, and Nikunj Kapadia, 2003, Delta-hedged gains and the negative market volatility risk premium, *The Review of Financial Studies* 16, 527–nÌf566.

Becker, Lucas, 2014, CVA hedge losses prompt focus on swaptions and guarantees, *Risk Magazine*.

Black, Fischer, and Myron S. Scholes, 1973, The pricing of options and corporate liabilities, *Journal of Political Economy* 81, 637–654.

Bollen, Nicolas P. B., and Robert E. Whaley, 2004, Does net buying pressure affect the shape of implied volatility functions?, *Journal of Finance* 59, 711–753.

Broadie, Mark, Mikhail Chernov, and Michael Johannes, 2009, Understanding index option returns, *The Review of Financial Studies* 22, 4493–4529.

Buchner, Matthias, and Bryan Kelly, 2022, A factor model for option returns, *Journal of Financial Economics* 143, 1140–1161.

Carr, Peter, and Liuren Wu, 2007, Stochastic skew in currency options, *Journal of Financial Economics* 86, 213–247.

———, 2020, Option Profit and Loss Attribution and Pricing: A New Framework, *Journal of Finance* 75, 2271–2316.

Castagna, Antonio, and Fabio Mercurio, 2007, The vanna-volga method for implied volatilities: tractability and robustness, *Risk Magazine* January, 106–111.

CFTC, 2024, Post-initial appropriate minimum block sizes and post-initial cap sizes for publicly reportable swap transactions, Available at: `https://www.cftc.gov`.

Chen, Hui, Scott Joslin, and Sophie Ni, 2019, Demand for crash insurance, intermediary constraints, and risk premia in financial markets, *Review of Financial Studies* 32, 228–265.

Chen, Long, Pierre Collin-Dufresne, and Robert S. Goldstein, 2009, On the relation between the credit spread puzzle and the equity premium puzzle, *Review of Financial Studies* 22, 3367–3409.

Chen, Steven Shu-Hsiu, Hitesh Doshi, and Sang Byung Seo, 2023, Synthetic options and implied volatility for the corporate bond market, *Journal of Financial and Quantitative Analysis* 58, 1295–1325.

Collin-Dufresne, Pierre, Kent Daniel, and Mehmet Saglam, 2020a, Liquidity regimes and optimal dynamic asset allocation, *Journal of Financial Economics* 136, 379–406.

Collin-Dufresne, Pierre, Benjamin Junge, and Anders B. Trolle, 2020b, Market structure and transaction costs of index CDSs, *Journal of Finance* 75, 2719–2763.

———, 2024, How integrated are credit and equity markets? Evidence from index options, *Journal of Finance* 79, 949–992.

Constantinides, George M., Jens Carsten Jackwerth, and Alexi Savov, 2013, The puzzle of index option returns, *The Review of Asset Pricing Studies* 3, 229–257.

Coval, Joshua D., and Tyler Shumway, 2001, Expected option returns, *Journal of Finance* 56, 983–1009.

Cremers, Martijn, Joost Driessen, and Pascal Maenhout, 2008, Explaining the level of credit spreads: Option-implied jump risk premia in a firm value model, *Review of Financial Studies* 21, 2209–2242.

Cremers, Martijn, Michael Halling, and David Weinbaum, 2015, Aggregate jump and volatility risk in the cross-section of stock returns, *Journal of Finance* 70, 577–614.

Culp, Christopher L., Yoshio Nozawa, and Pietro Veronesi, 2018, Option-based credit spreads, *American Economic Review* 108, 454–488.

Dew-Becker, Ian, and Stefano Giglio, 2023, Risk preferences implied by synthetic options, Working paper, Northwestern University.

Dew-Becker, Ian, Stefano Giglio, and Bryan Kelly, 2021, Hedging macroeconomic and financial uncertainty and volatility, *Journal of Financial Economics* 142, 23–45.

Doshi, Hitesh, Jan Ericsson, Mathieu Fournier, and Sang Byung Seo, 2024, The Risk and Return of Equity and Credit Index Options, *Journal of Financial Economics* 161.

Du, Du, Redouane Elkamhi, and Jan Ericsson, 2019, Time-varying asset volatility and the credit spread puzzle, *Journal of Finance* 74, 1841–1885.

Duarte, Jefferson, Christopher S. Jones, Mehdi Khorram, Haitao Mo, and Junbo L. Wang, 2023, Too good to be true: Look-ahead bias in empirical options research, Working paper, Rice University.

Durrleman, Valdo, 2010, From implied to spot volatilities, *Finance and Stochastics* 14, 157–177.

Fama, Eugene F., and Kenneth R. French, 2015, A five-factor asset pricing model, *Journal of Financial Economics* 115, 1–55.

Fournier, Mathieu, Kris Jacobs, and Piotr Orlowski, 2024, Modeling conditional factor risk premia implied by index option returns, *Journal of Finance* 79, 2289–2338.

Friewald, Nils, and Florian Nagler, 2019, Over-the-counter market frictions and yield spread changes, *Journal of Finance* 74, 3217–3257.

Gârleanu, Nicolae, Lasse H. Pedersen, and Allen M. Poteshman, 2009, Demand-based option pricing, *Review of Financial Studies* 22, 4259–4299.

Gibbons, Michael R., Stephen A. Ross, and Jay Shanken, 1989, A test of the efficiency of a given portfolio, *Econometrica* 57, 1121–1152.

He, Zhiguo, Bryan Kelly, and Asaf Manela, 2017, Intermediary asset pricing: New evidence from many asset classes, *Journal of Financial Economics* 126, 1–35.

He, Zhiguo, Paymon Khorrami, and Zhaogang Song, 2022, Commonality in credit spread changes: Dealer inventory and intermediary distress, *Review of Financial Studies* 35, 4630–4673.

Henderson, Vicky, and David Hobson, 2009, Utility indifference pricing: An overview, in René Carmona, ed.: *Indifference Pricing: Theory and Applications*, 44–74 (Princeton University Press).

Horenstein, Alex, Aurelio Vasquez, and Xiao Xiao, 2023, Common factors in equity option returns, Working Paper: University of Miami.

Huang, Jing-Zhi, and Ming Huang, 2012, How much of the corporate-Treasury yield spread is due to credit risk?, *Review of Asset Pricing Studies* 2, 153–202.

Hugonnier, Julien, Dimitri Kramkov, and Walter Schachermayer, 2005, On utility based pricing of contingent claims in incomplete markets, *Mathematical Finance* 15, 203–212.

Jones, Christopher S., 2006, A nonlinear factor analysis of S&P 500 index option returns, *Journal of Finance* 61, 2325–23633.

Jones, Philip E., Scott P. Mason, and Eric Rosenfeld, 1984, Contingent claims analysis of corporate capital structures: An empirical investigation, *Journal of Finance* 39, 611–25.

Kapadia, Nikunj, and Xiaoling Pu, 2012, Limited arbitrage between equity and credit markets, *Journal of Financial Economics* 105, 542–564.

Kozak, Serhiy, Stefan Nagel, and Shrihari Santosh, 2018, Interpreting factor models, *Journal of Finance* 73, 1183–1223.

Ledoit, Olivier, and Pedro Santa-Clara, 1998, Relative pricing of options with stochastic volatility, Working paper, UCLA.

Masabathula, Srichandra, and Nicholas Godec, 2023, Credit VIX: A new tool for measuring and managing credit risk, S&P Global.

Merton, Robert C., 1974, On the pricing of corporate debt: The risk structure of interest rates, *Journal of Finance* 29, 449–470.

Newey, Whitney K., and Kenneth D. West, 1987, A simple, positive semi-definite, heteroskedasticity and autocorrelation consistent covariance matrix, *Econometrica* 55, 703–708.

Rega-Jones, Natasha, 2020, CVA desks arm themselves for the next crisis, *Risk Magazine*.

Santa-Clara, Pedro, and Alessio Saretto, 2009, Option strategies: Good deals and margin calls, *Journal of Financial Markets* 12, 391–417.

Stambaugh, Robert F., and Yu Yuan, 2017, Mispricing factors, *The Review of Financial Studies* 30, 1270–1315.

Tipping, Michael E., and Christopher M. Bishop, 1999, Probabilistic principal component analysis, *Journal of the Royal Statistical Society* 61, 611–622.

	Calls			Puts			Δ-hedged calls			Δ-hedged puts		
	EQ	IG	L-S	EQ	IG	L-S	EQ	IG	L-S	EQ	IG	L-S
Panel A: Exposures												
Asset delta	4.24	3.00	1.24	-3.56	-2.74	-0.82	0.24	0.12	0.12	0.24	0.12	0.12
Asset gamma	0.71	0.39	0.33	0.87	0.81	0.06	0.79	0.60	0.19	0.79	0.60	0.20
Asset vega	0.98	-0.55	1.53	0.92	2.23	-1.31	0.95	0.85	0.09	0.95	0.84	0.11
Panel B: Finite-sample distributions of mean excess returns												
Mean	1.03	1.46	-0.43	-1.89	-2.29	0.40	-0.47	-0.42	-0.05	-0.46	-0.42	-0.04
2.5th %tile	-1.29	-0.48	-1.25	-4.52	-4.79	-0.25	-1.29	-1.13	-0.29	-1.32	-1.10	-0.30
97.5th %tile	3.32	3.32	0.40	0.84	0.29	1.06	0.33	0.26	0.19	0.35	0.24	0.22
Panel C: Sharpe ratios												
Std.dev.	3.85	3.44	1.39	4.72	4.86	1.21	1.38	1.22	0.38	1.41	1.17	0.42
SR	0.27	0.43	-0.31	-0.41	-0.48	0.33	-0.35	-0.35	-0.17	-0.34	-0.37	-0.13

Table 1: Simulated Option Exposures and Risk-Return Trade-Off
Simulations of daily excess returns on equity and credit (investment-grade) index options are based on the model in Collin-Dufresne et al. (2024) with parameter estimates from Doshi et al. (2024). The options are 1-month ATM puts and calls. Returns are for outright options and delta-hedged options, where the delta is with respect to the underlying index and computed using the Black-Scholes model. Results are reported for equity and credit options separately, and for a long-equity/short-credit option strategy. Panel A reports the factor exposures defined as the coefficients from regressing option excess returns on asset excess returns (delta), returns squared (gamma), and changes in asset volatility (vega). The factor exposures are normalized to reflect a one standard derivation change in each of the risk factors. Panel B reports the finite-sample distributions of mean excess returns obtained from 10,000 simulations of 10-years of daily returns (2520 observations). Mean returns are annualized. Panel C reports the annualized volatilities and Sharpe ratios (SR).

	IG				HY				EQ			
	-2	-1	0	1	-2	-1	0	1	-2	-1	0	1
Panel A: US market												
Mean	**-3.78**	**-2.83**	**-1.28**	**-3.23**	**-4.87**	**-3.36**	**-1.54**	**-3.72**	**-2.15**	**-1.36**	-0.43	-0.55
	(-5.86)	(-5.58)	(-4.98)	(-3.74)	(-7.90)	(-5.91)	(-5.01)	(-3.27)	(-2.31)	(-2.41)	(-1.73)	(-0.35)
Std.dev.	1.55	1.19	0.63	2.73	1.59	1.22	0.63	2.74	2.35	1.55	0.74	3.86
SR	-2.44	-2.39	-2.04	-1.18	-3.06	-2.75	-2.46	-1.36	-0.91	-0.88	-0.59	-0.14
Skew	3.30	3.45	2.71	1.47	3.99	3.26	1.95	2.08	5.58	3.92	2.45	2.58
Kurt	28.6	31.8	23.9	10.0	55.0	33.6	30.6	16.5	65.4	37.1	17.0	21.0
N obs	2513	2530	2528	2510	2449	2508	2518	2499	2560	2560	2560	2560
Panel B: European market												
Mean	**-3.90**	**-2.50**	**-1.05**	**-3.37**	**-3.59**	**-2.71**	**-1.15**	**-3.55**	-0.64	-0.58	-0.14	0.43
	(-6.98)	(-4.94)	(-3.98)	(-3.29)	(-4.69)	(-4.77)	(-4.22)	(-3.53)	(-0.69)	(-1.04)	(-0.52)	(0.32)
Std.dev.	1.60	1.21	0.64	2.65	1.76	1.29	0.63	2.32	2.43	1.60	0.75	3.35
SR	-2.43	-2.07	-1.64	-1.27	-2.03	-2.11	-1.84	-1.53	-0.26	-0.37	-0.18	0.13
Skew	3.76	3.26	3.41	3.39	4.23	3.72	3.05	2.90	5.48	3.76	2.91	2.74
Kurt	33.3	24.6	27.0	35.7	38.3	30.0	22.7	29.4	65.2	32.6	21.7	20.1
N obs	2444	2532	2536	2516	2334	2499	2508	2470	2547	2547	2547	2547

Table 2: Performance of Option Portfolios Sorted on Moneyness
Summary statistics of daily excess returns on option portfolios sorted on moneyness. Means, standard deviations, and Sharpe ratios ("SR") are annualized. t-statistics in parentheses are corrected for heteroscedasticity and serial correlation up to 63 lags (equal to three months) using the approach of Newey and West (1987). Mean estimates that are significant at the 5% level are highlighted in bold. Sample period is from January 1, 2013 to April 3, 2023.

	EQ-IG				EQ-HY			
	-2	-1	0	1	-2	-1	0	1
Panel A: US market								
Mean	**1.78**	**1.45**	**0.85**	**2.27**	**2.58**	**2.07**	**1.12**	**2.84**
	(2.83)	(3.91)	(4.38)	(2.33)	(3.88)	(4.89)	(5.29)	(3.34)
Std.dev.	2.31	1.50	0.73	3.55	2.23	1.50	0.74	3.46
SR	0.77	0.97	1.15	0.64	1.16	1.37	1.51	0.82
Skew	3.39	1.24	0.13	0.66	3.50	1.60	0.74	0.38
Kurt	59.8	32.6	11.7	10.3	64.7	35.4	16.1	9.0
N obs	2513	2530	2528	2510	2449	2508	2518	2499
Panel B: European market								
Mean	**3.31**	**2.11**	**1.03**	**4.13**	**3.34**	**2.36**	**1.14**	**4.12**
	(5.28)	(4.66)	(4.36)	(3.46)	(4.47)	(5.42)	(5.32)	(4.34)
Std.dev.	2.22	1.53	0.76	3.30	2.20	1.51	0.73	3.04
SR	1.49	1.38	1.35	1.25	1.52	1.57	1.55	1.36
Skew	2.50	1.08	0.36	0.36	1.93	1.09	0.82	1.84
Kurt	29.8	12.2	10.0	28.4	25.4	13.8	12.0	20.6
N obs	2418	2509	2513	2492	2305	2476	2485	2444

Table 3: Performance of Long-Short Option Portfolios Sorted on Moneyness
Summary statistics of daily excess returns on short credit vs. long equity option portfolios sorted on moneyness. Means, standard deviations, and Sharpe ratios ("SR") are annualized. t-statistics in parentheses are corrected for heteroscedasticity and serial correlation up to 63 lags (equal to three months) using the approach of Newey and West (1987). Mean estimates that are significant at the 5% level are highlighted in bold. Sample period is from January 1, 2013 to April 3, 2023.

	GMA			VGA			VNA			VLG		
	IG	HY	EQ	IG	HY	EQ	IG	HY	EQ	IG	HY	EQ
Panel A: US market												
Mean	**-0.64**	**-0.71**	-0.19	**-0.21**	**-0.32**	-0.11	**-1.35**	**-1.88**	**-0.99**	-0.15	0.14	-0.25
	(-4.77)	(-4.84)	(-1.42)	(-2.93)	(-4.15)	(-1.59)	(-4.80)	(-7.98)	(-3.37)	(-1.00)	(0.98)	(-1.67)
Std.dev.	0.39	0.41	0.45	0.22	0.22	0.19	0.81	0.71	0.89	0.44	0.45	0.38
SR	-1.66	-1.71	-0.42	-0.93	-1.46	-0.58	-1.66	-2.65	-1.11	-0.33	0.31	-0.67
Skew	1.58	3.43	2.97	0.05	0.75	1.17	0.50	-0.39	0.96	-0.43	7.73	2.64
Kurt	10.6	35.1	25.8	11.8	12.9	13.3	10.3	13.3	55.8	9.3	216.5	32.9
N obs	2521	2504	2560	2521	2504	2560	2508	2483	2560	2501	2482	2560
Panel B: European market												
Mean	**-0.60**	**-0.71**	-0.02	-0.12	**-0.14**	-0.03	**-0.84**	**-1.05**	-0.55	-0.16	-0.04	-0.08
	(-4.65)	(-5.79)	(-0.14)	(-1.69)	(-2.10)	(-0.60)	(-2.51)	(-3.36)	(-1.85)	(-1.55)	(-0.41)	(-0.69)
Std.dev.	0.43	0.37	0.43	0.22	0.22	0.16	0.77	0.72	0.81	0.42	0.40	0.27
SR	-1.41	-1.95	-0.04	-0.53	-0.63	-0.21	-1.09	-1.46	-0.67	-0.38	-0.11	-0.28
Skew	5.77	2.11	2.86	-0.42	1.08	0.98	-0.89	0.04	1.59	3.80	0.82	0.61
Kurt	99.4	17.6	19.7	28.2	13.8	10.4	41.5	8.1	43.1	87.0	23.7	15.4
N obs	2521	2461	2547	2521	2461	2547	2510	2459	2547	2510	2445	2547

Table 4: Performance of Factor-Mimicking Portfolios
Summary statistics of daily excess returns on factor-mimicking portfolios. Means, standard deviations, and Sharpe ratios ("SR") are annualized. t-statistics in parentheses are corrected for heteroscedasticity and serial correlation up to 63 lags (equal to three months) using the approach of Newey and West (1987). Mean estimates that are significant at the 5% level are highlighted in bold. Sample period is from January 1, 2013 to April 3, 2023.

	GMA		VGA		VNA		VLG	
	EQ-IG	EQ-HY	EQ-IG	EQ-HY	EQ-IG	EQ-HY	EQ-IG	EQ-HY
				Panel A: US market				
Mean	**0.64**	**0.74**	0.09	**0.22**	0.51	**1.18**	0.11	-0.29
	(3.89)	(4.85)	(1.45)	(2.96)	(1.57)	(3.41)	(0.46)	(-1.42)
Std.dev.	0.54	0.49	0.26	0.26	1.33	1.14	0.75	0.67
SR	1.19	1.51	0.35	0.84	0.38	1.03	0.14	-0.43
Skew	0.45	1.27	0.09	-0.32	0.08	1.43	1.70	-0.27
Kurt	16.5	18.2	11.8	13.0	29.8	25.0	22.4	76.1
N obs	2521	2504	2521	2504	2508	2483	2501	2482
				Panel B: European market				
Mean	**0.75**	**0.81**	0.10	**0.12**	0.26	0.46	0.24	0.19
	(5.17)	(6.49)	(1.60)	(2.12)	(0.68)	(1.26)	(1.35)	(1.13)
Std.dev.	0.54	0.45	0.25	0.24	1.21	1.05	0.70	0.66
SR	1.38	1.79	0.41	0.48	0.22	0.44	0.34	0.28
Skew	-3.05	1.04	0.57	-0.25	1.29	-0.13	-8.24	0.74
Kurt	91.7	10.8	19.3	11.2	46.5	10.3	240.0	58.0
N obs	2494	2436	2494	2436	2486	2433	2486	2419

Table 5: Performance of Long-Short Factor-Mimicking Portfolios
Summary statistics of daily excess returns on short credit vs. long equity factor-mimicking portfolios. Means, standard deviations, and Sharpe ratios ("SR") are annualized. t-statistics in parentheses are corrected for heteroscedasticity and serial correlation up to 63 lags (equal to three months) using the approach of Newey and West (1987). Mean estimates that are significant at the 5% level are highlighted in bold. Sample period is from January 1, 2013 to April 3, 2023.

	IG	HY	EQ
	Panel A: US market		
Max SR, options	2.94	3.28	1.72
Max SR, factors	2.77	3.64	1.37
Max SR, options+factors	3.05	3.95	1.87
GRS p-value	0.03	0.00	0.02
Average $\|\alpha\|$	0.14	0.27	0.27
Average $\|t\|$	0.53	0.90	0.95
Average R^2	0.82	0.87	0.93
N obs	2447	2382	2560
	Panel B: European market		
Max SR, options	3.62	3.14	1.65
Max SR, factors	2.75	2.66	1.15
Max SR, options+factors	3.75	3.48	1.78
GRS p-value	0.00	0.00	0.03
Average $\|\alpha\|$	0.41	0.29	0.27
Average $\|t\|$	1.52	0.99	1.01
Average R^2	0.89	0.89	0.94
N obs	2341	2118	2152

Table 6: Performance of Index-Specific Factor Pricing Models
The table reports the maximum Sharpe ratio of the option portfolios, the index-specific factors (IDX, GMA, VGA, VNA, and VLG), and the options and factors jointly; the p-value of the Gibbons et al. (1989) test of the alphas from the index-specific factor model being jointly zero; the average (across option portfolios) of the absolute alphas, absolute t-statistics, and R^2s; and the number of daily observations. Alphas are annualized and t-statistics are corrected for heteroscedasticity and serial correlation up to 63 lags (equal to three months) using the approach of Newey and West (1987). Sample period is from January 1, 2013 to April 3, 2023.

	Average $\|\alpha\|$		Average $\|t\|$		Average R^2	
	IG	HY	IG	HY	IG	HY
Panel A: US market						
mdl1	1.66	2.30	3.57	4.41	0.26	0.27
mdl1+F_t^1	0.67	0.98	2.03	2.72	0.73	0.74
mdl1+F_t^1+F_t^2	0.62	0.86	2.11	2.54	0.79	0.82
mdl2	1.61	2.31	3.38	4.52	0.27	0.29
mdl2+F_t^1	0.71	0.92	2.00	2.80	0.73	0.74
mdl2+F_t^1+F_t^2	0.67	0.81	2.16	2.66	0.79	0.82
mdl3	1.56	2.23	3.45	4.58	0.28	0.31
mdl3+F_t^1	0.71	0.92	2.04	2.79	0.74	0.74
mdl3+F_t^1+F_t^2	0.71	0.81	2.30	2.74	0.79	0.83
Panel B: European market						
mdl1	2.28	2.41	5.26	5.27	0.28	0.30
mdl1+F_t^1	0.68	0.45	2.39	1.87	0.81	0.79
mdl1+F_t^1+F_t^2	0.47	0.48	2.37	2.85	0.85	0.87
mdl2	2.25	2.38	5.17	5.38	0.29	0.31
mdl2+F_t^1	0.68	0.49	2.35	2.09	0.81	0.80
mdl2+F_t^1+F_t^2	0.48	0.53	2.30	3.13	0.85	0.88
mdl3	2.29	2.34	5.34	5.18	0.30	0.32
mdl3+F_t^1	0.66	0.50	2.29	2.11	0.81	0.80
mdl3+F_t^1+F_t^2	0.47	0.54	2.24	3.14	0.85	0.88

Table 7: Performance of Equity-Based Factor Models on Credit Options
The equity-based model with five factors (IDX, GMA, VGA, VNA, and VLG) is applied to the pricing of credit index options. Three versions are considered: the unconditional model (*mdl1*), a conditional version where factor exposures of credit option portfolios are conditioned on their greeks (*mdl2*), and a conditional version where factor exposures of credit option portfolios are conditioned on both their greeks and implied volatility (*mdl3*). To each equity-based model, one or two residual factors (F_t^1, F_t^2) constructed from the unexplained credit option portfolio returns are added sequentially. For each credit index, the table reports the average (across option portfolios) of the absolute alphas, absolute t-statistics, and R^2s. Alphas are annualized. t-statistics are corrected for heteroscedasticity and serial correlation up to 63 lags (equal to three months) using the approach of Newey and West (1987). Sample period is from January 1, 2013 to April 3, 2023.

	IG			HY		
	N trades	N capped	Volume	N trades	N capped	Volume
	Panel A: US market					
Mean	18.67	11.93	1.55	14.89	4.91	0.96
5th pcntile	3	2	0.25	2	0	0.10
Median	15	10	1.35	13	4	0.82
95th pcntile	40	28	3.49	34	14	2.30
	Panel B: European market					
Mean	10.87	7.30	0.79	6.24	2.57	0.37
5th pcntile	1	1	0.09	0	0	0.00
Median	8	6	0.64	5	2	0.27
95th pcntile	24	18	2.05	17	9	1.10

Table 8: Daily Order-Flow in Credit Index Options
Summary statistics of daily order flow in credit index options. Order-flow is measured in terms of number of trades, number of capped trades (i.e., where the notional amount of the underlying swap is above the reporting cap), and trading volume in billions (USD in US market and EUR in European market). Sample period is from January 1, 2013 to April 3, 2023.

	N capped			Volume		
	Panel A: US market					
Flow	**0.026**	**0.029**	**0.029**	**0.023**	**0.026**	**0.028**
	(3.322)	(3.847)	(4.295)	(3.194)	(3.633)	(4.294)
Flow × HKM	—	**-0.721**	—	—	-0.611	—
	—	(-1.979)	—	—	(-1.847)	—
Lagged flow	—	—	-0.008	—	—	-0.009
	—	—	(-0.857)	—	—	(-0.987)
R^2	0.016	0.019	0.017	0.015	0.018	0.016
N obs	2547	2547	2545	2547	2547	2545
	Panel B: European market					
Flow	**0.038**	**0.038**	**0.041**	**0.031**	**0.031**	**0.039**
	(4.460)	(4.483)	(5.752)	(3.930)	(3.938)	(5.934)
Flow × HKM	—	-0.603	—	—	-0.469	—
	—	(-1.334)	—	—	(-0.931)	—
Lagged flow	—	—	-0.009	—	—	**-0.018**
	—	—	(-1.191)	—	—	(-2.812)
R^2	0.030	0.031	0.031	0.023	0.023	0.027
N obs	2509	2456	2508	2509	2456	2508

Table 9: Regression of Credit Option Residual Factor on Order Flow
In each market, the credit option residual factor is regressed on credit option order flow. Frequency is daily. The residual factor is the first principal component of residuals from applying the equity-based factor model to the credit option portfolios. The independent variables are contemporaneous order flow, contemporaneous order flow interacted with the de-meaned HKM intermediary capital ratio, and order flow averaged over the past two trading days. Order-flow is measured as either number of capped trades (i.e., where the notional amount of the underlying swap is above the reporting cap) or trading volume, and is first standardized for each index and then summed over IG and HY. t-statistics in parentheses are corrected for heteroscedasticity and serial correlation up to 63 lags (equal to three months) using the approach of Newey and West (1987). Sample period is from January 1, 2013 to April 3, 2023.

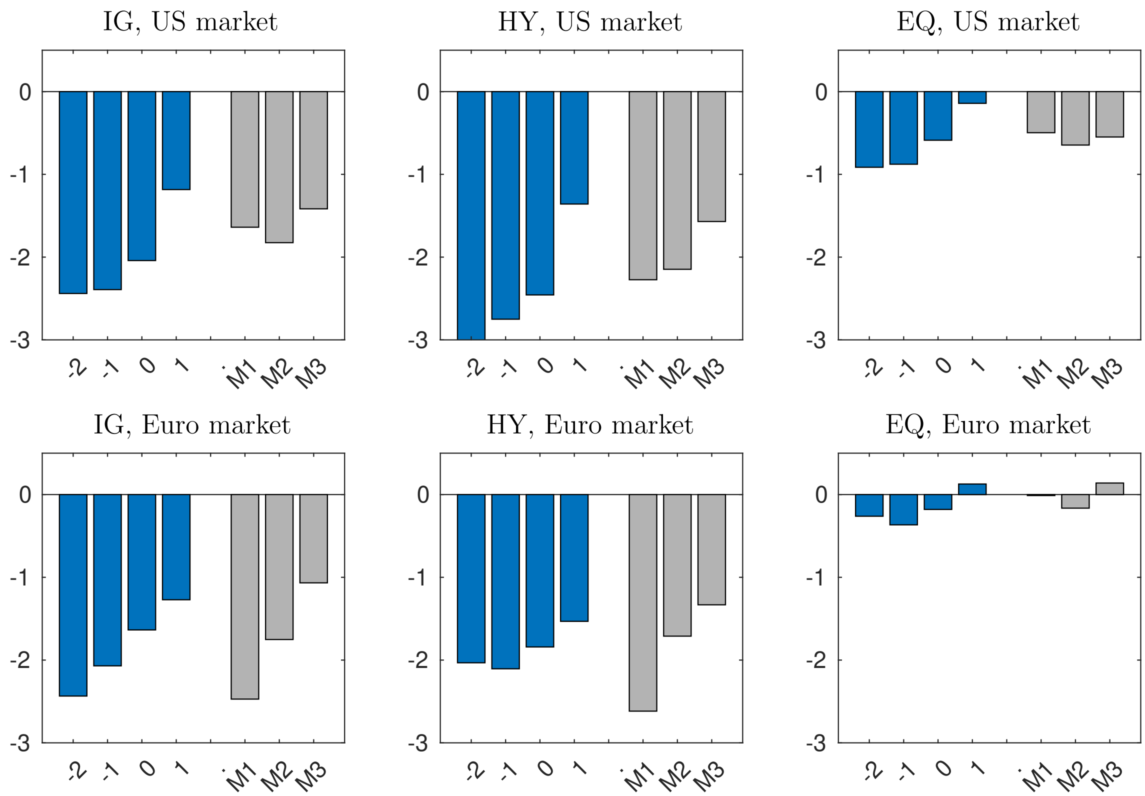

Figure 1: Performance of Option Portfolios, Sharpe Ratios
Annualized Sharpe ratios of option portfolios sorted on moneyness and maturity. -2, -1, 0, 1 refer to moneyness, m, defined in (3). M1, M2, and M3 refer to 1, 2, and 3 month options. Top panels are for the US market and bottom panels are for the European market. Left, middle, and right panels are for IG, HY, and EQ indexes, respectively. Returns are daily. Sample period is from January 1, 2013 to April 3, 2023.

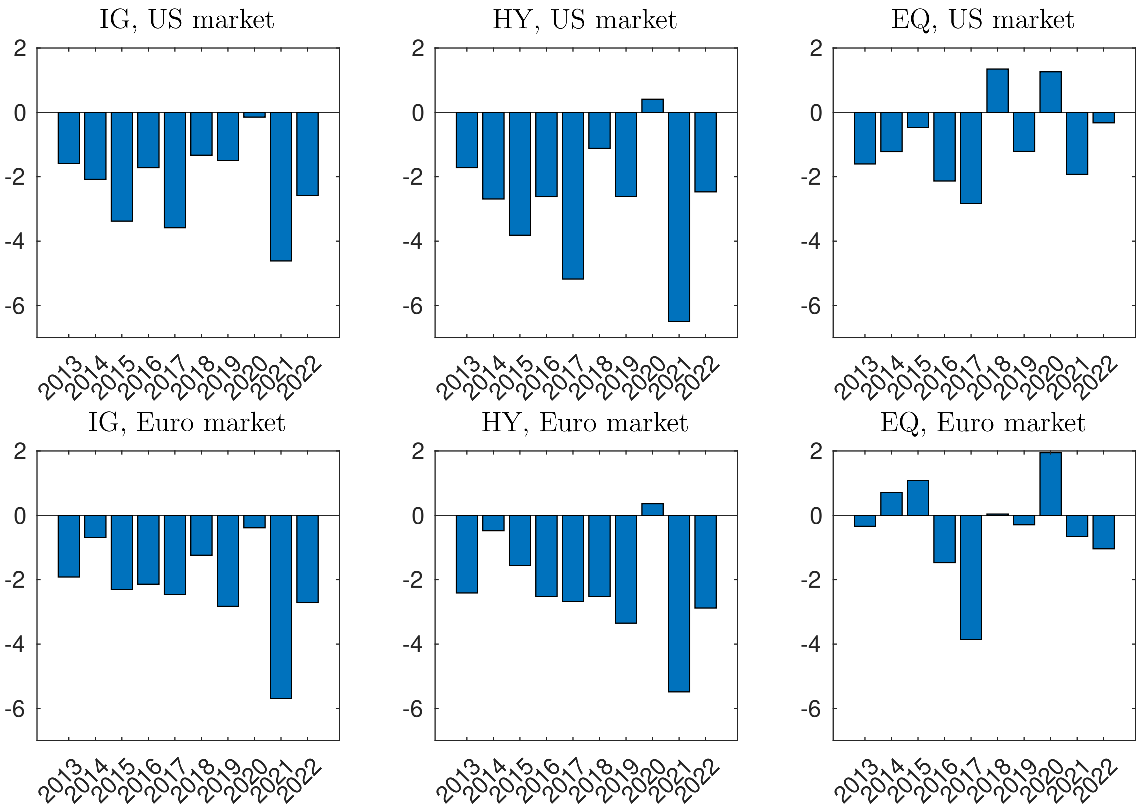

Figure 2: Average Sharpe Ratios on Option Portfolios per Year
For every full year in the sample: First, using daily returns, compute annualized Sharpe ratios on option portfolios sorted on moneyness and maturity (seven portfolios per index). Second, average the Sharpe ratios across portfolios. Top panels are for the US market and bottom panels are for the European market. Left, middle, and right panels are for IG, HY, and EQ indexes, respectively.

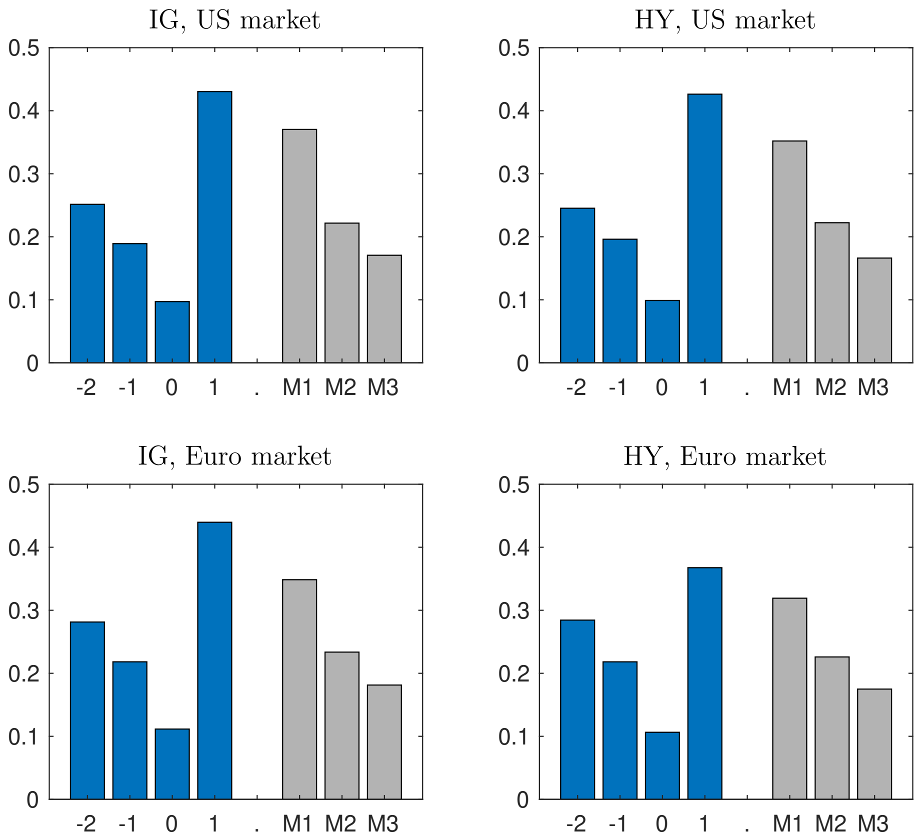

Figure 3: Loadings on Main Credit Option Residual Factor
In each market, the equity-based factor model is applied to the 14 credit option portfolios (two credit indexes, each with seven portfolios sorted on moneyness and maturity) and a principal component analysis (PCA) is applied to the residuals. -2, -1, 0, 1 refer to moneyness, m, defined in (3). M1, M2, and M3 refer to 1, 2, and 3 month options. The top (bottom) panels show the portfolio loadings on the first PC in the US (European) market. The left (right) panels are for the IG (HY) indexes.

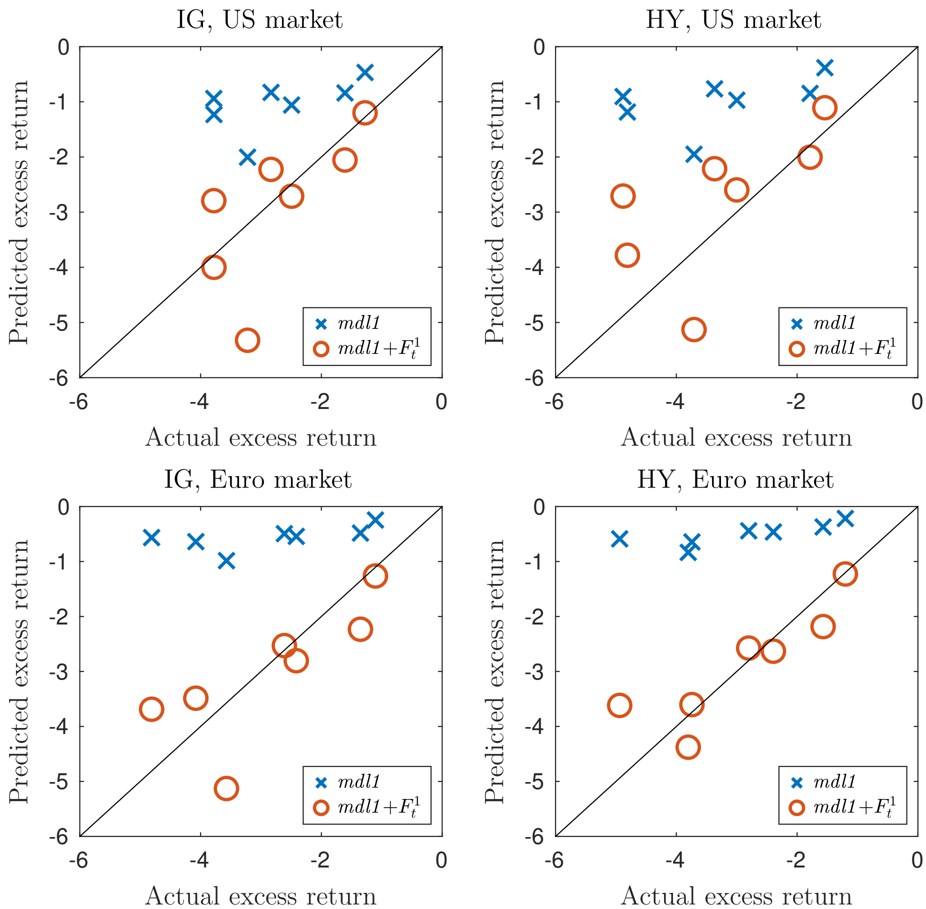

Figure 4: Fit of Equity-Based Factor Model to Credit Options
Predicted mean excess returns on credit option portfolios versus actual mean excess returns. Predicted returns are obtained from the risk exposures in two models: *mdl1* refers to the unconditional equity-based factor model and *mdl1*+F_t^1 refers to that model with the credit option residual factor added. The distance from the 45-degree line represents the alphas. The top (bottom) panels show results for the US (European) market. The left (right) panels are for the IG (HY) index options.

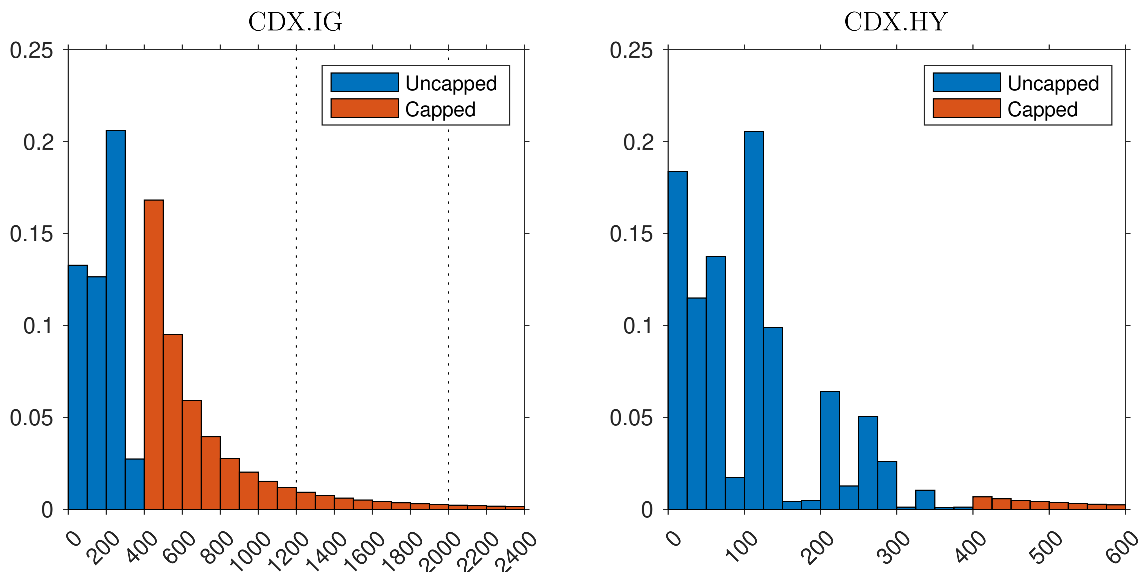

Figure 5: Empirical Distribution of Trade Sizes in US Credit Index Options
The figure shows the trade-size distributions for CDX.IG (left panel) and CDX.HY (right panel) options based on data from October 7, 2024 to June 13, 2025. We assume a Pareto distribution for capped trades with an estimated parameter of 1.81 (1.83) for CDX.IG (CDX.HY) options. Data consists of 4119 (3914) CDX.IG (CDX.HY) options of which 50.7% (6.5%) are capped. Trade size refers to the notional value of the underlying swap measured in million USD. The vertical dotted lines for CDX.IG mark the 67th and 75th percentiles of the notional-weighted size distribution as computed in CFTC (2024).

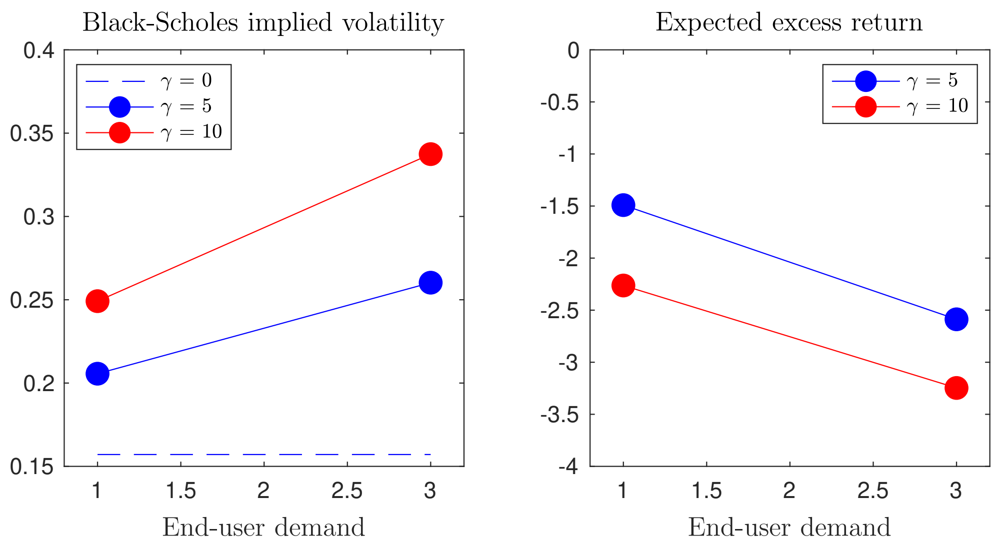

Figure 6: Illustration of Demand-Based Option Pricing Model
Implied volatility (left panel) and expected excess delta-hedged option return (right panel) for a 3-month ATM put option. The model has two volatility states $\sigma = \{0.1, 0.3\}$, two demand states resulting in $\theta = \{-1, -3\}$, and transition intensities $\lambda_x = 3$ and $\lambda_y = 1$. Further, $S_0 = K = 10$ and $r = 0.05$. Implied volatility and risk premia are shown for two levels of dealer risk aversion, $\gamma = 5$ and 10, and conditional on being in the low-volatility state.

Internet Appendix to:

Pricing of risk in credit and equity index options—
A role for option order flow?

IA.1 Return computations

We show how to mark-to-market an option when there are defaults in the underlying index. Consider a credit index put option at time t with expiration T, strike K^S, and price

$$\mathcal{P}_t(T, K^S) = \mathbb{E}_t^{\mathbb{Q}}\left[e^{-\int_t^T r_s ds}\left(K^S - S_T\right)^+\right].$$

Suppose that one of the index constituents defaults between t and $t+\Delta$. In this case, options on the series' original version are no longer quoted; only options on the series' new version are quoted. However, we can express the former in terms of the latter. Specifically, if the loss rate on the defaulted name is ℓ, we have that

$$\begin{aligned}
\mathcal{P}_{t+\Delta}(T, K^S) &= \mathbb{E}_{t+\Delta}^{\mathbb{Q}}\left[e^{-\int_{t+\Delta}^T r_s ds}\left(K^S - S_T\right)^+\right] \\
&= \mathbb{E}_{t+\Delta}^{\mathbb{Q}}\left[e^{-\int_{t+\Delta}^T r_s ds}\left(K^S - \left(\frac{N_T}{N_t}\tilde{S}_T + \frac{1}{N_t}\sum_{i=1}^{N_t - N_T}(1-\ell_i)\right)\right)^+\right] \\
&= \mathbb{E}_{t+\Delta}^{\mathbb{Q}}\left[e^{-\int_{t+\Delta}^T r_s ds}\left(K^S - \frac{1}{N_t}(1-\ell) - \left(\frac{N_T}{N_t}\tilde{S}_T + \frac{1}{N_t}\sum_{i=1}^{N_{t+\Delta} - N_T}(1-\ell_i)\right)\right)^+\right] \\
&= \frac{N_t - 1}{N_t} \times \mathbb{E}_{t+\Delta}^{\mathbb{Q}}\left[e^{-\int_{t+\Delta}^T r_s ds}\left(\frac{N_t}{N_t - 1}\left(K^S - \frac{1}{N_t}(1-\ell)\right) - \right.\right. \\
&\qquad \left.\left.\left(\frac{N_T}{N_{t+\Delta}}\tilde{S}_T + \frac{1}{N_{t+\Delta}}\sum_{i=1}^{N_{t+\Delta} - N_T}(1-\ell_i)\right)\right)^+\right] \\
&= \frac{N_t - 1}{N_t} \times \tilde{\mathcal{P}}_{t+\Delta}\left(T, \frac{N_t}{N_t - 1}\left(K^S - \frac{1}{N_t}(1-\ell)\right)\right),
\end{aligned}$$

where $\tilde{\mathcal{P}}$ denotes the price of an option on the series' new version. Therefore, at time $t+\Delta$, the value of the original option with strike K^S is given by $\frac{N_t-1}{N_t}$ times the value of an option on the series' new version with strike $\tilde{K}^S = \frac{N_t}{N_t-1}\left(K^S - \frac{1}{N_t}(1-\ell)\right)$.

In our empirical analyses, we always use actual quoted strikes. However, in this particular case, we need to use interpolation to get the correct option price.

Example 1. *In our dataset, the index series that has the most defaults while being on the run is CDX.HY Series 34, see Table IA.3. Version 1 of Series 34 (S34.V1) with 100 names is launched on March 20, 2020. On April 1, 2020, index member Whiting Petroleum files for bankruptcy. On May 6, 2020, the CDS settlement auction is held which results in a loss rate of* $\ell = 93\%$. *On May 7, 2020, Version 2 of Series 34 (S34.V2) with the 99 remaining names is launched.*

The return on the credit index from May 6 to May 7 is computed as follows: The closing index price of S34.V1 on May 6 is 0.9280. *The closing index price of S34.V2 on May 7 is* 0.9410. *Furthermore,* $r_t = 0.06\%$, $cpn = 5\%$, *and* $\Delta = \frac{1}{252}$. *Therefore, the one-day return on the credit index is*

$$R = \frac{\frac{99}{100}0.9410 + \frac{1}{100}(1 - 0.93) + (0.0006 + 0.05)\frac{1}{252}}{0.9280} - 1 = 0.48\%$$

(On the other hand, there is a -3.17% *return on the day that Whiting Petroleum files for bankruptcy.)*

Consider a put option on S34.V1 with strike $K^S = 0.92$ *and expiration on June 17. The closing price on May 6 is* 0.02550. *On May 7, the adjusted strike is* $\tilde{K}^S = 0.9286$. *Prices of put options on S34.V2 with strike* $K^S = \{0.92, 0.93\}$ *are* $\{0.01988, 0.02331\}$. *Interpolating to get the price corresponding to* $\tilde{K}^S$ *and multiplying by* $\frac{99}{100}$ *gives that the value of the original option is* 0.02260. *Therefore, the one-day return on the option is* -11.37%. *(On the other hand, there is a* 38.14% *return on this option on the day that Whiting Petroleum files for bankruptcy.)*

IA.2 Option greeks

We illustrate the properties of the relevant option greeks within the Black-Scholes model. Assume that the underlying index price follows a geometric Brownian motion with risk-neutral dynamics

$$\frac{dS_t}{S_t} = (r - q)dt + \sigma dZ_t,$$

where q is the payout rate. Consider a put and call option with strike K and time-to-expiry $\tau = T - t$. Define

$$d_1 = \frac{\ln(S/K) + \left(r - q + \frac{1}{2}\sigma^2\right)\tau}{\sigma\sqrt{\tau}}, \quad d_2 = d_1 - \sigma\sqrt{\tau}$$

and let φ and Φ denote the pdf and cdf of the standard normal distribution. Then, the put (P) and call (C) prices and their relevant greeks (scaled as in the paper) are given by

- Price:

$$P = e^{-r\tau}K\Phi(-d_2) - Se^{-q\tau}\Phi(-d_1), \quad C = Se^{-q\tau}\Phi(d_1) - e^{-r\tau}K\Phi(d_2)$$

- Gamma: $\gamma = \frac{\partial^2 P}{\partial S^2}S^2\sigma^2 = \frac{\partial^2 C}{\partial S^2}S^2\sigma^2$

$$\gamma = e^{-q\tau}\frac{\varphi(d_1)}{\sqrt{\tau}}S\sigma \tag{IA1}$$

- Vega: $\nu = \frac{\partial P}{\partial \sigma}\sigma = \frac{\partial C}{\partial \sigma}\sigma$

$$\nu = e^{-q\tau}\varphi(d_1)\sqrt{\tau}S\sigma \tag{IA2}$$

- Vanna: $\zeta = \frac{\partial^2 P}{\partial \sigma \partial S}S\sigma^2 = \frac{\partial^2 C}{\partial \sigma \partial S}S\sigma^2$

$$\zeta = -e^{-q\tau}\varphi(d_1)d_2 S\sigma \tag{IA3}$$

- Volga: $\omega = \frac{\partial^2 P}{\partial \sigma^2}\sigma^2 = \frac{\partial^2 C}{\partial \sigma^2}\sigma^2$

$$\omega = e^{-q\tau}\varphi(d_1)\sqrt{\tau}d_1 d_2 S\sigma \tag{IA4}$$

Example 1. *Assuming parameter values* $S_t = 100$*,* $r = 0.02$*,* $q = 0.01$*, and* $\sigma = 0.20$*, Figure IA1 shows gamma, vega, vanna, and volga for two-month options as a function of moneyness,* m*.*

Gamma and vega display the familiar patterns, being positive everywhere, highest for ATM options, and symmetric around the ATM level.

Vanna is asymmetric, being negative for low-strike options, approximately zero for ATM options, and positive for high-strike options. Intuitively, vanna is the change in vega for a change in the underlying. For a low-strike (OTM put or ITM call) option, an increase in the underlying brings the option further away from ATM, decreasing vega and making vanna negative. Conversely, for a high-strike (ITM put or OTM call) option, an increase in the underlying brings the option towards ATM, increasing vega and making vanna positive. Finally, around ATM, vega takes the maximum value making vanna approximately zero. This can also be seen analytically from Equation (IA3) where $\operatorname{sign}(\zeta) = \operatorname{sign}(-d_2)$ and $-d_2 = m + \frac{1}{2}\sigma\sqrt{\tau} \approx m$ for short-term options and reasonable levels of volatility.

Volga is roughly symmetric around the ATM level, being approximately zero for ATM options and positive for low-strike and high-strike options. Intuitively, volga is the convexity of the relation between option price and volatility. Around ATM, the relation is roughly linear making volga approximately zero, whereas away from ATM, the relation is convex making volga positive. That volga is symmetric can also be seen from Equation (IA4) since $\varphi(d_1)$ is approximately symmetric in m and $d_1 d_2 = (-m + \frac{1}{2}\sigma\sqrt{\tau})(-m - \frac{1}{2}\sigma\sqrt{\tau}) \approx m^2$, which is also symmetric in m (again, for short-term options and reasonable levels of volatility).

Example 2. *Continuing with the same parameter values, Figure IA2 shows gamma, vega, vanna, and volga for ATM options as a function of time-to-expiry,* τ*.*

Clearly, gamma is decreasing in τ and vega is increasing in τ, while vanna and volga are approximately zero.

Example 3. *Continuing with the same parameter values, we construct the gamma and vega factors using 1- and 3-month ATM options as well as the vanna and volga factors using 2-month options. Table IA.18 displays the resulting greeks. Clearly, the factors have the desired exposures*

The gamma factor (GMA) goes long one 1-month straddle and short $N = \frac{\nu_1}{\nu_2} = 0.5788$ 3-month straddles. Note from Equations (IA2) and (IA3) and with $m = 0$, that the *vega-vanna ratio* is independent of τ,

$$\frac{\nu}{\zeta} = \frac{2}{\sigma}.$$

Therefore, $\frac{\nu_1}{\nu_2} = \frac{\zeta_1}{\zeta_2}$ so not only is the vega exposure exactly zero but so is the vanna exposure.

The vega factor (VGA) goes long one 3-month straddle and short $N = \frac{\gamma_2}{\gamma_1} = 0.5759$ 1-month straddles.

The vanna factor (VNA) goes long one 2-month put with moneyness $m = -1$ and short $N = \frac{\nu_-^p}{\nu_+^c} = 0.9216$ 2-month calls with moneyness $m = 1$. Note from Equations (IA1) and (IA2), that the *vega-gamma ratio* is independent of m,

$$\frac{\nu}{\gamma} = \tau.$$

Also, note from Equations (IA2) and (IA4), that the *vega-volga ratio* depends on the absolute moneyness,

$$\frac{\nu}{\omega} = \frac{1}{m^2 - \frac{1}{4}\sigma^2\tau}.$$

Therefore, $\frac{\nu_-^p}{\nu_+^c} = \frac{\gamma_-^p}{\gamma_+^c} = \frac{\omega_-^p}{\omega_+^c}$ so not only is the vega exposure exactly zero but so are the gamma and volga exposures.

The volga factor (VLG) goes long one 2-month put with moneyness $m = -1$ and one 2-month call with moneyness $m = 1$, and shorts $N = \frac{\nu_-^p + \nu_+^c}{\nu_0^p + \nu_0^c} = 1.2141$ 2-month ATM straddles. By the same argument as above we have that not only is the vega exposure exactly zero but so is the gamma exposure.

IA.3 Data filters

First, we apply filters on the index options data in the following order:

1. The data include bid, ask, and mid prices. Use mid prices, but only those for which the associated bid price is positive.

2. For the spread-quoted IG options (CDX.IG and iTraxx.main), only use options with strikes on a 5 bps grid; say 80 bps, 85 bps,...

   For the spread-quoted HY option (iTraxx.Crossover), only use options with strikes on a 25 bps grid; say 400 bps, 425 bps,...

   For the price-quoted HY option (CDX.HY), only use options with strikes on a 0.0050 grid; say 1.0100, 1.0150,...

   We ignore options with strikes away from these "benchmark" grids because they typically have fewer dealers contributing to the composite quotes making them more noisy and less representative.

3. Impose standard no-arbitrage filters.

Second, on each trading day, we select the options that fall on the 4×3 moneyness-maturity grid described in the text.

Third, we remove a few outliers. A clear indication of an outlier is a large reversal in implied volatility from one day to the next. Specifically, we use the following procedure:

1. For each option, compute the percentage daily change in its implied volatility.

2. For each moneyness-maturity combination convert the time series of implied volatility changes into a time series of z-scores and eliminate observations for which a z-score

larger than three is followed on the next trading day by a z-score less than minus three, or vice versa.

For OTM and ATM puts with moneyness -2, -1, and 0 (ATM and OTM calls with moneyness 0 and 1) the fraction of observations that are removed is 0.40%, 0.26%, 0.12%, and 0.06% (0.46%, 0.37%, 0.23%, and 0.23%) for CDX.IG, CDX.HY, iTraxx.main, and iTraxx.Crossover, respectively.

Removing outliers mainly affects the higher-order moments of the return distributions and only to a very limited extent the mean returns and Sharpe ratios. This is largely because the procedure always removes return pairs with opposite signs.

IA.4 Holding period and transaction costs

In the paper we consider a holding period of one day. Here we consider an alternative strategy of holding options to expiry while delta hedging on a daily basis. The purpose is threefold:

1. demonstrate the robustness of the results to the choice of holding period,
2. study the impact of transaction costs, and
3. examine the profitability of selling options in a setting that is closer to actual option trading.

Specifically, we consider a strategy of selling 1-month ATM straddles. As in the paper, 1-month means the shortest option maturity with more than two weeks to expiration and ATM means the strike for which moneyness m is closest to zero.

IA.4.1 Selling straddles, no transaction costs

A straddle is sold on each trading day and delta hedged over the life of the options. We assume that the trader must put up a certain amount of capital, V_0, when selling options.

This amount along with the option premium received from selling options, P_0, is held in a margin account earning the risk-free rate. All cash-flows from the delta-hedge are brought forward to option expiry by investing/borrowing at the risk-free rate.

Specifically, consider a set of dates $t_0, t_1, ..., t_n$ where $t_0 = 0$ is the date the options are sold, $t_n = T$ is the option expiry, and $t_i - t_{i-1} = \delta$ is one trading day. The value of the delta-hedged credit index option portfolio at time T is

$$\begin{aligned} V_T =&(P_0 + V_0)e^{rT} - \left((U_T - K^U)^+ + (K^U - U_T)^+\right) \\ &- \Delta_0 U_0 e^{rT} - \sum_{i=1}^{n-1} \left(\left(\Delta_i - \Delta_{i-1}\right) U_i + \Delta_{i-1} c\delta\right) e^{r(T-i\delta)} + \Delta_{n-1} \left(U_T - c\delta\right), \end{aligned} \tag{IA5}$$

where the second term is the straddle payoff, the third term is the cost of the initial delta hedge, the fourth term is the cost of rebalancing the delta hedge $n-1$ times, and the last term is the final value of the delta hedge. We assume that the CDS index coupon, c, is paid continuously over time.[1]

Similarly, the value of the delta-hedged equity index option portfolio at time T is

$$\begin{aligned} V_T =&(P_0 + V_0)e^{rT} - \left((S_T - K)^+ + (K - S_T)^+\right) \\ &- \Delta_0 S_0 e^{rT} - \sum_{i=1}^{n-1} \left(\left(\Delta_i - \Delta_{i-1}\right) S_i - \Delta_{i-1} q_{i-1} S_{i-1}\delta\right) e^{r(T-i\delta)} + \Delta_{n-1} \left(S_T + q_{n-1} S_{n-1}\delta\right), \end{aligned} \tag{IA6}$$

where q is the dividend yield.

[1]For notational convenience, we write the interest rate as being constant. In the implementation, we account for time-varying interest rates.

IA.4.2 Selling straddles, with transaction costs

The credit index option data contains indicative bid and ask prices for options (except for a period in 2017 and 2018). We also have bid and ask prices for SPX options (via CBOE), but not for Eurostoxx 50 options (via OptionMetrics).

On each trading day, we compute the percentage spread between bid- and mid-prices, $\frac{P_t^{bid}-P_t^{mid}}{P_t^{mid}}$. Figure IA3 displays the frequency distribution of the spreads. The mean (median) spread is -7.9% (-7.2%) for CDX.IG, -8.6% (-7.8%) for CDX.HY, -6.4% (-6.0%) for iTraxx.main, -6.2% (-5.7%) for iTraxx.Crossover, and -1.7% (-1.5%) for SPX. As such, transaction costs for credit index options are about four to five times larger than those for equity index options, on average.

We implement the strategy from Section IA.4.1 with straddles sold at bid-prices rather than mid-prices. Because many bid-price data points are missing, we assume that transaction costs are constant across time and apply one transaction cost to all credit index options and another to both equity index options. Specifically, we assume that bid-prices are lower than mid-prices by 7.5% for credit index options and 1.5% for equity index options (to be conservative, we set the difference to be a factor five). We do not apply a bid-ask spread to the delta-hedge.[2] The amount of initial capital is the same as in the case of no transaction costs.

IA.4.3 Results

Table IA.19 shows the performance of three straddle-selling strategies:

1. Holding period of one day

2. Hold to expiration without transaction costs (as in Section IA.4.1)

[2]To start with, transaction costs are much lower for the underlying index. Moreover, trades for delta-hedging purposes are uninformed and can typically be executed at lower costs than the average trade. See Collin-Dufresne et al. (2020b) for an analysis of transaction costs in credit indexes.

3. Hold to expiration with transaction costs (as in Section IA.4.2)

Means, standard deviations, and Sharpe ratios are annualized; in cases 2 and 3 this is done based on an average holding period of one month. In all cases, t-statistics are computed using Newey and West (1987) with 63 lags.

Taking the US market as an example, with a daily holding period, the Sharpe ratios are 2.18, 2.46, and 0.56 for IG, HY, and equity, respectively. This largely mirrors the (absolute value of) Sharpe ratios for delta-hedged ATM put options in Figure 1 in the main paper. With hold-to-expiry, the ordering is maintained, even if the Sharpe ratios decrease somewhat to 1.46, 2.28, and 0.32, respectively.

Transaction costs reduce profitability; however, despite the relatively high costs of trading credit index options, the mean returns remain statistically significant and generate respectable Sharpe ratios of 0.73 for IG and 1.33 for HY. For comparison, the Sharpe ratio for EQ drops to 0.14.[3]

The general pattern is the same in the European market, and we conclude that our results are robust to variation in holding period and transaction costs.

IA.5 Index option returns in calibrated structural model

Doshi et al. (2024) estimate a structural credit risk model features three priced sources of systematic risk: diffusive risk, jump risk, and variance risk. The underlying asset dynamics are identical to the specification in Collin-Dufresne et al. (2024), although the debt structure and the conditions triggering default differ somewhat. Both papers allow for the consistent

[3]Note that the number of observations differ somewhat. With a daily holding period, the return computation necessitates that the option price at the end of the holding period is available. This is sometimes not the case, for instance on days when the underlying index series goes off the run (because only options on the on-the-run series are quoted). With hold-to-expiration, the return computation necessitates that the price of the underlying index series is available until option expiration. This is not a problem, even when the series goes off the run, because dealers continue to quote prices on first-off-the-run series. However, it does lead to a loss of observations at the end of the sample period.

pricing of credit and equity index options, with Collin-Dufresne et al. (2024) having analytical option prices based on transform analysis and Doshi et al. (2024) relying on simulation.

In this section, we briefly review this model that forms the basis for the simulation exercise in Section 3 in the paper. We also derive expressions for the factor exposures and mean and volatility of instantaneous excess returns of index options. Finally, we compute these values conditional on the variance state variable being equal to its long-run mean and compare with the simulated values reported in the paper.

IA.5.1 The model

We use the notation in Collin-Dufresne et al. (2024). The $\mathbb{P}$ dynamics are

$$\begin{aligned}
\frac{dA_t^i}{A_{t^-}^i} &= \frac{dA_t}{A_{t^-}} + \sigma_i dW_t^i + (e^{\gamma_i} - 1)dN_t^i - \lambda_i \nu_i dt \\
\frac{dA_t}{A_{t^-}} &= (r - \delta + \mu_t)dt + \sqrt{\omega_t}\left(\rho dW_t + \sqrt{1-\rho^2}dZ_t\right) + (e^{\gamma} - 1)dN_t - \lambda_t \nu dt \\
d\omega_t &= \kappa(\bar{\omega} - \omega_t)dt + \sigma_{\omega}\sqrt{\omega_t}dW_t,
\end{aligned}$$

where W_t^i, W_t, and Z_t are independent Brownian motions, N_t and N_t^i are independent Poisson counting processes with intensities $\lambda_t = \lambda_\omega \omega_t$ and λ_i, respectively, $\gamma \sim \mathcal{N}(m, v)$ and $\gamma_i \sim \mathcal{N}(m_i, v_i)$ are independent normal random variables, and we define $\nu = \mathbb{E}[e^{\gamma} - 1] = e^{m+\frac{v}{2}} - 1$ and $\nu_i = \mathbb{E}[e^{\gamma_i} - 1] = e^{m_i+\frac{v_i}{2}} - 1$.[4] The dividend payout rate is δ and the asset risk premium is μ.

With the risk premium specification in Doshi et al. (2024), the $\mathbb{Q}$ dynamics are of the form

$$\frac{dA_t^i}{A_{t^-}^i} = \frac{dA_t}{A_{t^-}} + \sigma_i dW_t^i + (e^{\gamma_i} - 1)dN_t^i - \lambda_i \nu_i dt$$

[4] We impose that λ_t is linear (rather than affine) in ω_t as in Doshi et al. (2024).

$$
\begin{aligned}
\frac{dA_t}{A_{t^-}} &= (r-\delta)dt + \sqrt{\omega_t}\left(\rho dW_t^{\mathbb{Q}} + \sqrt{1-\rho^2}dZ_t^{\mathbb{Q}}\right) + (e^{\gamma^{\mathbb{Q}}}-1)dN_t^{\mathbb{Q}} - \lambda_t^{\mathbb{Q}}\nu^{\mathbb{Q}}dt \\
d\omega_t &= \kappa^{\mathbb{Q}}(\bar{\omega}^{\mathbb{Q}} - \omega_t)dt + \sigma_{\omega}\sqrt{\omega_t}dW_t^{\mathbb{Q}},
\end{aligned}
$$

where $W_t^{\mathbb{Q}}$ and $Z_t^{\mathbb{Q}}$ are independent Brownian motions, $N_t^{\mathbb{Q}}$ is a Poisson counting process with intensity $\lambda_t^{\mathbb{Q}} = \lambda_\omega^{\mathbb{Q}}\omega_t$, $\gamma \sim \mathcal{N}(m^{\mathbb{Q}}, v)$, and $\nu^{\mathbb{Q}} = \mathbb{E}^{\mathbb{Q}}[e^{\gamma^{\mathbb{Q}}} - 1] = e^{m^{\mathbb{Q}}+\frac{v}{2}} - 1$.

In Doshi et al. (2024), there are three risk premium parameters, ξ_ω, $\xi_{A\perp\omega}$, and ξ_J. The asset risk premium is

$$
\mu_t = \mu_t^c + \left(\lambda_t\nu - \lambda_t^{\mathbb{Q}}\nu^{\mathbb{Q}}\right),
$$

with

$$
\mu_t^c = \left(\rho\xi_\omega + \sqrt{1-\rho^2}\xi_{A\perp\omega}\right)\omega_t
$$

being the premium for diffusive risk, and the remaining parameters are

$$
\begin{aligned}
\kappa^{\mathbb{Q}} &= \kappa + \sigma_\omega\xi_\omega \\
\theta^{\mathbb{Q}} &= \kappa\theta/\kappa^{\mathbb{Q}} \\
\lambda_\omega^{\mathbb{Q}} &= \lambda_\omega e^{\xi_J m + \frac{1}{2}\xi_J^2 v} \\
m^{\mathbb{Q}} &= m + \xi_J v.
\end{aligned}
$$

IA.5.2 Returns and factor exposures

Consider a derivative I_t. Could be an index or an index option. Applying Ito's Lemma

$$
\begin{aligned}
dI_t =& \frac{\partial I_t}{\partial t}dt + \frac{\partial^2 I_t}{\partial A_t^2}\left(dA_t^c\right)^2 + \frac{\partial^2 I_t}{\partial \omega_t^2}\left(d\omega_t\right)^2 + \frac{\partial^2 I_t}{\partial A_t \partial \omega_t}dA_t^c d\omega_t + \frac{\partial I_t}{\partial A_t}dA_t^c + \frac{\partial I_t}{\partial \omega_t}d\omega_t + \\
& \left(I(A_{t-}e^{\gamma}, \omega_t) - I_{t-}\right)dN_t. \qquad \text{(IA7)}
\end{aligned}
$$

Taking risk-neutral expectation of (IA7) and subtracting the result from (IA7) gives the expression for the realized dollar return:

$$
\begin{aligned}
dI_t - \mathbb{E}^{\mathbb{Q}}\left[dI_t\right] =& \frac{\partial I_t}{\partial A_t}\left(dA_t^c - \mathbb{E}^{\mathbb{Q}}\left[dA_t^c\right]\right) + \frac{\partial I_t}{\partial \omega_t}\left(d\omega_t - \mathbb{E}^{\mathbb{Q}}[d\omega_t]\right) + \\
& \left(I(A_{t-}e^{\gamma}, \omega_t) - I_{t-}\right) dN_t - \mathbb{E}^{\mathbb{Q}}\left[I(A_{t-}e^{\gamma}, \omega_t) - I_{t-}\right] \lambda_t^{\mathbb{Q}} dt. \qquad \text{(IA8)}
\end{aligned}
$$

We can write the realized excess return as

$$
R_t = \Delta_A \left(\frac{dA_t^c}{A_t} - \mathbb{E}^{\mathbb{Q}}\left[\frac{dA_t^c}{A_t}\right]\right) + \Delta_\omega \left(d\omega_t - \mathbb{E}^{\mathbb{Q}}[d\omega_t]\right) + \Delta_N dN_t - \mathbb{E}^{\mathbb{Q}}\left[\Delta_N\right] \lambda_t^{\mathbb{Q}} dt,
$$

where

$$
\Delta_A = \frac{\partial I_t}{\partial A_t}\frac{A_t}{I_t}, \quad \Delta_\omega = \frac{\partial I_t}{\partial \omega_t}\frac{1}{I_t}, \quad \Delta_N = \frac{I(A_{t-}e^{\gamma}, \omega_t) - I_{t-}}{I_{t-}}
$$

denote the exposures to diffusive asset risk, asset variance risk, and asset jump risk, respectively.

It follows that the annualized expected excess return is

$$
\frac{1}{dt}\mathbb{E}\left[R_t\right] = \Delta_A \mu_t^c + \Delta_\omega \sigma_\omega \xi_\omega \omega_t + \left(\mathbb{E}\left[\Delta_N\right]\lambda_\omega - \mathbb{E}^{\mathbb{Q}}\left[\Delta_N\right]\lambda_\omega^{\mathbb{Q}}\right)\omega_t, \qquad \text{(IA9)}
$$

and the annualized return variance is

$$
\frac{1}{dt}Var\left(R_t\right) = \left(\Delta_A\right)^2 \omega_t + \left(\Delta_\omega \sigma_\omega\right)^2 \omega_t + 2\Delta_A \Delta_\omega \sigma_\omega \rho \omega_t + \mathbb{E}\left[\left(\Delta_N\right)^2\right]\lambda_\omega \omega_t. \qquad \text{(IA10)}
$$

We consider

- Underlying index (credit or equity) with price S_t and excess return

$$
R_t^S = \frac{dS_t}{S_t} - (r - \delta_S)dt,
$$

where δ_S is the index yield.

- Naked options on the index with price P_t and excess return

$$R_t^P = \frac{dP_t}{P_t} - rdt,$$

- Delta-hedged options on the index, where the delta is computed using the Black-Scholes model and the delta-position is financed at the risk-free rate (so that the upfont cost remains P_t). The change in the value of such a delta-hedged option is

$$dP_t + \Delta_S^{BS} \left(dS_t - (r - \delta_S) S_t dt \right)$$

so that the excess return is

$$R_t^P - w R_t^S, \quad w = \Delta_S^{BS} \frac{S_t}{P_t}$$

IA.5.3 Conditional factor exposures and risk-return trade-off

Table IA.17 has the same structure as Table 1 in the paper, but here we use the expressions above for instantaneous returns and condition on the variance state variable being equal to its long-run mean, $\omega_t = \bar{\omega}$.

Panel A reports the conditional factor exposures. Note that the delta and gamma exposures in Table 1 become exposures to diffusive and jump risk in Table IA.17. The risk exposures are normalized to reflect a one standard derivation change in each of the risk factors, and in case of jump risk, the expected exposure is reported; that is, the table reports

$$\Delta_A \sqrt{\omega_t}, \quad \Delta_\omega \sigma_\omega \sqrt{\omega_t}, \quad \mathbb{E}\left[\Delta_N\right] \sqrt{\lambda_\omega \omega_t}.$$

The conditional (and instantaneous) values in Table IA.17 are similar to the unconditional (and daily) values in Table 1. The exception is the jump exposure in Table IA.17 which is not directly comparable to the gamma exposure in Table 1 in case of outright option returns.[5]

Panel B reports the conditional means and Sharpe ratios. Importantly, the mean excess returns are more negative for delta-hedged equity index options than credit index options, with the differences being very similar to the ones reported in Table 1.

IA.5.4 Marking-to-market of CDX and SPX Options

In our simulation exercise, options are bought at time 0 and sold (or marked-to-market) one day later at time t. The expressions for the time-0 option values are given in Collin-Dufresne et al. (2024). Here, we provide the expressions for the time-t option values.

The time-t value of a CDX call option with strike K and expiration at T_0 is

$$\begin{aligned}
C_t^{CDX} &= e^{-r(T_0-t)}\mathbb{E}[\max(U_{T_0}(x_{T_0}) - K, 0) \,|\, x_t] \\
&= e^{-r(T_0-t)}\mathbb{E}[(U_{T_0}(x_{T_0}) - K)\mathbf{1}_{\left\{A_{T_0} < \underline{A}(\omega_{T_0})\right\}} \,|\, x_t] \\
&= e^{-r(T_1-t)}\Big((1+C_1)\mathbb{E}[\mathbf{1}_{\left\{A_{T_0} < \underline{A}(\omega_{T_0}),A^i_{T_1} < \Phi(\omega_{T_1})\right\}} \,|\, x_t] - \frac{\alpha}{D_1+D_2}\mathbb{E}[A^i_{T_1}\mathbf{1}_{\left\{A_{T_0} < \underline{A}(\omega_{T_0}),A^i_{T_1} < \Phi(\omega_{T_1})\right\}} \,|\, x_t]\Big) \\
&\quad + e^{-r(T_2-t)}\Big(\mathbb{E}[\mathbf{1}_{\left\{A_{T_0} < \underline{A}(\omega_{T_0}),A^i_{T_1} \geq \Phi(\omega_{T_1}),A^i_{T_2} < D_2\right\}} \,|\, x_t] - \frac{\alpha}{D_2}\mathbb{E}[A^i_{T_2}\mathbf{1}_{\left\{A_{T_0} < \underline{A}(\omega_{T_0}),A^i_{T_1} \geq \Phi(\omega_{T_1}),A^i_{T_2} < D_2\right\}} \,|\, x_t]\Big) \\
&\quad - e^{-r(T_0-t)}\tilde{K}\mathbb{E}[\mathbf{1}_{\left\{A_{T_0} < \underline{A}(\omega_{T_0})\right\}} \,|\, x_t].
\end{aligned}$$

Similarly, the time-t value of an SPX call option with strike K and expiration at T_0 is

$$C_t^{SPX} = e^{-r(T_0-t)}\mathbb{E}[\max(S_{T_0}(x_{T_0}) - K, 0) \,|\, x_t]$$

[5] One should be careful when comparing the exposures for outright CDX options in Table IA.17 with the exposures in Figure 1 in Doshi et al. (2024). In our paper, CDX options refer to options on the index price, while in Doshi et al. (2024), CDX options refer to options on the index spread. Because price and spread are inversely related, CDX call (put) options here should be compared with CDX put (call) options in Doshi et al. (2024). With this is mind, exposures for outright index options in Table IA.17 are very similar to the exposures in Figure 1 in Doshi et al. (2024).

$$
\begin{aligned}
&= e^{-r(T_0-t)}\mathbb{E}[(S_{T_0}(x_{T_0}) - K)\mathbf{1}_{\{A_{T_0}\geq \overline{A}(\omega_{T_0})\}} \mid x_t] \\
&= e^{-r(T_0-t)}\mathbb{E}[A_{T_0}\mathbf{1}_{\{A_{T_0}\geq \overline{A}(\omega_{T_0})\}} \mid x_t] \\
&\quad - e^{-r(T_1-t)}\Big(D_1\mathbb{E}[\mathbf{1}_{\{A_{T_0}\geq \overline{A}(\omega_{T_0}), A^i_{T_1}\geq \Phi(\omega_{T_1})\}} \mid x_t] + \mathbb{E}[A^i_{T_1}\mathbf{1}_{\{A_{T_0}\geq \overline{A}(\omega_{T_0}), A^i_{T_1}< \Phi(\omega_{T_1})\}} \mid x_t]\Big) \\
&\quad - e^{-r(T_2-t)}\Big(D_2\mathbb{E}[\mathbf{1}_{\{A_{T_0}\geq \overline{A}(\omega_{T_0}), A^i_{T_1}\geq \Phi(\omega_{T_1}), A^i_{T_2}\geq D_2\}} \mid x_t] + \mathbb{E}[A^i_{T_2}\mathbf{1}_{\{A_{T_0}\geq \overline{A}(\omega_{T_0}), A^i_{T_1}\geq \Phi(\omega_{T_1}), A^i_{T_2}< D_2\}} \mid x_t]\Big) \\
&\quad - e^{-r(T_0-t)}K\mathbb{E}[\mathbf{1}_{\{A_{T_0}\geq \overline{A}(\omega_{T_0})\}} \mid x_t].
\end{aligned}
$$

IA.6 Distribution of trade sizes in US credit index options

This section descibes how we infer the distributions of capped trade sizes. We do this separately for CDX.IG and CDX.HY options.

IA.6.1 CDX.IG options

For the purpose of updating regulatory block and cap thresholds, CFTC (2024) uses all transactions from 2023 and computes the 67th and 75th percentiles of the notional-weighted size distribution. The x'th percentile is defined as the trade size below which trades account for x percent of total notional volume. For CDX.IG options, the 67th and 75th percentiles are 1.2 and 2.0 billion USD, repectively. While for other asset classes, including the underlying CDX contracts, the new cap thresholds were set at their 75th percentiles, for credit index options the CFTC decided to apply a uniform cap threshold of 0.4 billion USD.

We assume that the trade-size distribution in our sample from October 7, 2024 until June 13, 2025 is the same as in 2023 so that we can apply the percentiles from CFTC (2024) to the more recent sample. There are 2030 uncapped trades (with notionals less than 400 million) which have a combined notional of $V^{unc} = 337.07$ billion USD. There are $N^{cpd} = 2089$ capped trades. For these, we assume that the trade sizes are described by a Pareto distribution with density

$$f^{cpd}(x) = \frac{\alpha x_{\min}^{\alpha}}{x^{\alpha+1}}, \quad x > x_{\min}$$

and $x_{\min} = 0.4$ billion. Then, the cumulative notional of all trades up to size $x > 0.4$ is

$$\begin{aligned} V(x) &= V^{unc} + N^{cpd} \int_{0.4}^{x} u f^{cpd}(u) du \\ &= V^{unc} + N^{cpd} \frac{\alpha}{\alpha - 1} \left(0.4 - x \left(\frac{0.4}{x} \right)^{\alpha} \right), \end{aligned}$$

and the total notional is

$$V^{total} = V^{unc} + N^{cpd} \frac{\alpha}{\alpha - 1} 0.4.$$

We estimate α to minimize the sum of squared errors:

$$\begin{aligned} \epsilon_1 &= \frac{V(1.2)}{V^{total}} - 0.67 \\ \epsilon_2 &= \frac{V(2.0)}{V^{total}} - 0.75. \end{aligned}$$

which gives the estimate $\alpha = 1.81$. The fit is very good with error terms $\epsilon_1 = -0.0185$ and $\epsilon_2 = 0.0197$.

IA.6.2 CDX.HY options

In the case of CDX.HY, the 75th percentile computed in CFTC (2024) is below the cap threshold of 0.4 billion, so we cannot use the approach that we use for CDX.IG. Instead, we assume that the Pareto distribution for trade sizes applies not only to capped trades, but to trades larger than 200 million. There are 912 such trades of which 28.1% are capped. Since

$$\text{Prob}(X > x) = \left(\frac{x_{\min}}{x} \right)^{\alpha}$$

we get

$$\alpha = \frac{\log(0.281)}{\log\left(\frac{0.2}{0.4}\right)} = 1.83,$$

which, incidentally, is very close to he value for CDX.IG.

IA.6.3 CDX.IG options, alternative approach

A robust but conservative approach assumes that the true notionals of capped trades are either 0.4, 1.2, or 2.0 billion, and that the fraction of capped trades with these notionals are w_1, w_2, and $1 - w_1 - w_2$, respectively. Then, the total notional is

$$V^{total} = V^{unc} + N^{cpd}(w_1 0.4 + w_2 1.2 + (1 - w_1 - w_2)2.0).$$

We find w_1, w_2 as the solution to

$$\begin{aligned} \frac{V^{unc} + N^{cpd} w_1 0.4}{V^{total}} &= 0.67 \\ \frac{V^{unc} + N^{cpd}(w_1 0.4 + w_2 1.2)}{V^{total}} &= 0.75, \end{aligned}$$

which gives $w_1 = 85.59\%$ and $w_2 = 5.01\%$. With this approach, 2.5% (4.8%) of trades have notional values of 1.2 (2.0) billion, and the average daily trading volume is 9.18 billion.

Panel A: US market
New Year's Day
Martin Luther King Day
Presidents Day
Good Friday
Memorial Day
Juneteenth (from 2022)
Independence Day
Labor Day
Columbus Day
Veterans Day
Thanksgiving Day
Christmas Day
Panel B: European market
New Year's Day
Good Friday
Easter Monday
May 1st
U.K. May Day
U.K. Spring Bank Holiday
U.K. Summer Bank Holiday
December 24th
Christmas Day
U.K. Boxing Day
December 31st

Table IA.1: Non-Trading Days
The table shows the non-trading days in the US and European markets. In the European market, it is the union of non-trading days in the U.K. and on Eurex in Frankfurt.

	IG	HY	EQ
	Panel A: US market		
Mean	**0.012**	**0.047**	**0.126**
	(2.87)	(2.37)	(3.19)
Std.dev.	0.017	0.076	0.166
SR	0.68	0.62	0.76
Skew	0.81	0.46	-0.43
Kurt	44.3	30.3	12.3
N obs	2558	2556	2560
N defaults	0	21	—
	Panel B: European market		
Mean	**0.015**	**0.052**	0.095
	(2.99)	(2.54)	(1.86)
Std.dev.	0.019	0.072	0.196
SR	0.78	0.73	0.48
Skew	-0.64	-0.49	-0.57
Kurt	17.9	17.0	11.9
N obs	2568	2569	2547
N defaults	0	6	—

Table IA.2: Performance of Indexes
Summary statistics of daily excess returns on indexes. Means, standard deviations, and Sharpe ratios ("SR") are annualized. t-statistics in parentheses are corrected for heteroscedasticity and serial correlation up to 63 lags (equal to three months) using the approach of Newey and West (1987). Mean estimates that are significant at the 5% level are highlighted in bold. Sample period is from January 1, 2013 to April 3, 2023.

Default Date	Auction Date	Company Name	Loss Rate	Index Series
2014-04-29	2014-05-21	Texas Electric	91.50	22
2015-01-15	2015-02-19	Caesars Entertainment	84.12	23
2015-02-05	2015-03-05	RadioShack	88.50	23
2015-05-21	2015-06-23	Sabine Oil & Gas	84.12	24
2016-12-20	2017-02-02	iHeartCommunications	64.50	27
(2017-09-19	2017-10-11	Toys R Us	74.00	28)
2018-10-15	2019-01-17	Sears Roebuck	20.13	31
2018-12-12	2019-01-23	Parker Drilling	51.00	31
(2019-02-25	2019-04-03	Windstream Services	70.50	31)
2019-07-01	2019-07-24	Weatherford Int.	55.50	32
2019-11-12	2019-12-10	Dean Foods	90.75	33
2020-02-13	2020-03-10	McClatchy	98.00	33
2020-04-01	2020-05-06	Whiting Petroleum	93.00	34
2020-04-26	2020-05-22	Diamond Drilling	92.62	34
2020-05-07	2020-05-29	Neiman Marcus	97.00	34
2020-05-15	2020-06-09	J. C. Penney	99.88	34
2020-05-22	2020-06-24	Hertz	73.62	34
2020-06-03	2020-07-07	California Resources	98.88	34
2020-06-28	2020-08-04	Chesapeake Energy	96.50	34
2020-07-31	2020-09-10	Noble	99.00	34
2022-05-09	2022-06-07	Talen Energy Supply	30.00	38

Table IA.3: Defaults in CDX.HY
The table shows the defaults in the on-the-run series of CDX.HY. Loss rate is in percent. Note that although the defaults of Toys R Us and Windstream Services happen while Series 28 and 31 are on-the-run, the settlement auctions and, therefore, the version changes take place after the series have gone off-the-run.

Default Date	Auction Date	Company Name	Loss Rate	Index Series
(2013-09-15	2013-10-09	Codere	45.50	19)
2018-09-27	2018-11-29	Astaldi	69.12	30
2020-08-14	2020-09-08	Hema	31.50	33
2020-07-29	2020-09-15	Matalan	63.50	33
2020-11-29	2021-01-13	Europcar	0.00	34

Table IA.4: Defaults in iTraxx.Crossover
The table shows the defaults in the on-the-run series of iTraxx.Crossover. Loss rate is in percent. Note that although the default of Codere happens while Series 19 is on-the-run, the settlement auction and, therefore, the version change takes place after the series has gone off-the-run. Note also the 100% recovery in the case of Europcar.

	IG			HY			EQ		
	M1	M2	M3	M1	M2	M3	M1	M2	M3
Panel A: US market									
Mean	**-3.78**	**-2.50**	**-1.61**	**-4.81**	**-3.00**	**-1.79**	-1.43	-1.16	-0.78
	(-3.87)	(-4.99)	(-3.55)	(-5.45)	(-4.87)	(-3.19)	(-1.33)	(-1.57)	(-1.28)
Std.dev.	2.31	1.37	1.14	2.11	1.40	1.14	2.89	1.80	1.42
SR	-1.64	-1.83	-1.42	-2.27	-2.15	-1.57	-0.50	-0.65	-0.55
Skew	6.32	2.69	2.67	3.31	1.97	2.68	3.21	3.20	3.15
Kurt	88.9	22.3	28.5	32.0	23.4	21.2	24.0	25.3	25.2
N obs	2515	2525	2505	2491	2516	2496	2560	2560	2560
Panel B: European market									
Mean	**-4.64**	**-2.29**	**-1.25**	**-4.74**	**-2.27**	**-1.47**	-0.03	-0.28	0.19
	(-6.59)	(-4.40)	(-2.64)	(-6.29)	(-3.98)	(-2.87)	(-0.03)	(-0.44)	(0.34)
Std.dev.	1.88	1.30	1.17	1.81	1.33	1.10	2.73	1.73	1.36
SR	-2.47	-1.75	-1.07	-2.62	-1.71	-1.33	-0.01	-0.16	0.14
Skew	3.59	2.72	3.35	3.19	3.33	3.25	3.68	3.33	2.83
Kurt	31.5	18.8	30.7	25.6	26.1	26.7	30.5	25.9	20.8
N obs	2524	2521	2452	2458	2469	2289	2547	2547	2152

Table IA.5: Performance of Option Portfolios Sorted on Maturity
Summary statistics of daily excess returns on option portfolios sorted on maturity. Means, standard deviations, and Sharpe ratios ("SR") are annualized. t-statistics in parentheses are corrected for heteroscedasticity and serial correlation up to 63 lags (equal to three months) using the approach of Newey and West (1987). Mean estimates that are significant at the 5% level are highlighted in bold. Sample period is from January 1, 2013 to April 3, 2023.

	EQ-IG			EQ-HY		
	M1	M2	M3	M1	M2	M3
	Panel A: US market					
Mean	**2.25**	**1.41**	**0.97**	**3.31**	**1.86**	**0.93**
	(2.17)	(3.04)	(2.51)	(4.25)	(4.46)	(2.90)
Std.dev.	2.96	1.71	1.39	2.70	1.70	1.40
SR	0.76	0.82	0.70	1.23	1.10	0.66
Skew	-2.02	1.81	1.49	1.00	1.45	-1.02
Kurt	52.8	24.5	23.1	23.8	19.2	27.6
N obs	2515	2525	2505	2491	2516	2496
	Panel B: European market					
Mean	**4.62**	**2.22**	**1.30**	**4.67**	**2.20**	**1.24**
	(5.68)	(4.58)	(3.65)	(6.69)	(4.93)	(3.38)
Std.dev.	2.54	1.61	1.31	2.40	1.61	1.22
SR	1.82	1.38	0.99	1.95	1.36	1.01
Skew	1.24	1.01	0.75	1.58	1.34	0.41
Kurt	16.4	13.5	17.0	14.2	17.1	10.9
N obs	2501	2498	2106	2435	2446	2041

Table IA.6: Performance of Long-Short Option Portfolios Sorted on Maturity
Summary statistics of daily excess returns on short credit vs. long equity option portfolios sorted on maturity. Means, standard deviations, and Sharpe ratios ("SR") are annualized. t-statistics in parentheses are corrected for heteroscedasticity and serial correlation up to 63 lags (equal to three months) using the approach of Newey and West (1987). Mean estimates that are significant at the 5% level are highlighted in bold. Sample period is from January 1, 2013 to April 3, 2023.

	IG			HY			EQ		
	M1-M2	M2-M3	M1-M3	M1-M2	M2-M3	M1-M3	M1-M2	M2-M3	M1-M3
				Panel A: US market					
Mean	**-0.69**	**-1.00**	**-0.27**	**-0.78**	**-1.14**	**-0.32**	-0.15	-0.29	**-0.13**
	(-4.69)	(-4.93)	(-3.80)	(-5.11)	(-5.21)	(-5.09)	(-1.01)	(-1.45)	(-2.18)
Std.dev.	0.46	0.59	0.25	0.47	0.59	0.24	0.53	0.68	0.18
SR	-1.49	-1.71	-1.07	-1.65	-1.93	-1.34	-0.28	-0.43	-0.73
Skew	1.37	1.59	0.91	2.50	2.53	2.02	3.03	2.97	2.66
Kurt	10.1	10.6	11.8	25.3	20.8	20.7	26.8	25.4	27.5
N obs	2471	2444	2494	2468	2447	2477	2560	2560	2560
				Panel B: European market					
Mean	**-0.75**	**-1.01**	**-0.34**	**-0.84**	**-1.20**	**-0.26**	0.06	0.11	-0.05
	(-5.92)	(-5.67)	(-5.33)	(-5.97)	(-6.02)	(-3.98)	(0.42)	(0.51)	(-0.81)
Std.dev.	0.43	0.59	0.23	0.43	0.53	0.24	0.48	0.66	0.20
SR	-1.75	-1.72	-1.47	-1.97	-2.26	-1.08	0.13	0.17	-0.25
Skew	1.88	3.22	1.25	1.74	1.92	1.74	2.76	2.86	2.59
Kurt	13.8	37.4	25.5	16.1	15.1	20.3	18.9	19.5	19.7
N obs	2461	2386	2416	2335	2163	2243	2545	2150	2152

Table IA.7: Performance of Gamma-Mimicking Portfolios
Summary statistics of daily excess returns on gamma-mimicking portfolios. Means, standard deviations, and Sharpe ratios ("SR") are annualized. t-statistics in parentheses are corrected for heteroscedasticity and serial correlation up to 63 lags (equal to three months) using the approach of Newey and West (1987). Mean estimates that are significant at the 5% level are highlighted in bold. Sample period is from January 1, 2013 to April 3, 2023.

	IG			HY			EQ		
	M1-M2	M2-M3	M1-M3	M1-M2	M2-M3	M1-M3	M1-M2	M2-M3	M1-M3
					Panel A: US market				
Mean	**-0.27**	**-0.25**	-0.09	**-0.40**	**-0.38**	**-0.14**	**-0.17**	-0.13	-0.03
	(-3.30)	(-2.65)	(-1.71)	(-4.36)	(-3.86)	(-2.74)	(-2.08)	(-1.51)	(-0.61)
Std.dev.	0.29	0.29	0.20	0.28	0.27	0.18	0.23	0.24	0.11
SR	-0.94	-0.86	-0.45	-1.44	-1.38	-0.80	-0.75	-0.56	-0.23
Skew	0.65	0.23	0.43	0.68	0.85	0.38	1.35	1.10	0.83
Kurt	11.3	11.7	13.8	12.5	8.8	9.9	13.4	13.9	11.5
N obs	2471	2444	2494	2468	2447	2477	2560	2560	2560
					Panel B: European market				
Mean	**-0.17**	-0.17	-0.01	**-0.16**	**-0.19**	-0.07	-0.10	0.02	0.07
	(-2.02)	(-1.76)	(-0.29)	(-2.08)	(-2.00)	(-1.47)	(-1.59)	(0.30)	(1.76)
Std.dev.	0.25	0.29	0.19	0.27	0.27	0.19	0.19	0.21	0.11
SR	-0.70	-0.59	-0.07	-0.61	-0.68	-0.38	-0.53	0.11	0.63
Skew	1.40	0.51	0.69	1.62	0.70	0.50	0.93	1.04	0.96
Kurt	13.8	18.8	15.1	24.5	8.6	9.9	10.8	11.0	12.4
N obs	2461	2386	2416	2335	2163	2243	2545	2150	2152

Table IA.8: Performance of Vega-Mimicking Portfolios

Summary statistics of daily excess returns on vega-mimicking portfolios. Means, standard deviations, and Sharpe ratios ("SR") are annualized. t-statistics in parentheses are corrected for heteroscedasticity and serial correlation up to 63 lags (equal to three months) using the approach of Newey and West (1987). Mean estimates that are significant at the 5% level are highlighted in bold. Sample period is from January 1, 2013 to April 3, 2023.

	IG			HY			EQ		
	M1	M2	M3	M1	M2	M3	M1	M2	M3
				Panel A: US market					
Mean	**-2.10**	**-1.11**	**-0.62**	**-3.73**	**-1.19**	**-0.63**	**-1.92**	**-0.64**	-0.41
	(-4.02)	(-3.98)	(-3.14)	(-10.20)	(-5.45)	(-3.70)	(-4.42)	(-2.33)	(-1.88)
Std.dev.	1.52	0.82	0.62	1.17	0.69	0.57	1.37	0.82	0.63
SR	-1.38	-1.35	-1.00	-3.18	-1.72	-1.12	-1.39	-0.78	-0.64
Skew	1.50	0.12	0.17	-0.10	0.21	0.50	0.87	0.63	-0.07
Kurt	26.0	8.2	10.0	7.6	7.1	9.2	46.1	68.5	55.6
N obs	2163	2418	2431	2307	2440	2414	2560	2559	2560
				Panel B: European market					
Mean	-1.13	**-0.83**	**-0.50**	**-2.21**	**-0.92**	**-0.60**	**-1.10**	-0.36	-0.30
	(-1.73)	(-2.97)	(-2.45)	(-3.96)	(-3.20)	(-2.87)	(-2.42)	(-1.39)	(-1.43)
Std.dev.	1.29	0.68	0.67	1.12	0.75	0.65	1.25	0.73	0.55
SR	-0.87	-1.21	-0.74	-1.98	-1.23	-0.92	-0.88	-0.50	-0.55
Skew	3.19	-0.06	-0.93	-0.12	0.41	0.24	1.86	1.24	0.75
Kurt	58.6	8.2	86.9	8.2	10.7	10.9	41.0	47.8	36.5
N obs	2210	2445	2379	1921	2314	2180	2545	2547	2151

Table IA.9: Performance of Vanna-Mimicking Portfolios
Summary statistics of daily excess returns on vanna-mimicking portfolios. Means, standard deviations, and Sharpe ratios ("SR") are annualized. t-statistics in parentheses are corrected for heteroscedasticity and serial correlation up to 63 lags (equal to three months) using the approach of Newey and West (1987). Mean estimates that are significant at the 5% level are highlighted in bold. Sample period is from January 1, 2013 to April 3, 2023.

	IG			HY			EQ		
	M1	M2	M3	M1	M2	M3	M1	M2	M3
Panel A: US market									
Mean	-0.41	-0.11	-0.10	0.22	-0.05	-0.07	-0.22	**-0.30**	**-0.25**
	(-1.21)	(-0.74)	(-1.10)	(0.94)	(-0.43)	(-0.66)	(-1.00)	(-2.12)	(-2.13)
Std.dev.	0.81	0.46	0.41	0.69	0.43	0.38	0.53	0.38	0.32
SR	-0.51	-0.23	-0.25	0.32	-0.11	-0.18	-0.41	-0.78	-0.78
Skew	-0.03	-0.02	-0.00	1.58	0.15	-0.12	2.25	2.54	2.56
Kurt	18.8	6.8	9.1	56.0	8.3	5.3	28.1	32.2	33.5
N obs	2135	2418	2425	2306	2438	2413	2560	2559	2560
Panel B: European market									
Mean	**-0.50**	-0.04	-0.11	0.01	-0.12	-0.05	-0.05	-0.10	-0.13
	(-3.28)	(-0.35)	(-1.26)	(0.06)	(-0.98)	(-0.54)	(-0.27)	(-0.99)	(-1.50)
Std.dev.	0.57	0.43	0.42	0.50	0.46	0.42	0.42	0.28	0.24
SR	-0.88	-0.09	-0.27	0.02	-0.25	-0.13	-0.11	-0.38	-0.53
Skew	-0.30	0.23	3.97	0.80	-0.66	1.99	-0.31	1.21	1.10
Kurt	9.4	7.1	92.8	12.3	33.4	37.5	16.3	20.1	16.1
N obs	2182	2440	2369	1844	2305	2166	2543	2547	2151

Table IA.10: Performance of Volga-Mimicking Portfolios
Summary statistics of daily excess returns on volga-mimicking portfolios. Means, standard deviations, and Sharpe ratios ("SR") are annualized. t-statistics in parentheses are corrected for heteroscedasticity and serial correlation up to 63 lags (equal to three months) using the approach of Newey and West (1987). Mean estimates that are significant at the 5% level are highlighted in bold. Sample period is from January 1, 2013 to April 3, 2023.

	EQ-IG			EQ-HY		
	M1-M2	M2-M3	M1-M3	M1-M2	M2-M3	M1-M3
			Panel A: US market			
Mean	**0.78**	**0.95**	**0.22**	**0.90**	**1.08**	**0.24**
	(3.86)	(3.83)	(3.09)	(4.70)	(4.45)	(3.60)
Std.dev.	0.66	0.82	0.30	0.59	0.72	0.25
SR	1.19	1.17	0.72	1.51	1.49	0.96
Skew	0.35	0.44	0.28	1.42	1.35	0.16
Kurt	19.8	17.4	13.7	21.0	17.9	12.0
N obs	2471	2444	2494	2468	2447	2477
			Panel B: European market			
Mean	**1.01**	**1.19**	**0.34**	**1.05**	**1.33**	**0.23**
	(6.75)	(5.07)	(4.40)	(7.09)	(7.02)	(3.26)
Std.dev.	0.54	0.78	0.28	0.52	0.66	0.28
SR	1.86	1.53	1.19	2.03	2.03	0.81
Skew	1.39	-0.26	0.90	1.42	1.04	-0.31
Kurt	12.5	33.7	11.7	14.4	9.3	17.9
N obs	2436	2049	2081	2310	1914	1996

Table IA.11: Performance of Long-Short Gamma-Mimicking Portfolios
Summary statistics of daily excess returns on short credit vs. long equity gamma-mimicking portfolios. Means, standard deviations, and Sharpe ratios ("SR") are annualized. t-statistics in parentheses are corrected for heteroscedasticity and serial correlation up to 63 lags (equal to three months) using the approach of Newey and West (1987). Mean estimates that are significant at the 5% level are highlighted in bold. Sample period is from January 1, 2013 to April 3, 2023.

	EQ-IG			EQ-HY		
	M1-M2	M2-M3	M1-M3	M1-M2	M2-M3	M1-M3
	Panel A: US market					
Mean	0.10	0.12	0.05	**0.22**	**0.27**	0.11
	(1.29)	(1.40)	(0.83)	(2.62)	(2.75)	(1.85)
Std.dev.	0.34	0.34	0.23	0.33	0.32	0.20
SR	0.29	0.35	0.20	0.67	0.84	0.56
Skew	-0.11	-0.12	-0.45	-0.41	0.05	-0.08
Kurt	8.8	12.4	13.9	13.5	6.3	9.4
N obs	2471	2444	2494	2468	2447	2477
	Panel B: European market					
Mean	0.08	**0.19**	0.05	0.05	0.14	**0.12**
	(0.98)	(1.97)	(0.91)	(0.72)	(1.86)	(2.45)
Std.dev.	0.28	0.31	0.21	0.30	0.29	0.20
SR	0.30	0.59	0.24	0.16	0.49	0.62
Skew	-0.75	0.01	-0.82	-1.75	-0.05	0.08
Kurt	11.2	13.7	13.6	32.1	6.2	7.2
N obs	2436	2049	2081	2310	1914	1996

Table IA.12: Performance of Long-Short Vega-Mimicking Portfolios
Summary statistics of daily excess returns on short credit vs. long equity vega-mimicking portfolios. Means, standard deviations, and Sharpe ratios (“SR”) are annualized. t-statistics in parentheses are corrected for heteroscedasticity and serial correlation up to 63 lags (equal to three months) using the approach of Newey and West (1987). Mean estimates that are significant at the 5% level are highlighted in bold. Sample period is from January 1, 2013 to April 3, 2023.

	EQ-IG			EQ-HY		
	M1	M2	M3	M1	M2	M3
	Panel A: US market					
Mean	0.39	0.38	0.09	**2.49**	0.63	0.38
	(0.66)	(1.12)	(0.36)	(4.55)	(1.87)	(1.54)
Std.dev.	2.24	1.24	0.97	1.86	1.06	0.86
SR	0.17	0.31	0.09	1.34	0.59	0.44
Skew	-0.02	0.73	0.60	1.95	1.31	0.65
Kurt	18.8	25.4	24.3	30.2	21.9	12.7
N obs	2163	2417	2431	2307	2439	2414
	Panel B: European market					
Mean	-0.27	0.52	0.15	0.81	0.44	0.07
	(-0.35)	(1.57)	(0.66)	(1.18)	(1.24)	(0.27)
Std.dev.	1.84	1.04	1.02	1.55	1.08	0.91
SR	-0.14	0.50	0.15	0.52	0.40	0.08
Skew	-3.43	0.35	1.78	-0.15	-0.05	-0.85
Kurt	67.7	14.0	110.2	9.3	14.8	14.5
N obs	2187	2422	2052	1899	2292	1962

Table IA.13: Performance of Long-Short Vanna-Mimicking Portfolios
Summary statistics of daily excess returns on short credit vs. long equity vanna-mimicking portfolios. Means, standard deviations, and Sharpe ratios ("SR") are annualized. t-statistics in parentheses are corrected for heteroscedasticity and serial correlation up to 63 lags (equal to three months) using the approach of Newey and West (1987). Mean estimates that are significant at the 5% level are highlighted in bold. Sample period is from January 1, 2013 to April 3, 2023.

	EQ-IG			EQ-HY		
	M1	M2	M3	M1	M2	M3
Panel A: US market						
Mean	0.67	-0.10	-0.08	-0.16	**-0.37**	-0.25
	(1.32)	(-0.43)	(-0.60)	(-0.40)	(-2.14)	(-1.76)
Std.dev.	1.33	0.73	0.65	1.18	0.63	0.56
SR	0.51	-0.13	-0.12	-0.13	-0.58	-0.45
Skew	1.95	1.04	0.27	8.45	0.49	0.53
Kurt	23.4	17.4	16.9	232.7	10.0	8.6
N obs	2135	2417	2425	2306	2437	2413
Panel B: European market						
Mean	**0.69**	0.05	0.12	0.11	0.24	-0.04
	(2.55)	(0.26)	(0.84)	(0.36)	(1.11)	(-0.30)
Std.dev.	0.89	0.61	0.73	0.77	0.78	0.70
SR	0.77	0.08	0.16	0.14	0.31	-0.06
Skew	0.30	0.08	-7.98	0.08	5.94	-5.70
Kurt	8.7	7.8	261.0	11.6	176.0	145.8
N obs	2159	2417	2049	1821	2283	1948

Table IA.14: Performance of Long-Short Volga-Mimicking Portfolios
Summary statistics of daily excess returns on short credit vs. long equity volga-mimicking portfolios. Means, standard deviations, and Sharpe ratios ("SR") are annualized. t-statistics in parentheses are corrected for heteroscedasticity and serial correlation up to 63 lags (equal to three months) using the approach of Newey and West (1987). Mean estimates that are significant at the 5% level are highlighted in bold. Sample period is from January 1, 2013 to April 3, 2023.

	IG				HY				EQ			
	-2	-1	0	1	-2	-1	0	1	-2	-1	0	1
					Panel A: US market							
α	**-2.84**	**-2.00**	**-0.81**	**-1.22**	**-3.98**	**-2.60**	**-1.16**	**-1.76**	0.17	0.01	0.02	**0.81**
	(-5.04)	(-4.82)	(-3.76)	(-2.11)	(-6.32)	(-5.34)	(-4.66)	(-2.58)	(0.58)	(0.14)	(0.48)	(2.09)
IDX	**-1.62**	**-1.65**	**-0.90**	**-5.55**	**-1.95**	**-1.72**	**-0.95**	**-4.89**	**0.64**	-0.26	-0.16	**-1.49**
	(-4.19)	(-5.77)	(-5.96)	(-8.20)	(-3.25)	(-3.97)	(-5.41)	(-10.42)	(2.36)	(-1.62)	(-1.70)	(-2.61)
GMA	**0.49**	**0.50**	**0.29**	**0.90**	**0.65**	**0.55**	**0.31**	**1.29**	**2.63**	**1.96**	**1.05**	**4.89**
	(3.60)	(5.56)	(6.49)	(5.60)	(3.77)	(4.92)	(6.18)	(7.11)	(29.29)	(26.95)	(27.43)	(17.98)
VGA	**1.40**	**1.06**	**0.60**	**2.31**	**1.00**	**0.97**	**0.49**	**2.05**	**4.36**	**3.33**	**1.89**	**9.52**
	(4.19)	(4.83)	(5.41)	(5.53)	(3.09)	(4.65)	(4.48)	(5.31)	(25.00)	(45.50)	(63.35)	(27.66)
VNA	0.02	0.03	0.02	-0.01	0.09	0.06	0.01	-0.08	**0.92**	**0.42**	**0.04**	**-1.53**
	(0.19)	(0.42)	(0.47)	(-0.09)	(0.89)	(0.62)	(0.17)	(-0.48)	(11.18)	(10.99)	(2.19)	(-6.53)
VLG	0.24	0.17	0.08	0.19	0.09	0.17	0.08	**0.36**	**2.02**	**0.84**	0.04	**2.88**
	(1.59)	(1.85)	(1.86)	(1.07)	(0.46)	(1.42)	(1.26)	(2.17)	(10.49)	(10.28)	(0.78)	(11.47)
R^2	0.20	0.27	0.28	0.29	0.18	0.26	0.27	0.32	0.94	0.97	0.96	0.90
					Panel B: European market							
α	**-3.44**	**-2.12**	**-0.86**	**-2.59**	**-3.10**	**-2.36**	**-0.98**	**-2.97**	0.34	-0.06	-0.01	0.44
	(-7.57)	(-5.32)	(-4.32)	(-3.27)	(-4.85)	(-5.95)	(-4.96)	(-4.36)	(1.39)	(-0.54)	(-0.15)	(1.13)
IDX	**-2.16**	**-1.57**	**-0.79**	**-3.93**	**-2.36**	**-1.71**	**-0.84**	**-3.92**	0.47	-0.17	-0.11	-0.72
	(-6.19)	(-8.99)	(-7.34)	(-7.06)	(-4.35)	(-6.45)	(-7.73)	(-10.91)	(1.96)	(-1.45)	(-1.63)	(-1.50)
GMA	**0.62**	**0.53**	**0.30**	**1.01**	**0.74**	**0.62**	**0.29**	**0.82**	**3.52**	**2.54**	**1.30**	**5.78**
	(4.45)	(4.32)	(4.39)	(5.73)	(3.70)	(4.74)	(4.56)	(4.31)	(28.42)	(37.81)	(38.79)	(20.01)
VGA	**1.20**	**0.71**	**0.38**	**2.20**	**1.02**	**0.93**	**0.53**	**2.20**	**5.06**	**3.68**	**1.92**	**8.54**
	(3.60)	(4.05)	(4.29)	(6.71)	(2.75)	(4.29)	(4.48)	(4.97)	(23.70)	(39.36)	(47.15)	(32.30)
VNA	**0.34**	**0.23**	**0.11**	**0.15**	**0.35**	**0.26**	**0.09**	0.14	**1.07**	**0.48**	0.04	**-1.12**
	(5.30)	(5.63)	(4.81)	(2.06)	(3.89)	(4.46)	(3.72)	(1.72)	(12.63)	(9.05)	(1.42)	(-6.91)
VLG	0.07	0.18	0.08	0.51	-0.15	-0.01	-0.04	0.34	**2.29**	**0.85**	0.05	**2.35**
	(0.24)	(0.84)	(0.66)	(1.43)	(-0.33)	(-0.03)	(-0.33)	(0.95)	(15.10)	(12.14)	(1.02)	(5.11)
R^2	0.25	0.28	0.27	0.27	0.25	0.29	0.29	0.32	0.93	0.96	0.96	0.91

Table IA.15: Equity Factor Exposures for Option Portfolios Sorted on Moneyness

The table shows the factor loadings from regressing daily excess returns on IG option portfolios onto a constant (α) and the daily excess returns on the equity factors. The α coefficient is annualized. The regression also includes the factor returns lagged one day to take potential non-synchronicity into account, but for brevity the factor loadings are not displayed. t-statistics in parentheses are corrected for heteroscedasticity and serial correlation up to 63 lags (equal to three months) using the approach of Newey and West (1987). Coefficients that are significant at the 5% level are highlighted in bold. Sample period is from January 1, 2013 to April 3, 2023.

	IG			HY			EQ		
	M1	M2	M3	M1	M2	M3	M1	M2	M3
Panel A: US market									
α	**-2.55**	**-1.43**	**-0.77**	**-3.62**	**-2.03**	**-0.94**	**0.36**	0.14	0.25
	(-2.82)	(-3.97)	(-2.47)	(-5.00)	(-4.66)	(-2.28)	(1.97)	(0.68)	(1.22)
IDX	**-1.89**	**-2.51**	**-2.62**	**-1.89**	**-2.68**	**-2.57**	**0.43**	**-0.56**	**-0.83**
	(-3.28)	(-9.18)	(-8.20)	(-3.84)	(-8.40)	(-12.65)	(1.99)	(-2.28)	(-3.41)
GMA	**0.86**	**0.45**	**0.33**	**1.24**	**0.56**	**0.31**	**4.75**	**1.97**	**1.17**
	(5.89)	(5.09)	(4.83)	(7.12)	(5.86)	(3.75)	(33.92)	(17.58)	(12.73)
VGA	**1.61**	**1.39**	**0.94**	**1.44**	**1.03**	**0.89**	**5.13**	**4.85**	**4.35**
	(4.34)	(5.87)	(4.31)	(4.68)	(6.07)	(5.37)	(48.04)	(35.51)	(22.46)
VNA	0.07	-0.00	0.01	0.03	-0.01	0.03	-0.05	-0.02	-0.04
	(0.73)	(-0.03)	(0.16)	(0.20)	(-0.09)	(0.54)	(-0.56)	(-0.21)	(-0.48)
VLG	**0.43**	0.16	0.01	**0.39**	0.11	0.09	**1.91**	**1.38**	**1.05**
	(2.93)	(1.70)	(0.09)	(2.14)	(1.23)	(0.76)	(17.84)	(9.21)	(6.66)
R^2	0.15	0.31	0.33	0.23	0.31	0.33	0.96	0.91	0.88
Panel B: European market									
α	**-4.25**	**-1.87**	**-0.87**	**-4.35**	**-1.93**	**-1.20**	0.44	0.10	0.15
	(-7.88)	(-5.61)	(-2.83)	(-8.06)	(-5.15)	(-3.57)	(1.76)	(0.68)	(1.02)
IDX	**-1.76**	**-2.23**	**-2.27**	**-1.78**	**-2.32**	**-1.91**	0.33	-0.26	**-0.44**
	(-5.41)	(-10.80)	(-9.71)	(-6.63)	(-11.09)	(-13.63)	(1.59)	(-1.09)	(-2.27)
GMA	**0.93**	**0.53**	**0.36**	**1.02**	**0.49**	**0.40**	**5.25**	**2.69**	**1.69**
	(4.92)	(5.10)	(4.04)	(4.86)	(3.59)	(4.00)	(40.45)	(22.79)	(15.10)
VGA	**1.26**	**1.00**	**0.85**	**1.13**	**1.09**	**1.12**	**5.07**	**4.97**	**4.48**
	(5.36)	(5.96)	(6.94)	(3.63)	(4.77)	(4.82)	(31.98)	(42.57)	(41.33)
VNA	**0.27**	**0.19**	**0.12**	**0.31**	**0.14**	**0.12**	0.18	0.08	0.02
	(4.04)	(4.94)	(3.96)	(3.98)	(2.90)	(3.89)	(1.53)	(1.18)	(0.41)
VLG	0.42	0.21	0.05	0.23	-0.02	0.10	**1.90**	**1.27**	**0.96**
	(1.53)	(0.99)	(0.21)	(0.70)	(-0.09)	(0.54)	(11.53)	(7.65)	(4.92)
R^2	0.23	0.35	0.34	0.25	0.33	0.35	0.95	0.93	0.91

Table IA.16: Equity Factor Exposures for Option Portfolios Sorted on Maturity
The table shows the factor loadings from regressing daily excess returns on HY option portfolios onto a constant (α) and the daily excess returns on the equity factors. The α coefficient is annualized. The regression also includes the factor returns lagged one day to take potential non-synchronicity into account, but for brevity the factor loadings are not displayed. t-statistics in parentheses are corrected for heteroscedasticity and serial correlation up to 63 lags (equal to three months) using the approach of Newey and West (1987). Coefficients that are significant at the 5% level are highlighted in bold. Sample period is from January 1, 2013 to April 3, 2023.

	Calls			Puts			Δ-hedged calls			Δ-hedged puts		
	EQ	IG	L-S	EQ	IG	L-S	EQ	IG	L-S	EQ	IG	L-S
Panel A: Exposures												
Asset diffusive	4.49	3.15	1.34	-3.64	-2.82	-0.82	0.33	0.17	0.17	0.34	0.16	0.18
Asset jumps	-0.84	-0.74	-0.10	1.90	1.44	0.46	0.56	0.35	0.21	0.56	0.35	0.21
Asset variance	1.11	-0.62	1.74	1.02	2.47	-1.44	1.07	0.92	0.15	1.07	0.92	0.14
Panel B: Mean excess returns and Sharpe ratios												
Mean	1.34	1.77	-0.43	-2.35	-2.78	0.43	-0.55	-0.51	-0.04	-0.54	-0.51	-0.03
Std.dev.	4.02	3.64	1.42	4.81	4.99	1.26	1.13	0.94	0.28	1.12	0.94	0.28
SR	0.33	0.49	-0.30	-0.49	-0.56	0.34	-0.48	-0.54	-0.14	-0.48	-0.54	-0.11

Table IA.17: Conditional Option Exposures and Risk-Return Trade-Off
Instantaneous excess returns on equity and credit (investment-grade) index options are computed from the model in Collin-Dufresne et al. (2024) with parameter estimates from Doshi et al. (2024). The options are 1-month ATM puts and calls. Returns are for outright options and delta-hedged options, where the delta is with respect to the underlying index and computed using the Black-Scholes model. Results are reported for equity and credit options separately, and for a long-equity/short-credit option strategy. Panel A reports the conditional factor exposures normalized to reflect a one standard derivation change in each of the risk factors. Panel B reports the conditional annualized means, volatilities, and Sharpe ratios (SR). All values are conditional on the variance state variable being equal to its long-run mean.

	γ	ν	ζ	ω
GMA	36.81	0	0	0.01
VGA	0	5.30	0.53	-0.02
VNA	0	0	-9.27	0
VLG	0	0	0.39	3.94

Table IA.18: Greeks of Gamma, Vega, Vanna, and Volga Factors
The figure shows the greeks for the gamma (GMA), vega (VGA), vanna (VNA), and volga (VLG) factors in the Black-Scholes model. Parameter values are $S_t = 100$, $r = 0.02$, $q = 0.01$, and $\sigma = 0.20$.

	IG			HY			EQ		
Holding period	Daily	Expiry	Expiry	Daily	Expiry	Expiry	Daily	Expiry	Expiry
T-cost	—	—	7.5%	—	—	7.5%	—	—	1.5%
Panel A: US market									
Mean	**1.93**	**1.81**	**0.91**	**2.16**	**2.16**	**1.26**	0.62	0.32	0.14
	(5.11)	(5.93)	(2.98)	(5.36)	(8.03)	(4.69)	(1.75)	(1.27)	(0.56)
Std.dev.	0.89	1.24	1.24	0.88	0.95	0.95	1.11	1.00	1.00
SR	2.18	1.46	0.73	2.46	2.28	1.33	0.56	0.32	0.14
Skew	-2.22	-2.00	-2.00	-3.12	-0.79	-0.79	-2.66	-1.53	-1.53
Kurt	17.2	9.1	9.1	24.8	4.2	4.2	18.6	8.6	8.6
N obs	2485	2501	2501	2465	2512	2512	2560	2537	2537
Panel B: European market									
Mean	**1.77**	**1.97**	**1.07**	**1.96**	**1.82**	**0.92**	0.17	0.22	0.04
	(5.26)	(9.15)	(4.97)	(5.42)	(8.31)	(4.20)	(0.50)	(0.80)	(0.16)
Std.dev.	0.85	0.83	0.83	0.82	0.92	0.92	1.06	1.02	1.02
SR	2.08	2.37	1.29	2.38	1.98	1.00	0.16	0.22	0.04
Skew	-3.21	-0.84	-0.84	-2.95	-1.81	-1.81	-2.71	-1.06	-1.06
Kurt	27.3	5.0	5.0	23.0	13.9	13.9	18.0	4.8	4.8
N obs	2480	2507	2507	2369	2425	2425	2545	2527	2527

Table IA.19: Performance of Straddles

Summary statistics of daily excess returns on straddles. Means, standard deviations, and Sharpe ratios ("SR") are annualized. t-statistics in parentheses are corrected for heteroscedasticity and serial correlation up to 63 lags (equal to three months) using the approach of Newey and West (1987). Mean estimates that are significant at the 5% level are highlighted in bold. Sample period is from January 1, 2013 to April 3, 2023.

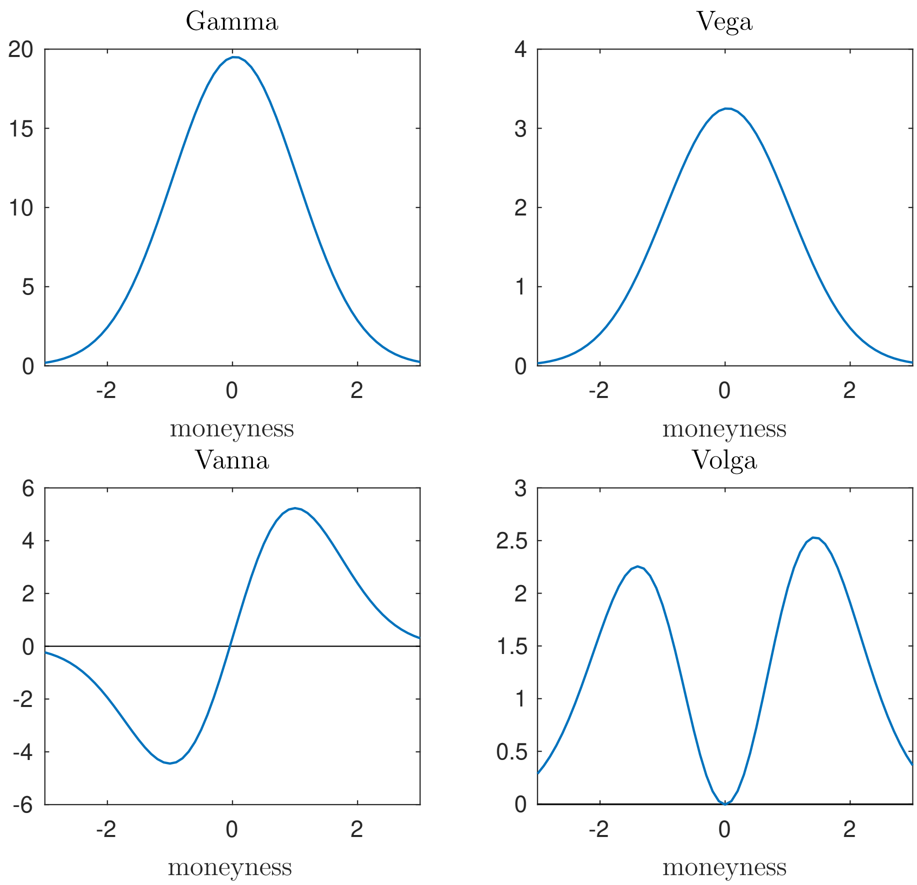

Figure IA1: Option Greeks as Function of Moneyness
The figure shows gamma, vega, vanna, and volga for two-month options in the Black-Scholes model as a function of moneyness, m. Parameter values are $S_t = 100$, $r = 0.02$, $q = 0.01$, and $\sigma = 0.20$.

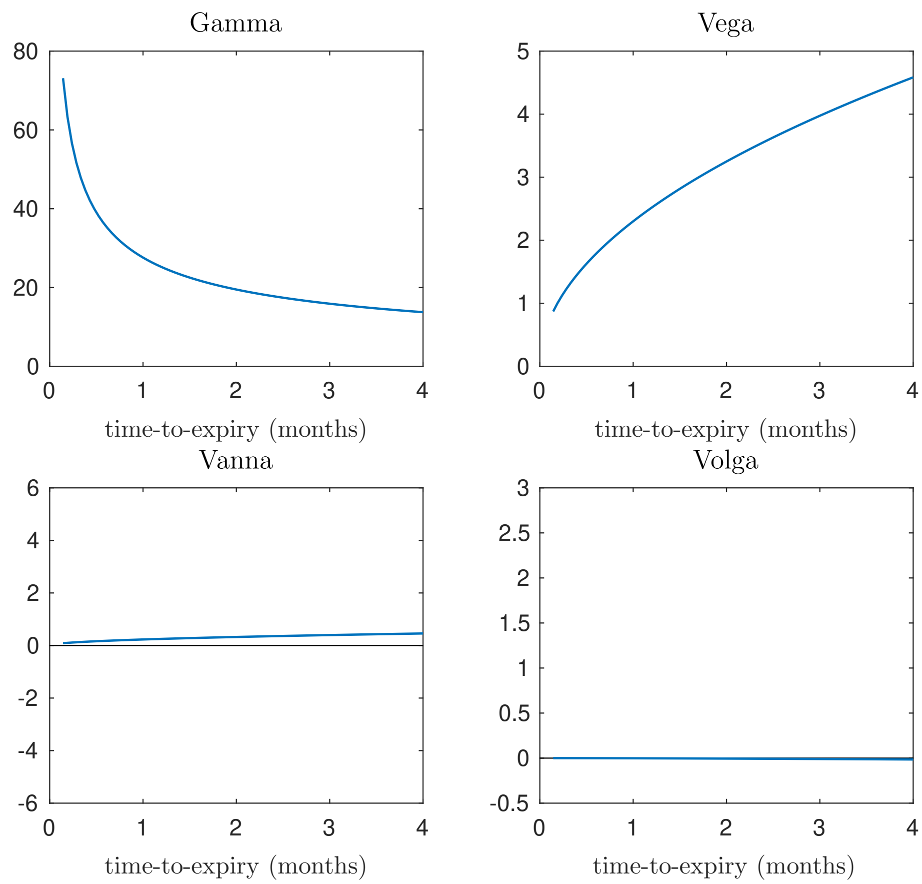

Figure IA2: Option Greeks as Function of Time-to-Expiry
The figure shows gamma, vega, vanna, and volga for ATM options in the Black-Scholes model as a function of time-to-expiry, τ. Parameter values are $S_t = 100$, $r = 0.02$, $q = 0.01$, and $\sigma = 0.20$.

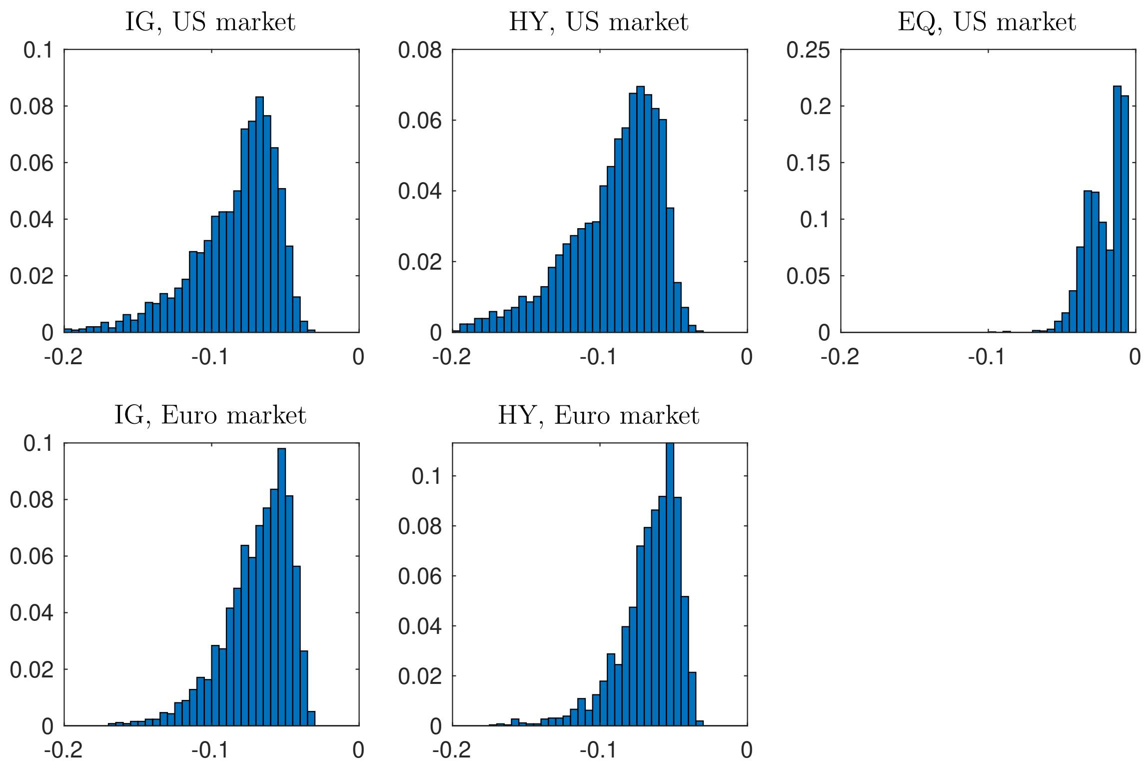

Figure IA3: Percentage Bid-Mid Spreads on ATM Straddles
Frequency distribution of percentage bid-mid spreads, $\frac{P_t^{bid}-P_t^{mid}}{P_t^{mid}}$, on 1-month ATM straddles. Note that data is missing for the European equity index option. Daily data from January 1, 2013 to April 3, 2023.

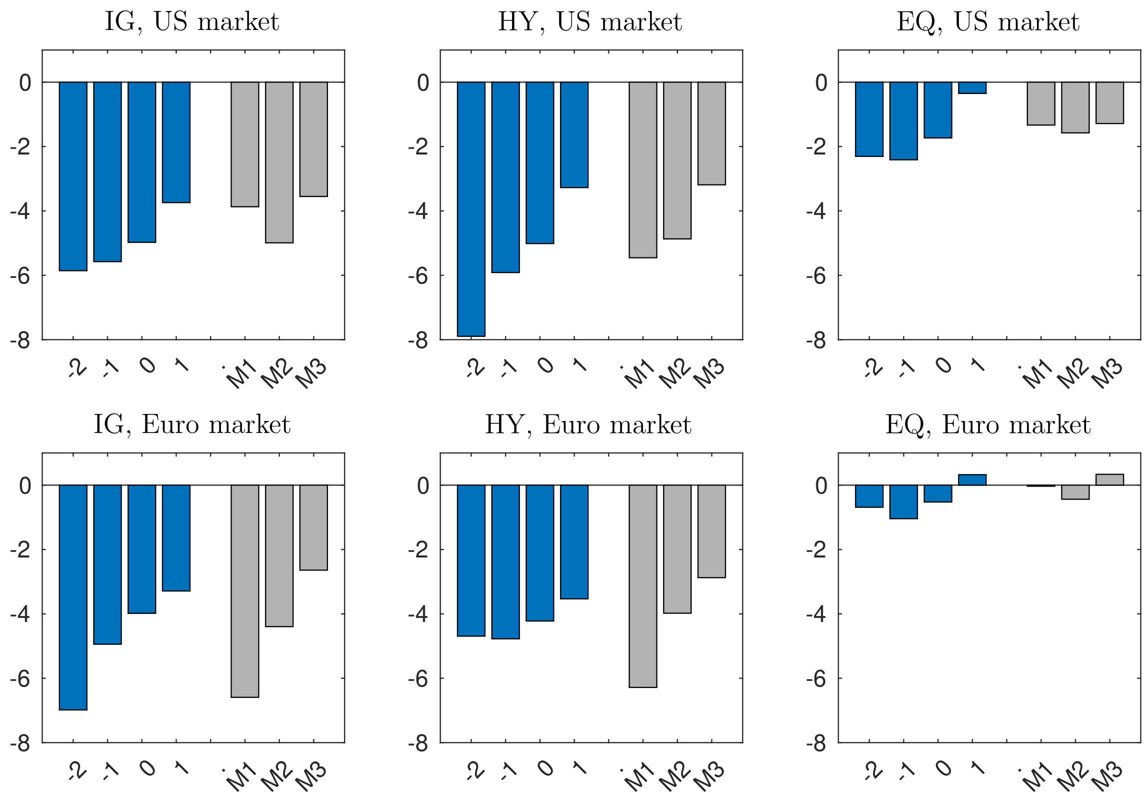

Figure IA4: Performance of Option Portfolios, t-statistics
t-statistics for the mean excess daily returns of option portfolios sorted on moneyness and maturity. -2, -1, 0, 1 refer to moneyness, m, defined in (3). M1, M2, and M3 refer to 1, 2, and 3 month options. Top panels are for the US market and bottom panels are for the European market. Left, middle, and right panels are for IG, HY, and EQ indexes, respectively. The t-statistics are corrected for heteroscedasticity and serial correlation up to 63 lags (equal to three months) using the approach of Newey and West (1987). Sample period is from January 1, 2013 to April 3, 2023.

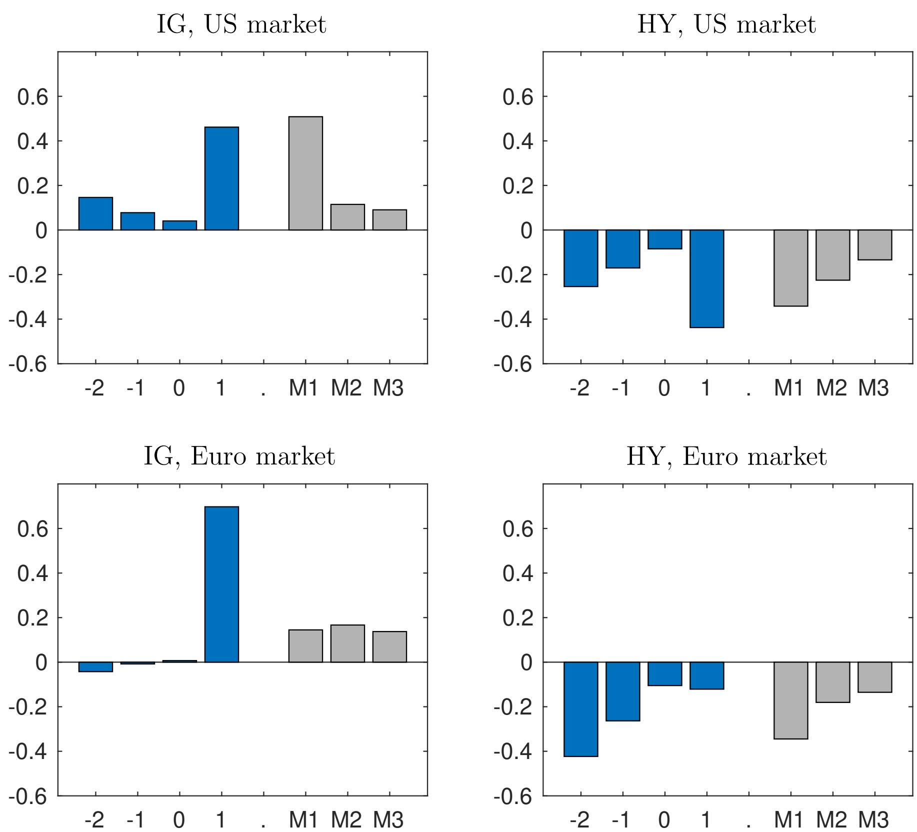

Figure IA5: Loadings on Second Credit Option Residual Factor
In each market, the equity-based factor model is applied to the 14 credit option portfolios (two credit indexes each with seven portfolios sorted on moneyness and maturity) and a principal component analysis (PCA) is applied to the residuals. -2, -1, 0, 1 refer to moneyness, m, defined in (3). M1, M2, and M3 refer to 1, 2, and 3 month options. The top (bottom) panels show the portfolio loadings on the second PC in the US (European) market. The left (right) panels are for the IG (HY) indexes.

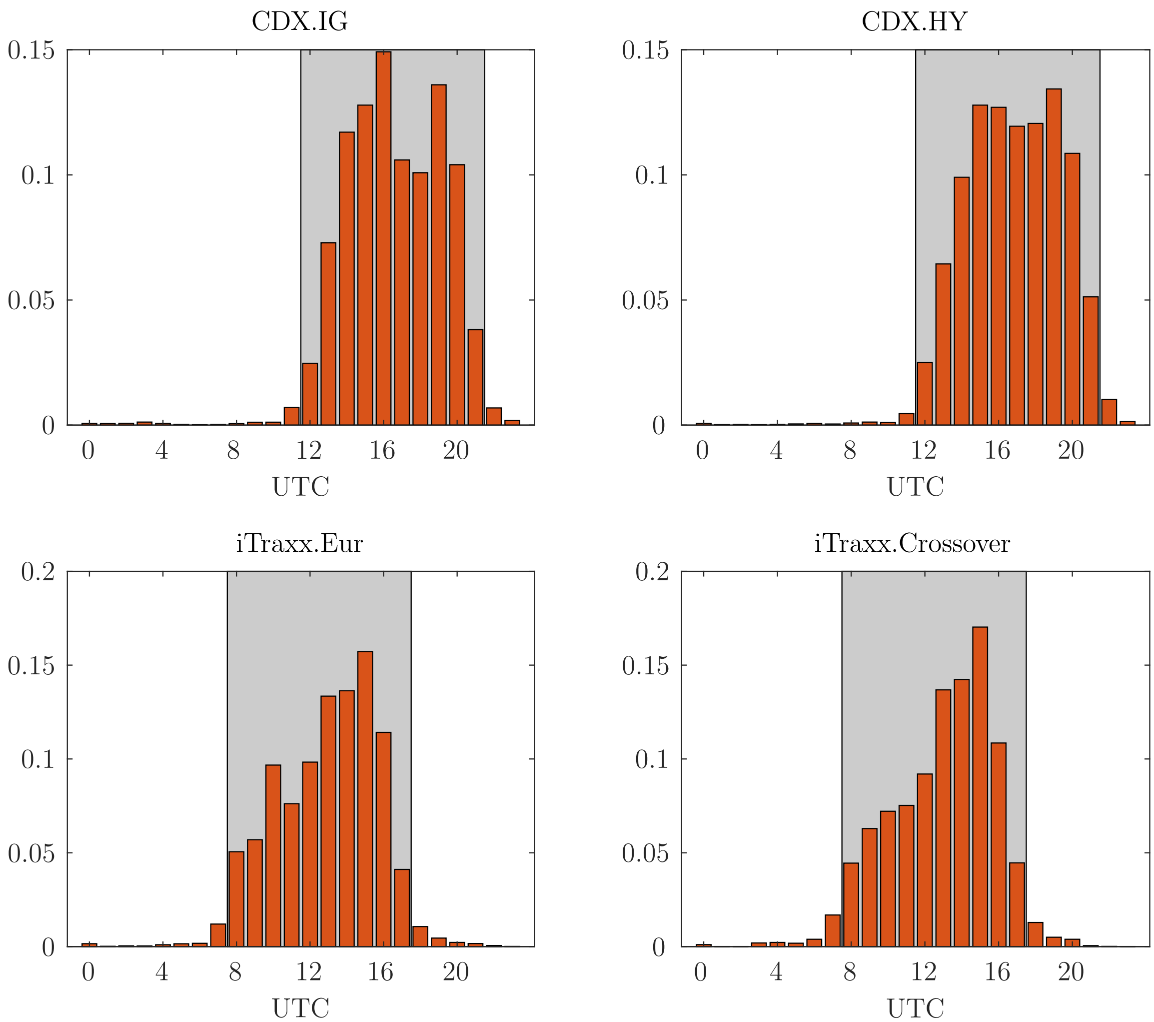

Figure IA6: Distribution of Execution Times for Option Trades
The figure shows for each index the empirical distribution of the execution time stamps on option trades in Coordinated Universal Time (UTC). The grey shaded area marks typical trading hours in New York (for the US indices) and London (for the European indices).